Development of local Coupled Cluster response methods for high-spin open-shell molecules

Dissertation

zur Erlangung des Doktorgrades der Naturwissenschaften (Dr. rer. nat.)

der Fakultät Chemie und Pharmazie

der Universität Regensburg

vorgelegt von

David David

aus Tal Nasri, Haska, Syrien

im Jahr 2018

Promotionsgesuch eingereicht am:	17.12.2018
Tag des Kolloquiums:	01.02.2019
Diese Arbeit wurde angeleitet von:	Prof. Dr. Martin Schütz

Prüfungsausschuss	
Vorsitzender:	Prof. Dr. Hubert Motschmann
Erstgutachter:	Prof. Dr. Bernhard Dick
Zweitgutachter:	PD Dr. Denis Usvyat
Drittprüfer:	Prof. Dr. Stefan Dove

Danksagung

Ich möchte mich an dieser Stelle bei allen bedanken, die zur Entstehung dieser Dissertationsarbeit beigetragen haben. Mein besonderer Dank gilt hierbei:

Dem leider inzwischen verstorbenen Herrn *Prof. Dr. Martin Schütz* für die Vergabe des sehr interessanten und anspruchsvollen Themas sowie für seine Geduld und stets kompetente Betreuung.

Herrn *PD Dr. Denis Usvyat* für die ständige Bereitschaft zur Diskussion unendlich vieler Fragen und für die Übernahme der weiteren Betreuung.

Herrn *Prof. Dr. Bernhard Dick* für die vielen fachlichen Ratschläge sowie für die freundliche Übernahme der Zweitbegutachtung.

Klaus Ziereis und *Thomas Dargel* für die kompetente Hilfe bei technischen Angelegenheiten.

Dr. Oliver Masur, *Dr. Katrin Ledermüller*, *Dr. Stefan Loibl*, *Martin Christlmaier*, *Alexander Krach*, *Alexander Schinabeck*, *Petra Eichenseher*, *Dr. Marco Lorenz* und *Dr. Thomas Merz* für eine angenehme Atmosphäre am Arbeitskreis.

Meinem Kollegen *Matthias Hinreiner* für die vielfältigen und sehr bereichernden Diskussionen während der Mittagspausen.

Meinem Kollegen und Freund *Dr. Gero Wälz*, der mir in fachlichen als auch privaten Angelegenheiten stets zur Seite stand.

Vor allen aber meinem Herrn und Gott, ***Jesus Christus***, der meinem Leben einen ewigen Sinn verleiht sowie meiner Frau *Nensina*, meiner Tochter *Mariel*, meinen Eltern *Gaivarghis* und *Amira* und meinen Geschwistern *Shamiram*, *Fouad* und *Ninab* für ihre Liebe.

Contents

1. Introduction

Open-shell molecules, radicals, play an important role in different fields of chemistry and biology. To give some examples one can think about DNA-damage in biological systems, polymerisation reactions or photocatalysis in synthetic chemistry. To understand and predict reactions in which radicals are involved needs the ability to describe the ground and excited states of these molecules. But this is still a challenging task for large high-spin open-shell molecules (100 atoms). Especially if one aims at a compromise between accuracy and computational costs.

Probably the most widely used methods are Density Functional Theory (DFT) [1,2] and time dependent (TD-)DFT. The reason is that these methods are computationally less demanding than correlated, wave function based, methods which go beyond Configuration Interaction Singles (CIS). Yet TD-DFT, depending on the used functional, may fail to produce even qualitatively reasonable results especially in case of charge transfer states [3].

Coupled Cluster (CC) theory [4–7] is well established as a wave function based method for the description of dynamical correlation effects. The restriction of the cluster operator to singles and doubles (CCSD) has also been used to describe high-spin open-shell systems along with a single-reference determinant, but often a straight forward usage of unrestricted spin-orbital formalism has been avoided [8–11]. The main reasons are spin contamination and computational costs.

However, if a restricted open-shell Hartree-Fock (ROHF) reference determinant is

chosen instead of unrestricted Hartree-Fock (UHF), the excitation energies despite the remaining spin contamination, which arises from not solving the CC spin equations, are in good agreement (absolute error < 0.1 eV) with the Multi-Reference Configuration Interaction (MR-CI) results for a set of diatomic molecules described in reference [12].

CCSD scales as $\mathcal{O}(\mathcal{N}^6)$ with molecular size $\mathcal{N}$ and a straight forward, unrestricted spin-orbital formulation, even if based on a ROHF reference implies a computational cost factor of 3 compared to the corresponding closed-shell calculation [13].

Thus the search for reduction of computational costs along with a straight forward implementation using unrestricted spin-orbital formulation, but maintaining the ROHF reference and reaching a reasonable accuracy, lead to the work presented here.

Firstly, one chooses the approximate CC2 Model [14] which scales as $\mathcal{O}(\mathcal{N}^5)$ with molecular size $\mathcal{N}$ instead of CCSD ($\mathcal{O}(\mathcal{N}^6)$).

Secondly, one starts with a ROHF reference and generates out of it the semi-canonical spin orbitals [15]. The occupied ones are transformed to localized spin orbitals and atomic orbitals are projected to the virtuals as proposed by Pulay [16].

Thirdly, Density Fitting (DF) approximation [17–19], for reduction of the prefactor of the scaling behaviour, and local approximations in order to reach a lower order scaling of CC2, are applied. Note that a canonical, non local, implementation of CC2 based only on the DF approximation for high-spin open-shell molecules is available in the TURBOMOLE package [20].

Fourthly, inspired by the work of D. Kats and M. Schütz [21], the laplace-transform (LT) trick is used to enable a multistate CC2 response method along with local approximations in analogy to what is already available in MOLPRO [22] for closed-shell molecules. So the new method will be called $\mathbf{LT-DF-LUCC2}$ (laplace-transformed density fitted local unrestricted CC2).

At the beginning basic concepts which are necessary for the development of the presented method are introduced. It follows the choice of the reference wave function and the description of local spin orbitals. Then the derivation of the working equations for the ground and excited state of high-spin open-shell molecules as well as corresponding local approximations are outlined. Finally the application of that method to calculate excitation energies, ionization potentials and electron affinities is demonstrated.

2. Basic concepts

In this chapter several basic concepts are introduced for the understanding of the method presented in this thesis. As the method is based on Coupled Cluster (CC) theory, response theory, construction and evaluation of CC diagrams, density fitting and Laplace transformation, these concepts are explained.

2.1. Coupled Cluster theory and the CC2 model

It is well known that the movement of two electrons with opposite spin is not correlated within the use of a single Slater Determinant (SD). To capture this dynamic electron correlation, or to describe the coulomb hole correctly, many theoretical methods have been developed. Among the wave function based methods like Configuration Interaction (CI) or perturbation theory along with the Møller-Plesset (MP) partitioning of the electronic Hamiltonian, the Coupled Cluster (CC) theory [4–7] is very successful and widely used.

A SD which contains occupied Hartree Fock spin orbitals, is usually used as a reference determinant to generate the CC wave function $|\mathrm{CC}\rangle$ through the exponential ansatz.

$$|\mathrm{CC}\rangle = \exp(\mathbf{T})\,|\Phi_0\rangle \tag{2.1}$$

In equation (2.1), $|\Phi_0\rangle$ symbolizes the reference determinant and $\mathbf{T}$ is the total cluster operator, which is defined as

$$\mathbf{T} = \sum_{i=1}^{N_{elec}} \mathrm{T}_i. \tag{2.2}$$

Here each summand T_i implies replacement of i occupied spin orbitals by virtual ones. This replacement is often referred to as generating excited determinants. Each cluster operator T_i contains products of amplitudes t_{μ_i} and corresponding excitation operators τ_{μ_i} to generate all possible i-fold excited determinants. For example, the singles and doubles cluster operators are defined as

$$\begin{aligned} \mathrm{T}_1 &= \sum_{\mu_1} t_{\mu_1}\tau_{\mu_1} = \sum_{IA} t_A^I a_A^\dagger a_I \\ \mathrm{T}_2 &= \sum_{\mu_2} t_{\mu_2}\tau_{\mu_2} = \frac{1}{4}\sum_{IJAB} t_{AB}^{IJ} a_A^\dagger a_B^\dagger a_J a_I \end{aligned} \tag{2.3}$$

The capital letters $I, J, ...$ and $A, B, ...$ represent occupied and virtual spin orbitals, respectively, while the explicit spin (α or β) of the corresponding orbital is not yet specified. The second quantization operator a_I annihilates the occupied spin orbital I from $|\Phi_0\rangle$ and $a_A^\dagger$ introduces the virtual spin orbital A in it. Thus $a_A^\dagger$ and a_I are referred to as the creation and annihilation operators, respectively. The factor $\frac{1}{4}$ is included to avoid double counting of spin orbital pairs.

Due to the exponential ansatz, even if the cluster operator is truncated, one has formally all possible higher excitations. The products of amplitudes are referred to as disconnected cluster amplitudes. Irrespective of the truncation level of $\mathbf{T}$, the CC models are size consistent. That means, that the total energy of a system composed of noninteracting subsystems is the same as the sum of the energies of each subsystem calculated separately. This is fulfilled because the exponential ansatz makes the CC wave function multiplicative separable and the corresponding expectation values of the Hamiltonians additive. But in cases where the reference method fails to be size

consistent, also the correlated method will not be. In general for the CC models, the mathematically stronger requirement that the energy scales correctly with the number of the correlated electrons is fulfilled. This feature is referred to as size extensivity.

For the calculation of the CC energy a projective technique is used instead of the usual quantum mechanical expectation value equation.

$$\mathrm{E} = \langle \Phi_0 | \exp(-\mathbf{T}) \mathbf{H} \exp(\mathbf{T}) | \Phi_0 \rangle = \langle \Phi_0 | \bar{\mathbf{H}} | \Phi_0 \rangle \tag{2.4}$$

The reason for that is that $\exp(\mathbf{T})^\dagger$ would act on the left as an excitation operator giving rise to much more matrix elements of the Hamilton operator $\mathbf{H}$ than in equation (2.4). The Hamiltonian can be written in second quantized form as

$$\mathbf{H} = \sum_{PQ} h_{PQ} a_P^\dagger a_Q + \frac{1}{4} \sum_{PQRS} \langle PQ||RS\rangle \, a_P^\dagger a_Q^\dagger a_S a_R. \tag{2.5}$$

With the following definition of the one electron integral,

$$h_{PQ} = \int \psi_P^*(x_1) h(r_1) \psi_Q(x_1) dx_1, \tag{2.6}$$

which describes the kinetic energy of a single electron with three space and one spin coordinate hidden in x_1 as well as the coulomb attraction between an electron and all nuclei. The antisymmetrized two electron integrals are defined as

$$\begin{aligned} \langle PQ||RS\rangle &= \langle PQ|RS\rangle - \langle PQ|SR\rangle \\ \langle PQ|RS\rangle &= \int \psi_P^*(x_1) \psi_Q^*(x_2) \frac{1}{r_{12}} \psi_R(x_1) \psi_S(x_2) dx_1 dx_2 \end{aligned} \tag{2.7}$$

$PQRS...$ indicate general spin orbitals which can be either occupied or virtual.

Use of the similarity transformed Hamiltonian $\bar{\mathbf{H}}$ is justified by the fact that, in case of no truncation, its eigenvalues represent the complete eigenvalue spectrum of the hermitian Hamilton operator $\mathbf{H}$. $\bar{\mathbf{H}}$ can be written in the Baker-Campbell-Hausdorff (BCH) expansion,

$$\bar{\mathbf{H}} = \mathbf{H} + [\mathbf{H}, \mathbf{T}] + \frac{1}{2!}[[\mathbf{H}, \mathbf{T}], \mathbf{T}] + \frac{1}{3!}[[[\mathbf{H}, \mathbf{T}], \mathbf{T}], \mathbf{T}] + \frac{1}{4!}[[[[\mathbf{H}, \mathbf{T}], \mathbf{T}], \mathbf{T}], \mathbf{T}], \tag{2.8}$$

which terminates exactly after the fifth term, because each commutator reduces the number of the general creation and annihilation operators of the Hamiltonian by one. Thus after the fifth term only creation and annihilation operator strings with either occupied or virtual spin orbital index remain and these commute. Equation (2.4) is called the linked CC energy equation. For the determination of the CC amplitudes, the so-called linked CC amplitudes equations have to be solved.

$$\Omega_{\mu_i} = \langle \mu_i | \exp(-\mathbf{T}) \mathbf{H} \exp(\mathbf{T}) | \Phi_0 \rangle \stackrel{!}{=} 0 \tag{2.9}$$

While $|\mu_i\rangle$ represents all possilbe i-fold excited determinants. Solving the CC amplitudes equations iteratively, yields the corresponding amplitudes t_{μ_i} for which the residuums vector Ω_{μ_i} becomes zero. These amplitudes determine the final CC energy (2.4).

By restriction of the Cluster operator $\mathbf{T}$ to singles and doubles excitations one arrives at the well known CCSD model. The singles and doubles amplitudes equations for that model can be written in a compact form as

$$\Omega_{\mu_1} = \langle \mu_1 | \hat{\mathbf{H}} + [\hat{\mathbf{H}}, \mathrm{T}_2] | \Phi_0 \rangle \tag{2.10}$$

and

$$\Omega_{\mu_2} = \langle \mu_2 | \hat{\mathbf{H}} + [\hat{\mathbf{H}}, \mathrm{T}_2] + \frac{1}{2!} [[\hat{\mathbf{H}}, \mathrm{T}_2], \mathrm{T}_2] | \Phi_0 \rangle, \tag{2.11}$$

where the T_1-dressed (similarity transformed) Hamilton operator $\hat{\mathbf{H}}$ is defined as

$$\hat{\mathbf{H}} = \exp(-\mathrm{T}_1) \mathbf{H} \exp(\mathrm{T}_1). \tag{2.12}$$

For the singles amplitudes equation (2.10), the expansion series of $\exp(-\mathrm{T}_2)\hat{\mathbf{H}} \exp(\mathrm{T}_2)$ terminates after the second term, because the action of further products of T_2 can not be compensated by the Hamiltonian in order that only singly excited determinants remain on the bra side. In an analogous manner of reasoning the commutator

series in the doubles equation (2.11) terminates after the third term.
If the Hamiltonian is partitioned into a Fock operator $\mathbf{F}$ and a fluctuation potential operator $\mathbf{W}$, describing the difference between the real electron-electron repulsion and the Fock potential, the CC2 model [14] is obtained from CCSD by simplifying the doubles equation (2.11) as

$$\Omega_{\mu_2} = \langle \mu_2 | \hat{\mathbf{H}} + [\mathbf{F}, \mathrm{T}_2] | \Phi_0 \rangle. \tag{2.13}$$

In closed-shell cases the Fock operator is usually regarded to be of zeroth order ($\mathbf{F}^{[0]}$) in the fluctuation potential, $\mathbf{W}^{[1]}$, which it self is of first order. The fact that off-diagonal elements of the Fock operator for closed-shell molecules are zero, gives a leading contribution of the singles amplitudes of second order [24]. And only the first order doubles amplitudes contribute to the second order energy correction.
However, in open-shell cases off-diagonal Fock elements are not zero and thus partitioning the Hamiltonian as

$$\mathbf{H} = \mathbf{F}^{[0]} + \mathbf{F}^{[1]} + \mathbf{W}^{[1]} \tag{2.14}$$

leads to a contribution of the singles amplitudes in first order. $\mathbf{F}^{[0]}$ and $\mathbf{F}^{[1]}$ represent the diagonal and off-diagonal parts of the Fock operator, respectively. Nevertheless, in CC2 the singles are formally assumed to be of zeroth order to obtain a doubles equation (2.13) which is correct only to first order as in the closed-shell case [14]. Finally it is this form of the doubles equation which enables building the so-called "effective singles eigenvalue problem" which will be explained in detail in chapter 5.

2.2. T_1-dressed normal-ordered Hamiltonian with explicit spin

Before examination of the effect of T_1-dressing and normal-ordering on the Hamilton operator (2.5), it is given in its explicit spin form as

$$\begin{aligned}\mathbf{H} = &\sum_{p_\alpha q_\alpha} h_{p_\alpha q_\alpha} a^\dagger_{p_\alpha} a_{q_\alpha} + \sum_{p_\beta q_\beta} h_{p_\beta q_\beta} a^\dagger_{p_\beta} a_{q_\beta} \\ &+ \frac{1}{4} \sum_{p_\alpha q_\alpha r_\alpha s_\alpha} \langle p_\alpha q_\alpha || r_\alpha s_\alpha \rangle \, a^\dagger_{p_\alpha} a^\dagger_{q_\alpha} a_{s_\alpha} a_{r_\alpha} \\ &+ \frac{1}{4} \sum_{p_\beta q_\beta r_\beta s_\beta} \langle p_\beta q_\beta || r_\beta s_\beta \rangle \, a^\dagger_{p_\beta} a^\dagger_{q_\beta} a_{s_\beta} a_{r_\beta} \\ &+ \sum_{p_\alpha q_\beta r_\alpha s_\beta} \langle p_\alpha q_\beta | r_\alpha s_\beta \rangle \, a^\dagger_{p_\alpha} a^\dagger_{q_\beta} a_{s_\beta} a_{r_\alpha} \ . \end{aligned} \tag{2.15}$$

The one and two electron integrals entering the equation above have been introduced in the previous section in equations (2.6) and (2.7). The sole difference is that the spin of the orbitals is given explicitly for valid spin combinations in equation (2.15). One can express the singles cluster operator T_1 with explicit spin as

$$\mathrm{T}_1 = \sum_{i_\alpha a_\alpha} t^{i_\alpha}_{a_\alpha} a^\dagger_{a_\alpha} a_{i_\alpha} + \sum_{i_\beta a_\beta} t^{i_\beta}_{a_\beta} a^\dagger_{a_\beta} a_{i_\beta} \ . \tag{2.16}$$

Similarity transformation of equation (2.15) leads to the following expression

$$\begin{aligned}\hat{\mathbf{H}} = &\sum_{p_\alpha q_\alpha} h_{p_\alpha q_\alpha} \exp(-\mathrm{T}_1) a^\dagger_{p_\alpha} a_{q_\alpha} \exp(\mathrm{T}_1) + \sum_{p_\beta q_\beta} h_{p_\beta q_\beta} \exp(-\mathrm{T}_1) a^\dagger_{p_\beta} a_{q_\beta} \exp(\mathrm{T}_1) \\ &+ \frac{1}{4} \sum_{p_\alpha q_\alpha r_\alpha s_\alpha} \langle p_\alpha q_\alpha || r_\alpha s_\alpha \rangle \exp(-\mathrm{T}_1) a^\dagger_{p_\alpha} a^\dagger_{q_\alpha} a_{s_\alpha} a_{r_\alpha} \exp(\mathrm{T}_1) \\ &+ \frac{1}{4} \sum_{p_\beta q_\beta r_\beta s_\beta} \langle p_\beta q_\beta || r_\beta s_\beta \rangle \exp(-\mathrm{T}_1) a^\dagger_{p_\beta} a^\dagger_{q_\beta} a_{s_\beta} a_{r_\beta} \exp(\mathrm{T}_1) \\ &+ \sum_{p_\alpha q_\beta r_\alpha s_\beta} \langle p_\alpha q_\beta | r_\alpha s_\beta \rangle \exp(-\mathrm{T}_1) a^\dagger_{p_\alpha} a^\dagger_{q_\beta} a_{s_\beta} a_{r_\alpha} \exp(\mathrm{T}_1) \ . \end{aligned} \tag{2.17}$$

For the one-electron part with σ spin, ($\sigma = \alpha$ or β), one gets

$$\sum_{p_\sigma q_\sigma} h_{p_\sigma q_\sigma} \exp(-\mathrm{T}_1) a^\dagger_{p_\sigma} a_{q_\sigma} \exp(\mathrm{T}_1) =$$
$$= \sum_{p_\sigma q_\sigma} h_{p_\sigma q_\sigma} \exp(-\mathrm{T}_1) a^\dagger_{p_\sigma} \underbrace{\exp(\mathrm{T}_1)\exp(-\mathrm{T}_1)}_{=1} a_{q_\sigma} \exp(\mathrm{T}_1) \ . \tag{2.18}$$

Using the BCH expansion, like in equation (2.8), and applying the anticommutation relations

$$[a^\dagger_{p_\sigma}, a^\dagger_{q_\tau}]_+ = 0, \ [a_{p_\sigma}, a_{q_\tau}]_+ = 0, \ [a^\dagger_{p_\sigma}, a_{q_\tau}]_+ = \delta_{p_\sigma q_\tau}\delta_{\sigma\tau}, \tag{2.19}$$

for the creation and annihilation operators, one obtains

$$\hat{a}^\dagger_{p_\sigma} = \exp(-\mathrm{T}_1) a^\dagger_{p_\sigma} \exp(\mathrm{T}_1) = a^\dagger_{p_\sigma} - \sum_{i_\sigma a_\sigma} t^{i_\sigma}_{a_\sigma} a^\dagger_{a_\sigma} \delta_{p_\sigma i_\sigma} \tag{2.20}$$

and

$$\hat{a}_{q_\sigma} = \exp(-\mathrm{T}_1) a_{q_\sigma} \exp(\mathrm{T}_1) = a_{q_\sigma} + \sum_{i_\sigma a_\sigma} t^{i_\sigma}_{a_\sigma} a_{i_\sigma} \delta_{q_\sigma a_\sigma} \ . \tag{2.21}$$

One has to note that for a set of non-orthogonal orbitals the anticommutator between a creation and an annihilation operator becomes

$$[a^\dagger_{p_\sigma}, a_{q_\tau}]_+ = S_{p_\sigma q_\tau}\delta_{\sigma\tau} \tag{2.22}$$

where $S_{p_\sigma q_\tau}$ is the overlap integral between the spin orbitals p_σ and q_τ. But the use of a biorthogonal basis yields exactly the same relationships as given in equation (2.19) [25]. The matrices $\mathbf{X}^\sigma$ and $\mathbf{Y}^\sigma$,

$$\mathbf{X}^\sigma = \mathbf{1} - \mathbf{t_1}^\sigma \text{ with } [\mathbf{t_1}]_{\mathrm{p_\sigma q_\sigma}} = \{t^{q_\sigma}_{p_\sigma}, \text{ if } \mathrm{p}_\sigma \in \text{virt. \& } \mathrm{q}_\sigma \in \text{occ. else } 0$$
$$\mathbf{Y}^\sigma = \mathbf{1} + (\mathbf{t_1}^\sigma)^{\mathrm{T}} \ , \tag{2.23}$$

are introduced and have for an example with two occupied and two virtual spin orbitals the following structure.

$$\mathbf{X}^\sigma = \begin{array}{c} \\ i_\sigma \\ j_\sigma \\ a_\sigma \\ b_\sigma \end{array} \begin{array}{c} \begin{array}{cccc} i_\sigma & j_\sigma & a_\sigma & b_\sigma \end{array} \\ \begin{pmatrix} 1 & 0 & 0 & 0 \\ 0 & 1 & 0 & 0 \\ -t^{i_\sigma}_{a_\sigma} & -t^{j_\sigma}_{a_\sigma} & 1 & 0 \\ -t^{i_\sigma}_{b_\sigma} & -t^{j_\sigma}_{b_\sigma} & 0 & 1 \end{pmatrix} \end{array} ; \mathbf{Y}^\sigma = \begin{array}{c} \\ i_\sigma \\ j_\sigma \\ a_\sigma \\ b_\sigma \end{array} \begin{array}{c} \begin{array}{cccc} i_\sigma & j_\sigma & a_\sigma & b_\sigma \end{array} \\ \begin{pmatrix} 1 & 0 & t^{i_\sigma}_{a_\sigma} & t^{i_\sigma}_{b_\sigma} \\ 0 & 1 & t^{j_\sigma}_{a_\sigma} & t^{j_\sigma}_{b_\sigma} \\ 0 & 0 & 1 & 0 \\ 0 & 0 & 0 & 1 \end{pmatrix} \end{array} \tag{2.24}$$

σ can be either α or β. In case of using PAOs for the virtual space, each element of the occupied-virtual block of $\mathbf{Y}^\sigma$ has to be multiplied with the corresponding element of the PAO-overlap matrix. The similarity transformed creation and annihilation operators can be written as

$$\hat{a}^\dagger_{p_\sigma} = \sum_{r_\sigma} a^\dagger_{r_\sigma} [\mathbf{X}^\sigma]_{r_\sigma p_\sigma} = \sum_{r_\sigma} a^\dagger_{r_\sigma} X_{r_\sigma p_\sigma} \tag{2.25}$$

and

$$\hat{a}_{q_\sigma} = \sum_{s_\sigma} a_{s_\sigma} [\mathbf{Y}^\sigma]_{s_\sigma q_\sigma} = \sum_{s_\sigma} a_{s_\sigma} Y_{s_\sigma q_\sigma}. \tag{2.26}$$

From equations (2.20) and (2.21) as well as from the structure of $\mathbf{X}^\sigma$ and $\mathbf{Y}^\sigma$ one can immediately see that $\hat{a}^\dagger_{p_\sigma} = a^\dagger_{p_\sigma}$ if $p_\sigma \in$ virtual and $\hat{a}_{q_\sigma} = a_{q_\sigma}$ if $q_\sigma \in$ occupied space. If equations (2.25) and (2.26) are used, the one electron part of the dressed Hamiltonian in second quantized form can be written as

$$\begin{aligned} \sum_{p_\sigma q_\sigma} h_{p_\sigma q_\sigma} \hat{a}^\dagger_{p_\sigma} \hat{a}_{q_\sigma} &= \sum_{p_\sigma q_\sigma} h_{p_\sigma q_\sigma} \sum_{r_\sigma} a^\dagger_{r_\sigma} X_{r_\sigma p_\sigma} \sum_{s_\sigma} a_{s_\sigma} Y_{s_\sigma q_\sigma} \\ &\overset{\substack{r_\sigma \leftrightarrow p_\sigma \\ s_\sigma \leftrightarrow q_\sigma}}{=} \sum_{p_\sigma q_\sigma} \sum_{r_\sigma s_\sigma} X_{p_\sigma r_\sigma} h_{r_\sigma s_\sigma} Y_{q_\sigma s_\sigma} a^\dagger_{p_\sigma} a_{q_\sigma} \\ &= \sum_{p_\sigma q_\sigma} \hat{h}_{p_\sigma q_\sigma} a^\dagger_{p_\sigma} a_{q_\sigma} \ . \end{aligned} \tag{2.27}$$

It follows again from the structure of $\mathbf{X}^\sigma$ and $\mathbf{Y}^\sigma$ that $\hat{h}_{i_\sigma a_\sigma} = h_{i_\sigma a_\sigma}$ and that $\hat{h}_{p_\sigma q_\sigma} \neq \hat{h}_{q_\sigma p_\sigma}$. Analogously the $\alpha\alpha$ and the $\beta\beta$ two-electron part of the Hamiltonian can be formulated as

$$\begin{aligned}
&\frac{1}{4}\sum_{p_\sigma q_\sigma r_\sigma s_\sigma} \langle p_\sigma q_\sigma || r_\sigma s_\sigma \rangle \, \hat{a}^\dagger_{p_\sigma} \hat{a}^\dagger_{q_\sigma} \hat{a}_{s_\sigma} \hat{a}_{r_\sigma} \\
=&\frac{1}{4}\sum_{p_\sigma q_\sigma r_\sigma s_\sigma} \langle p_\sigma q_\sigma || r_\sigma s_\sigma \rangle \sum_{t_\sigma} a^\dagger_{t_\sigma} X_{t_\sigma p_\sigma} \sum_{u_\sigma} a^\dagger_{u_\sigma} X_{u_\sigma q_\sigma} \sum_{v_\sigma} a_{v_\sigma} Y_{v_\sigma s_\sigma} \sum_{w_\sigma} a_{w_\sigma} Y_{w_\sigma r_\sigma} \\
=&\frac{1}{4}\sum_{p_\sigma q_\sigma r_\sigma s_\sigma} \sum_{t_\sigma u_\sigma v_\sigma w_\sigma} \langle t_\sigma u_\sigma || w_\sigma v_\sigma \rangle \, X_{p_\sigma t_\sigma} X_{q_\sigma u_\sigma} Y_{s_\sigma v_\sigma} Y_{r_\sigma w_\sigma} a^\dagger_{p_\sigma} a^\dagger_{q_\sigma} a_{s_\sigma} a_{r_\sigma} \\
=&\frac{1}{4}\sum_{p_\sigma q_\sigma r_\sigma s_\sigma} \langle p_\sigma q_\sigma \hat{||} r_\sigma s_\sigma \rangle \, a^\dagger_{p_\sigma} a^\dagger_{q_\sigma} a_{s_\sigma} a_{r_\sigma}
\end{aligned} \tag{2.28}$$

The dressed two-electron integrals $\langle p_\sigma q_\sigma \hat{||} r_\sigma s_\sigma \rangle = \langle p_\sigma q_\sigma \hat{|} r_\sigma s_\sigma \rangle - \langle p_\sigma q_\sigma \hat{|} s_\sigma r_\sigma \rangle$ have only the permutational symmetry of the electrons, i. e. $\langle p_\sigma q_\sigma \hat{|} r_\sigma s_\sigma \rangle = \langle q_\sigma p_\sigma \hat{|} s_\sigma r_\sigma \rangle$. Applying the same strategy for expressing the $\alpha\beta$ part of the two-electron part and putting together the remaining parts after dressing, leads to the following equation for the dressed Hamilton operator with explicit spin.

$$\begin{aligned}
\hat{\mathbf{H}} = &\sum_{p_\alpha q_\alpha} \hat{h}_{p_\alpha q_\alpha} a^\dagger_{p_\alpha} a_{q_\alpha} + \frac{1}{4}\sum_{p_\alpha q_\alpha r_\alpha s_\alpha} \langle p_\alpha q_\alpha \hat{||} r_\alpha s_\alpha \rangle \, a^\dagger_{p_\alpha} a^\dagger_{q_\alpha} a_{s_\alpha} a_{r_\alpha} \\
&+ \sum_{p_\beta q_\beta} \hat{h}_{p_\beta q_\beta} a^\dagger_{p_\beta} a_{q_\beta} + \frac{1}{4}\sum_{p_\beta q_\beta r_\beta s_\beta} \langle p_\beta q_\beta \hat{||} r_\beta s_\beta \rangle \, a^\dagger_{p_\beta} a^\dagger_{q_\beta} a_{s_\beta} a_{r_\beta} \\
&+ \sum_{p_\alpha q_\beta r_\alpha s_\beta} \langle p_\alpha q_\beta \hat{|} r_\alpha s_\beta \rangle \, a^\dagger_{p_\alpha} a^\dagger_{q_\beta} a_{s_\beta} a_{r_\alpha}
\end{aligned} \tag{2.29}$$

In the final analysis it can be clearly seen that the effect of dressing is carried over to the integrals and the creation and annihilation operators are retained in their undressed form. Hence the normal-ordering of the dressed Hamiltonian can be performed in exactly the same way as for the undressed operator.

A normal-ordered string of operators is one in which all annihilation operators stand

to the right of the creation operators. This can be achieved by using the anticommutation relations (2.19).

A more convenient way to normal-order any string of creation and annihilation operators is the application of Wick's theorem which states that every string can be normal-ordered by writing it as linear combinations of pairwise contractions of operators, i.e.

$$\begin{aligned} ABC\dots IJK =& \{ABC\dots IJK\}_{\mathrm{v}} + \sum_{s} \{\overbrace{AB}C\dots IJK\}_{\mathrm{v}} \\ &+ \sum_{d} \{\overbrace{\overbrace{AB}C\dots I}JK\}_{\mathrm{v}} + \dots \end{aligned} \tag{2.30}$$

The first term in the equation above denotes the totally normal-ordered string with respect to the true vacuum state (v). The first sum is over all possible single pair contractions and the second one over all possible double pair contractions.

The generalised Wicks theorem states that products of normal-ordered operator strings can be normal-ordered by writing the complete string as a sum of the normal-ordered string and the pairwise contractions between operators of the involved normal-ordered strings and no contractions within a normal-ordered string itself.

$$\begin{aligned} \{ABCD\dots\}_{\mathrm{v}}\{IJKL\dots\}_{\mathrm{v}} =& \{ABCD\dots IJKL\dots\}_{\mathrm{v}} + \sum_{s} \{\overbrace{ABCD\dots I}JKL\dots\} \\ &+ \sum_{d} \{\overbrace{\overbrace{ABCD\dots I}JKL\dots}\} + \dots \end{aligned} \tag{2.31}$$

A contraction between two operators is defined as the pair it self minus the normal-ordered form of the pair.

$$\overbrace{AB} = AB - \{AB\}_{\mathrm{v}} \tag{2.32}$$

For each permutation of two operators one has to multiply the operator string with -1. If one examines the four possible pairs of creation and annihilation operators

(same spin) for a contraction, one gets

$$\overbrace{a_{p_\sigma} a^\dagger_{q_\sigma}} = a_{p_\sigma} a^\dagger_{q_\sigma} - \{a_{p_\sigma} a^\dagger_{q_\sigma}\}_{\mathrm{v}} = a_{p_\sigma} a^\dagger_{q_\sigma} + a^\dagger_{q_\sigma} a_{p_\sigma} = \delta_{p_\sigma q_\sigma} \tag{2.33}$$

as the only nonzero combination.

As any matrix element $\langle\psi_2|\mathbf{O}|\psi_1\rangle$ can be written as $\langle|(A_2)^\dagger \mathbf{O} A_1|\rangle$ with $|\psi_1\rangle = A_1\,|\rangle$ and $|\psi_2\rangle = A_2\,|\rangle$, where $|\rangle$ is the true vacuum state, only fully contracted terms of the string $(A_2)^\dagger \mathbf{O} A_1$ give nonzero results.

However, it is more convenient to work with a slater determinant (SD) as a reference state, (also called the Fermi vacuum) than the true vacuum state. For the use of a SD as a reference state a so-called particle hole formalism has to be introduced and creation and annihilation operators with respect to this reference state have to be defined. The quasi-particle creation operators are

$$a_{i_\sigma} \text{ and } a^\dagger_{a_\sigma}\ , \tag{2.34}$$

because a_{i_σ} working on a SD creates a hole (the spin orbital i_σ is occupied) and $a^\dagger_{a_\sigma}$ creates a particle. And the quasi-particle annihilation operators are

$$a^\dagger_{i_\sigma} \text{ and } a_{a_\sigma}\ , \tag{2.35}$$

because they annihilate possible holes and particles.

With the quasi-particle operators a normal-ordered string is one, in which all quasi-particle annihilation operators stand to the right of the quasi-particle creation operators. When all eight possible combinations of quasi-particle creation and annihilation operators (same spin) are examined, the only two pairs giving a nonzero result after performing the contraction are

$$\overbrace{a_{a_\sigma} a^\dagger_{b_\sigma}} = a_{a_\sigma} a^\dagger_{b_\sigma} - \{a_{a_\sigma} a^\dagger_{b_\sigma}\} = a_{a_\sigma} a^\dagger_{b_\sigma} + a^\dagger_{b_\sigma} a_{a_\sigma} = \delta_{a_\sigma b_\sigma} \tag{2.36}$$

and

$$\overbrace{a^\dagger_{i_\sigma} a_{j_\sigma}} = a^\dagger_{i_\sigma} a_{j_\sigma} - \{a^\dagger_{i_\sigma} a_{j_\sigma}\} = a^\dagger_{i_\sigma} a_{j_\sigma} + a_{j_\sigma} a^\dagger_{i_\sigma} = \delta_{i_\sigma j_\sigma}\ . \tag{2.37}$$

Now it is straight forward to get the normal-order of the dressed Hamilton operator (2.29) with respect to the Fermi vacuum. The one-electron part for example can be normal-ordered as

$$\begin{aligned}\sum_{p_\sigma q_\sigma} \hat{h}_{p_\sigma q_\sigma} a^\dagger_{p_\sigma} a_{q_\sigma} &= \sum_{p_\sigma q_\sigma} \hat{h}_{p_\sigma q_\sigma} \{a^\dagger_{p_\sigma} a_{q_\sigma}\} + \sum_{p_\sigma q_\sigma} \hat{h}_{p_\sigma q_\sigma} \{\overbrace{a^\dagger_{p_\sigma} a_{q_\sigma}}\} \\ &= \sum_{p_\sigma q_\sigma} \hat{h}_{p_\sigma q_\sigma} \{a^\dagger_{p_\sigma} a_{q_\sigma}\} + \sum_{p_\sigma q_\sigma} \hat{h}_{p_\sigma q_\sigma} \delta_{p_\sigma q_\sigma} \delta_{p_\sigma \in i_\sigma} \\ &= \sum_{p_\sigma q_\sigma} \hat{h}_{p_\sigma q_\sigma} \{a^\dagger_{p_\sigma} a_{q_\sigma}\} + \sum_{i_\sigma} \hat{h}_{i_\sigma i_\sigma} \ . \end{aligned} \tag{2.38}$$

Wicks theorem (2.30) and the contraction of equation (2.37) have been used. Normal-ordering of the remaining parts of the dressed Hamilton operator and considering the particle permutational symmetry of the dressed two-electron integrals leads to

$$\begin{aligned}\hat{\mathbf{H}} =& \sum_{p_\alpha q_\alpha} \big[\hat{h}_{p_\alpha q_\alpha} + \sum_{i_\alpha} \langle i_\alpha p_\alpha \hat{||} i_\alpha q_\alpha\rangle + \sum_{i_\beta} \langle i_\beta p_\alpha \hat{|} i_\beta q_\alpha\rangle \big] \{a^\dagger_{p_\alpha} a_{q_\alpha}\} \\ &+ \sum_{p_\beta q_\beta} \big[\hat{h}_{p_\beta q_\beta} + \sum_{i_\beta} \langle i_\beta p_\beta \hat{||} i_\beta q_\beta\rangle + \sum_{i_\alpha} \langle i_\alpha p_\beta \hat{|} i_\alpha q_\beta\rangle \big] \{a^\dagger_{p_\beta} a_{q_\beta}\} \\ &+ \frac{1}{4} \sum_{p_\alpha q_\alpha r_\alpha s_\alpha} \langle p_\alpha q_\alpha \hat{||} r_\alpha s_\alpha\rangle \{a^\dagger_{p_\alpha} a^\dagger_{q_\alpha} a_{s_\alpha} a_{r_\alpha}\} \\ &+ \frac{1}{4} \sum_{p_\beta q_\beta r_\beta s_\beta} \langle p_\beta q_\beta \hat{||} r_\beta s_\beta\rangle \{a^\dagger_{p_\beta} a^\dagger_{q_\beta} a_{s_\beta} a_{r_\beta}\} \\ &+ \sum_{p_\alpha q_\beta r_\alpha s_\beta} \langle p_\alpha q_\beta \hat{|} r_\alpha s_\beta\rangle \{a^\dagger_{p_\alpha} a^\dagger_{q_\beta} a_{s_\beta} a_{r_\alpha}\} \\ &+ \sum_{i_\alpha} \hat{h}_{i_\alpha i_\alpha} + \frac{1}{2} \sum_{i_\alpha j_\alpha} \langle i_\alpha j_\alpha \hat{||} i_\alpha j_\alpha\rangle + \sum_{i_\beta} \hat{h}_{i_\beta i_\beta} + \frac{1}{2} \sum_{i_\beta j_\beta} \langle i_\beta j_\beta \hat{||} i_\beta j_\beta\rangle + \sum_{i_\alpha j_\beta} \langle i_\alpha j_\beta \hat{|} i_\alpha j_\beta\rangle \\ =& \hat{\mathrm{F}}^\alpha_{\mathrm{N}} + \hat{\mathrm{F}}^\beta_{\mathrm{N}} + \hat{\mathrm{V}}^{\alpha\alpha}_{\mathrm{N}} + \hat{\mathrm{V}}^{\beta\beta}_{\mathrm{N}} + \hat{\mathrm{V}}^{\alpha\beta}_{\mathrm{N}} + \langle\Phi_0|\hat{\mathbf{H}}|\Phi_0\rangle \\ =& \hat{\mathbf{H}}_{\mathrm{N}} + \langle\Phi_0|\hat{\mathbf{H}}|\Phi_0\rangle \ . \end{aligned} \tag{2.39}$$

The normal-ordering of the non similarity transformed Hamiltonian has been demonstrated in detail in reference [26]. The general statement that the normal-order of an operator is the same as the operator itself minus its expectation value holds also

in the case of the dressed Hamiltonian.

$$\hat{\mathbf{H}}_{\mathrm{N}} = \hat{\mathrm{F}}_{\mathrm{N}}^{\alpha} + \hat{\mathrm{F}}_{\mathrm{N}}^{\beta} + \hat{\mathrm{V}}_{\mathrm{N}}^{\alpha\alpha} + \hat{\mathrm{V}}_{\mathrm{N}}^{\beta\beta} + \hat{\mathrm{V}}_{\mathrm{N}}^{\alpha\beta} \tag{2.40}$$

The CC2 singles (2.10) and doubles (2.13) amplitudes equations remain unchanged wether one uses the non normal-ordered or the normal-ordered dressed Hamilton operator, as will be shown later. But it is much easier to work with the already normal-ordered strings of the dressed Hamiltonian when analyzing any matrix elements.

However, looking at the energy equation of CC2,

$$\begin{aligned} E_{\mathrm{CC2}} &= \langle\Phi_0|\exp(-\mathrm{T}_2)\hat{\mathbf{H}}\exp(\mathrm{T}_2)|\Phi_0\rangle \\ &= \langle\Phi_0|\exp(-\mathrm{T}_2)(\hat{\mathbf{H}}_{\mathrm{N}} + \langle\Phi_0|\hat{\mathbf{H}}|\Phi_0\rangle)\exp(\mathrm{T}_2)|\Phi_0\rangle \\ &= \langle\Phi_0|\exp(-\mathrm{T}_2)\hat{\mathbf{H}}_{\mathrm{N}}\exp(\mathrm{T}_2)|\Phi_0\rangle + \langle\Phi_0|\hat{\mathbf{H}}|\Phi_0\rangle\ , \end{aligned} \tag{2.41}$$

one can conclude that the expression

$$\langle\Phi_0|\exp(-\mathrm{T}_2)\hat{\mathbf{H}}_{\mathrm{N}}\exp(\mathrm{T}_2)|\Phi_0\rangle = E_{\mathrm{CC2}} - \langle\Phi_0|\hat{\mathbf{H}}|\Phi_0\rangle \tag{2.42}$$

represents a sort of correlation energy. But one has to be careful, because $\langle\Phi_0|\hat{\mathbf{H}}|\Phi_0\rangle$ is not the Hartree-Fock energy $\langle\Phi_0|\mathbf{H}|\Phi_0\rangle$. That is the reason why the CC2 correlation energy is calculated using the non-dressed normal-ordered Hamilton operator $\mathbf{H}_{\mathrm{N}}$ instead of $\hat{\mathbf{H}}_{\mathrm{N}}$.

2.3. Construction and evaluation of Coupled Cluster diagrams

Using Wicks theorem as introduced in equations (2.30) and (2.31), it is straight forward to derive working equations from the CC2 amplitudes equations (2.10) and

(2.13). But this is a rather tedious way compared to the diagrammatic technique. In reference [26] the rules for construction and evaluation of Coupled Cluster diagrams have been shown for the case of orthogonal spin orbitals. Here the construction and evaluation of diagrams within the use of the T1-dressed normal-ordered Hamiltonian (2.40) and the non-orthogonal PAOs will be discussed.

For the construction of CC diagrams the quasi particle-hole formalism and the corresponding quasi creation and annihilation operators as introduced in section 2.2 are needed. A so-called hole line is one directed downward and symbolizes an occupied orbital in the reference determinant. The particle line is directed upward and symbolizes a virtual orbital.

The Hamilton operator fragments are described by horizontal lines which are dashed. $\hat{\mathrm{F}}^{\sigma}_{\mathrm{N}}$ is an one-electron operator an thus has one vertice on which creation and annihilation operators can act.

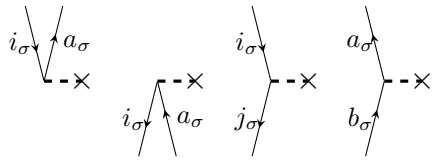

Figure 2.1.: $\hat{\mathrm{F}}^{\sigma}_{\mathrm{N}}$ fragments with excitation levels $+1$, -1, 0 and 0 (from left to right)

In figure 2.1 the four possible $\hat{\mathrm{F}}^{\sigma}_{\mathrm{N}}$ fragments are shown, where σ can be either α or β. This yields in total eight diagrams. In the most left fragment two quasi creation operators are symbolized by two lines above the horizontal operator line (also called interaction line). The excitation level is calculated by subtracting the number of quasi particle lines under the interaction line (annihilation operator lines) from the quasi particle lines above it (creation operator lines) and dividing the result by two. One gets, e.g. for the most right fragment of figure 2.1 an excitation level of $\frac{(1-1)}{2} = 0$. Also the non-dressed Fock operator which appears in the CC2 doubles equation (2.13) will be represented by the same diagrams. It will be clear from

the context if it is a dressed or a non-dressed fragment of the Hamiltonian. A line pointing toward a vertice is called incoming line and when pointing away it is called outgoing line. Both lines on a vertice have to correspond to the same spin.
For the two-electron operator $\hat{\mathrm{V}}_{\mathrm{N}}^{\sigma\sigma}$ or $\hat{\mathrm{V}}_{\mathrm{N}}^{\sigma\tau}$ (with $\sigma = \alpha$ and $\tau = \beta$ or vice versa) there are two vertices and correspondingly two incoming and two outgoing lines. Diagrams for a $\hat{\mathrm{V}}_{\mathrm{N}}^{\sigma\sigma}$ and $\hat{\mathrm{V}}_{\mathrm{N}}^{\sigma\tau}$ fragment with an excitation level of +2 and +1, respectively, are shown in figure 2.2.

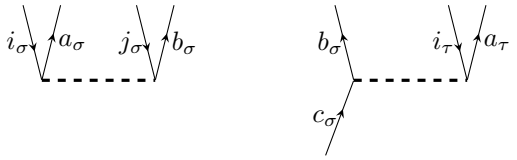

Figure 2.2.: $\hat{\mathrm{V}}_{\mathrm{N}}^{\sigma\sigma}$ and $\hat{\mathrm{V}}_{\mathrm{N}}^{\sigma\tau}$ fragments with excitation levels +2 and +1

The amplitudes of the cluster operators are illustrated by solid horizontal lines. As the cluster operators contain only quasi creation operators, they are already normal-ordered with respect to Fermi vacuum. The α or β singles cluster operator $\mathrm{T}_1^\sigma = \sum_{i_\sigma a_\sigma} t_{a_\sigma}^{i_\sigma} \{a_{a_\sigma}^\dagger a_{i_\sigma}\}$ corresponds to an excitation level of +1 and is represented as shown in figure 2.3.

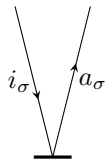

Figure 2.3.: Diagrammatic representation of T_1^σ

Doubles cluster operators,

$$\mathrm{T}_2^{\sigma\sigma} = \frac{1}{4} \sum_{i_\sigma a_\sigma j_\sigma b_\sigma} t_{a_\sigma b_\sigma}^{i_\sigma j_\sigma} \{a_{a_\sigma}^\dagger a_{b_\sigma}^\dagger a_{j_\sigma} a_{i_\sigma}\}$$

or

$$\mathrm{T}_2^{\sigma\tau} = \sum_{i_\sigma a_\sigma j_\tau b_\tau} t_{a_\sigma b_\tau}^{i_\sigma j_\tau} \{a_{a_\sigma}^\dagger a_{b_\tau}^\dagger a_{j_\tau} a_{i_\sigma}\}$$

where σ and τ can be either α or β, correspond to an excitation level of +2. $\mathrm{T}_2^{\sigma\tau}$ is diagrammatically represented as drawn in figure 2.4.

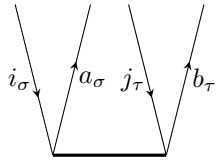

Figure 2.4.: Diagrammatic representation of $\mathrm{T}_2^{\sigma\tau}$

Having these elements at hand, one can draw diagrams corresponding to matrix elements in a simple way. For example the matrix element $\langle \Phi_{i_\sigma}^{a_\sigma} | \hat{\mathrm{F}}_{\mathrm{N}}^{\sigma} | \Phi_0 \rangle$ is represented by the diagram in figure 2.5.

Figure 2.5.: Diagrammatic representation of $\langle \Phi_{i_\sigma}^{a_\sigma} | \hat{\mathrm{F}}_{\mathrm{N}}^{\sigma} | \Phi_0 \rangle$

The reference determinant is represented by the empty space under the horizontal line corresponding to $\hat{\mathrm{F}}_{\mathrm{N}}^{\sigma}$ and the singly excited determinant $\langle \Phi_{i_\sigma}^{a_\sigma} |$ by the two external lines. So on the top of the diagram is the bra-side and on the bottom the ket-side of the matrix element. In between are the fragments of the Hamilton operator. In figure 2.5 one has to use the $\hat{\mathrm{F}}_{\mathrm{N}}^{\sigma}$ fragment with the excitation level +1 to match the excitation level on the bra-side. The agreement of the excitation level of the bra-side

and the parts of the Hamiltonian working on the ket-side has to be fulfilled when representing matrix elements by CC diagrams.
As a further example the diagram for the matrix element $\langle\Phi_0|(\hat{\mathrm{V}}_{\mathrm{N}}^{\sigma\sigma}\mathrm{T}_2^{\sigma\sigma})_{\mathrm{c}}|\Phi_0\rangle$ is shown in figure 2.6. There one has only internal lines, i.e. lines which start and end at

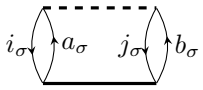

Figure 2.6.: Diagrammatic representation of $\langle\Phi_0|(\hat{\mathrm{V}}_{\mathrm{N}}^{\sigma\sigma}\mathrm{T}_2^{\sigma\sigma})_{\mathrm{c}}|\Phi_0\rangle$

operator interaction lines. No external lines like in figure 2.5 occur, because the overall excitation level of the diagram is zero.
The subscript c indicates that the cluster operators standing to the right of the Hamilton operator fragment have to be connected at least once to it. This result is obtained when carrying out Wicks theorem on the commutators introduced by the Baker-Campbell-Hausdorff expansion of the T1-dressed and normal-ordered Hamiltonian of equation (2.40).
The evaluation of CC diagrams is carried out according to the following rules.

- The sign is calculated as $(-1)^{l+h}$, with l and h as abbreviations for loops and hole lines in a diagram.
- Each pair of equivalent lines, which start and end at the same operator interaction line and have the same spin, like (i_σ, j_σ) or (a_σ, b_σ) in figure 2.6, yields a prefactor of $\frac{1}{2}$.
- A summation is carried over each index of an internal line.
- The Fock operator fragment, e.g. $\hat{\mathrm{F}}_{\mathrm{N}}^{\sigma}$, contributes an integral $\langle\mathrm{out}|\hat{f}|\mathrm{in}\rangle$, where "out" is the outgoing and "in" the incoming line on the vertice of the operator. And a cluster operator interaction line contributes the corresponding ampli-

tude to the expression, e.g. $t^{i_\sigma j_\sigma}_{a_\sigma b_\sigma}$ from the diagram in figure 2.6. The indexes are taken first from the left and then from the right vertice of the amplitude.

- The two-electron operator $\hat{\mathrm{V}}^{\sigma\sigma}_{\mathrm{N}}$ contributes a dressed integral of the form $\langle$l-out r-out$\hat{|}|$l-in r-in$\rangle$, where l and r mean the left and right vertice of the operator. But $\hat{\mathrm{V}}^{\sigma\tau}_{\mathrm{N}}$, with $\sigma = \alpha$ and $\tau = \beta$ or vice versa, contributes the integral $\langle$l-out r-out$\hat{|}$l-in r-in$\rangle$. Whereas in chemist notation the corresponding integrals would be (l-out l-in$\hat{|}$r-out r-in) $-$ (l-out r-in$\hat{|}$r-out l-in) for $\hat{\mathrm{V}}^{\sigma\sigma}_{\mathrm{N}}$ and (l-out l-in$\hat{|}$r-out r-in) for $\hat{\mathrm{V}}^{\sigma\tau}_{\mathrm{N}}$.

- If a diagram contains n equivalent vertices, the algebraic expression is multiplied by a factor of $\frac{1}{n!}$. For example the diagrammatic representation of the matrix element $\langle\Phi_0|(\mathrm{V}^{\alpha\alpha}_{\mathrm{N}}\mathrm{T}^{\alpha}_{1}\mathrm{T}^{\alpha}_{1})_{\mathrm{c}}|\Phi_0\rangle$, which appears in the CC2 energy equation, contains two equivalent vertices (figure 2.7), because both T^{α}_{1} fragments are connected the same way to $\mathrm{V}^{\alpha\alpha}_{\mathrm{N}}$ and both vertices have incoming and outgoing lines of the same spin. According to this rule the representation of the matrix element $\langle\Phi_0|(\mathrm{V}^{\alpha\beta}_{\mathrm{N}}\mathrm{T}^{\alpha}_{1}\mathrm{T}^{\beta}_{1})_{\mathrm{c}}|\Phi_0\rangle$ does not contain equivalent vertices.

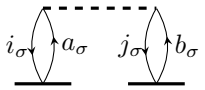

Figure 2.7.: Diagrammatic representation of $\langle\Phi_0|(\mathrm{V}^{\alpha\alpha}_{\mathrm{N}}\mathrm{T}^{\alpha}_{1}\mathrm{T}^{\alpha}_{1})_{\mathrm{c}}|\Phi_0\rangle$

- For each external outgoing line of an amplitude vertice, i.e. the line is not connected to a fragment of the Hamilton operator, the corresponding amplitude has to be multiplied by the PAO overlap matrix. This rule has to be applied for example when evaluating the matrix element $\langle\Phi^{a_\sigma}_{i_\sigma}|(\hat{\mathrm{F}}^{\sigma}_{\mathrm{N}}\mathrm{T}^{\sigma\sigma}_{2})_{\mathrm{c}}|\Phi_0\rangle$. One possible corresponding diagrammatic representation is shown in figure 2.8.

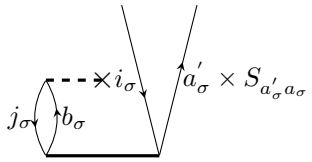

Figure 2.8.: One possible diagrammatic representation of $\langle \Phi_{i_\sigma}^{a_\sigma} | (\hat{\mathrm{F}}_{\mathrm{N}}^{\sigma} \mathrm{T}_2^{\sigma\sigma})_{\mathrm{c}} | \Phi_0 \rangle$.

- Each pair of unique external hole or particle lines with the same spin, i.e. external lines which originate from different operator interaction lines or end on different ones, yields a permutation operator. If i_σ and j_σ represent the unique external lines, the permutation operator would act on a corresponding function as $P(i_\sigma, j_\sigma) f(i_\sigma, j_\sigma) = f(i_\sigma, j_\sigma) - f(j_\sigma, i_\sigma)$. A diagram that contains unique external lines is shown in figure 2.9.

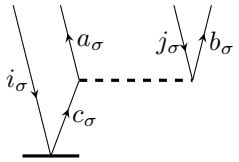

Figure 2.9.: A diagram containing the unique external lines i_σ and j_σ

These rules are applied to the diagram shown in figure 2.6. This yields

$$\langle \Phi_0 | (\hat{\mathrm{V}}_{\mathrm{N}}^{\sigma\sigma} \mathrm{T}_2^{\sigma\sigma})_{\mathrm{c}} | \Phi_0 \rangle = \frac{1}{4} \sum_{i_\sigma j_\sigma a_\sigma b_\sigma} t_{a_\sigma b_\sigma}^{i_\sigma j_\sigma} \, \langle i_\sigma j_\sigma | \hat{|} | a_\sigma b_\sigma \rangle \ .$$

2.4. Response theory

Examination of the response of a system to external perturbations gives information about its properties. Is the perturbation time independent, the static properties of the system can be studied. When the considered system is opposed to some time dependent perturbations, the dynamic properties can be examined. The Hamilton operator acting on the wave function of the system has to be modified according to the perturbation.

In case of a time independent perturbation, e.g. a static electric field, within a variational theory, response functions can be identified from a taylor expansion of the expectation value of the space operator entering the perturbation. But it is also possible to get the response functions as derivatives of the quantum mechanical energy expression with respect to the electric field parameters. This is also known as the Hellmann-Feynman theorem,

$$\frac{\mathrm{d}\,\langle\Phi_0|\mathbf{H}_0|\Phi_0\rangle}{\mathrm{d}\epsilon_X} = \left\langle \Phi_0 \left| \frac{\partial \mathbf{H}_0}{\partial \epsilon_X} \right| \Phi_0 \right\rangle \ , \tag{2.43}$$

which is a consequence of the variational principle.
As in this work the interest is for excitation energies, the time dependent Schrödinger equation has to be considered.

$$\mathbf{H}(t)\,|\Psi(t)\rangle = i\frac{\partial\,|\Psi(t)\rangle}{\partial t} \tag{2.44}$$

The time dependent Hamiltonian is a sum of the time independent part $\mathbf{H}_0$ and a time dependent perturbation $\mathrm{V}(t)$ ($\hbar$ is set to 1). The time dependent wave function is given as

$$|\Psi(t)\rangle = \exp(-iF(t))\,|\tilde{\Psi}(t)\rangle\,. \tag{2.45}$$

If the Hamiltonian itself would be time independent, the wave function would be time dependent only through the phase factor $\exp(-iE_0t)$. Inserting equation (2.45) into equation (2.44) leads to

$$\mathbf{H}(t)\exp(-iF(t))\,|\tilde{\Psi}(t)\rangle = \dot{F}(t)\exp(-iF(t))\,|\tilde{\Psi}(t)\rangle + i\exp(-iF(t))\,|\frac{\partial\tilde{\Psi}(t)}{\partial t}\rangle \ . \tag{2.46}$$

Dividing by the phase factor and projecting onto $\langle\tilde{\Psi}(t)|$ yields

$$Q(t) = \dot{F}(t) = \left\langle \tilde{\Psi}(t) \left| \mathbf{H}(t) - i\frac{\partial}{\partial t} \right| \tilde{\Psi}(t) \right\rangle . \tag{2.47}$$

The so-called quasienergy $Q(t)$ reduces to the ordinary energy E_0 in case of a time independent wave function. Taking the derivative of the quasienergy in analogy to equation (2.43) gives

$$\frac{\mathrm{d}Q(t)}{\mathrm{d}\epsilon_X(\omega)} = \left\langle \tilde{\Psi}(t) \left| \frac{\partial \mathbf{H}(t)}{\partial \epsilon_X(\omega)} \right| \tilde{\Psi}(t) \right\rangle - i\frac{\partial}{\partial t} \left\langle \tilde{\Psi}(t) \left| \frac{\partial \tilde{\Psi}(t)}{\partial \epsilon_X(\omega)} \right\rangle \right. . \tag{2.48}$$

In contrast to the time independent Hellman-Feynman theorem, equation (2.48) contains an additional term with a time derivative. The time average of a time differentiated periodic function is defined as

$$\left\{ \frac{\partial f(t)}{\partial t} \right\}_T = \frac{1}{T} \int_{-\frac{T}{2}}^{\frac{T}{2}} \frac{\partial f(t)}{\partial t} dt \ . \tag{2.49}$$

By taking the time average of equation (2.48), the second term on the right hand side vanishes. This has been been shown in detail for the derivatives of the quasienergy in reference [27]. There the time dependent perturbation $\mathrm{V}(t)$ and the perturbed wave functions to all orders are described as Fourier series. With

$$\mathrm{V}(t) = \sum_{k=-N}^{N} \exp(-i\omega_k t) \sum_X \epsilon_X(\omega_k) X, \tag{2.50}$$

the time average of equation (2.48) becomes

$$\frac{d\{Q(t)\}_T}{d\epsilon_X(\omega)} = \left\{ \left\langle \tilde{\Psi}(t) \left| X \right| \tilde{\Psi}(t) \right\rangle \exp(-i\omega t) \right\}_T . \tag{2.51}$$

Finally response functions are identified using equation (2.51). The linear response function becomes

$$\langle\langle X; Y \rangle\rangle_{\omega_{k_1}} = \frac{d^2\{Q(t)\}_T}{d\epsilon_X(\omega_0) d\epsilon_Y(\omega_{k_1})} \ , \ \omega_0 = -\omega_{k_1} \ . \tag{2.52}$$

For nonvariational theories as Coupled Cluster, a Lagrangian technique is used. The Lagrange functional can be written in general as

$$L\Big(c(t), \dot{c}(t), \lambda(t)\Big) = Q\Big(c(t), \dot{c}(t)\Big) + \lambda(t) e\Big(c(t), \dot{c}(t)\Big) \ , \tag{2.53}$$

with $c(t)$ as wave function parameters and $\lambda(t)$ as multipliers. The time averaged Lagrangian takes over the role of $\{Q(t)\}_T$, i.e. the response functions are identified as derivatives of the time-averaged Lagrange functional. The Lagrangian of all orders higher than zero are also expanded as Fourier series. For example the first and second order Lagrangian (order with respect to time) can be written as

$$\begin{aligned} L^{(1)}(t) &= \sum_{k_1=-N}^{N} \exp(-i\omega_{k_1}t) L^{(1)}(\omega_{k_1}) = \sum_{k_1} \exp(-i\omega_{k_1}t) \sum_{X} \epsilon_X(\omega_{k_1}) L^X(\omega_{k_1}) \\ L^{(2)}(t) &= \frac{1}{2} \sum_{k_1,k_2} \exp(-i(\omega_{k_1}+\omega_{k_2})t) \sum_{XY} \epsilon_X(\omega_{k_1}) \epsilon_Y(\omega_{k_2}) L^{XY}(\omega_{k_1},\omega_{k_2}) \ . \end{aligned} \tag{2.54}$$

When the variational conditions are fulfilled, the Fourier components become the response functions. The Lagrangian for a Coupled Cluster model can be written in general as

$$\begin{aligned} L(t) = &\langle \Phi_0 \,|\, \mathbf{H}(t) \exp(T(t)) \,|\, \Phi_0 \rangle \\ &+ \sum_{i,\mu_i} \lambda_{\mu_i}(t) \left\langle \mu_i \middle| \exp\left(-T(t)\right) \Big(\mathbf{H}(t) - i\frac{\partial}{\partial t} \Big) \exp(T(t)) \middle| \Phi_0 \right\rangle . \end{aligned} \tag{2.55}$$

The time dependent Lagrange multipliers $\lambda_{\mu_i}(t)$ and Coupled Cluster amplitudes $t_{\mu_i}(t)$ are also described in terms of Fourier series to all orders higher than zero [27]. The Lagrangian for the CC2 or UCC2 model, without explicit writing of the spin dependence, is defined as

$$\begin{aligned} L_{UCC2}(t) = &\langle \Phi_0 \,|\, \mathbf{H}(t) \exp(T_1(t) + T_2(t)) \,|\, \Phi_0 \rangle \\ &+ \sum_{\mu_1} \lambda_{\mu_1} \Big(\left\langle \mu_1 \middle| \hat{\mathbf{H}}(t) + [\hat{\mathbf{H}}(t), T_2(t)] \middle| \Phi_0 \right\rangle - i\frac{\partial t_{\mu_1}}{\partial t} \Big) \\ &+ \sum_{\mu_2} \lambda_{\mu_2} \Big(\left\langle \mu_2 \middle| \hat{\mathbf{H}}(t) + [\mathbf{F} + \hat{\mathbf{V}}(t), T_2(t)] \middle| \Phi_0 \right\rangle - i\frac{\partial t_{\mu_2}}{\partial t} \Big) \ . \end{aligned} \tag{2.56}$$

Here the dressed quantities are similarity transformed with the zeroth and first order singles cluster operator. To get the linear response function according to the 2n+1 rule, only zeroth and first order amplitudes and multipliers are considered

for the second order Lagrangian which is given in the supplementary in equation (A.1) for unrestricted CC2. Using several variational conditions and the fact that the Hamiltonian is only linearly dependent on the field strength parameters, the expression for the linear response function reduces to

$$\langle\langle X;Y\rangle\rangle_{\omega_{k_1}} = P(X(\omega_0),Y(\omega_{k_1}))\Big\{ \underbrace{\frac{\partial^2\{^{2n+1}L^{(2)}_{UCC2}(t)\}_T}{\partial\epsilon_X(\omega_0)\partial t^{(1)}(\omega_{k1})}}_{=\eta^X} t^Y(\omega_{k_1}) + \frac{1}{2}\underbrace{\frac{\partial^2\{^{2n+1}L^{(2)}_{UCC2}(t)\}_T}{\partial t^{(1)}(\omega_0)\partial t^{(1)}(\omega_{k1})}}_{=\mathbf{F}} t^X(\omega_0)t^Y(\omega_{k_1})\Big\} \ . \quad (2.57)$$

While

$$P(X(\omega_0),Y(\omega_{k_1}))f^{XY}(\omega_0,\omega_{k_1}) = f^{XY}(\omega_0,\omega_{k_1}) + f^{YX}(\omega_{k_1},\omega_0) \quad (2.58)$$

and

$$t^X(\omega) = \frac{\partial t^{(1)}(\omega)}{\partial\epsilon_X(\omega)} \ . \quad (2.59)$$

The variational condition for the first order multipliers gives an equation for the first order amplitudes and has been used to simplify the expression for the linear response function.

$$\begin{aligned} 0 = \frac{\partial L^{XY}(\omega_0,\omega_{k_1})}{\partial\lambda^X(\omega_0)} =& \frac{\partial^2\{^{2n+1}L^{(2)}_{UCC2}(t)\}_T}{\partial\lambda^{(1)}(\omega_0)\partial\epsilon_Y(\omega_{k_1})} + \frac{\partial^2\{^{2n+1}L^{(2)}_{UCC2}(t)\}_T}{\partial\lambda^{(1)}(\omega_0)\partial t^{(1)}(\omega_{k_1})}t^Y(\omega_{k_1}) \\ =& \xi^Y + (\mathbf{A}-\omega_{k_1}\mathbf{1})t^Y(\omega_{k_1}) \end{aligned} \quad (2.60)$$

$\mathbf{A}$ represents the so-called Jacobi matrix and $\omega_0 = -\omega_{k_1}$. The second derivative of $\{^{2n+1}L^{(2)}_{UCC2}(t)\}_T$ (A.4) with respect to spin dependent first order multipliers and amplitudes will be considered in detail in section 5.1. Representing equation (2.60) in a basis where the nonsymmetric Jacobian is diagonal leads to

$${}^{diag}t^Y(\omega_{k_1}) = -\sum_l \frac{{}^{diag}\xi^Y}{(\omega_l-\omega_{k_1})} \ . \quad (2.61)$$

Thus the linear response function (2.57) in that basis has poles where ω_{k_1} equals $\pm\omega_l$, the eigenvalues of $\mathbf{A}$. So the determination of the excitation energies reduces to the diagonalization of the Jacobian.

2.5. Density fitting

Construction of the two-electron repulsion integrals, e.g. $(ia|jb)$, is computationally time consuming and represents for example in MP2 the bottleneck of the calculation [28]. Density Fitting (DF) reduces the computational cost for the evaluation of the these integrals [17–19].

$$\begin{aligned}(rs|tu) &= \int \psi_r^*(r_1)\psi_s(r_1)\frac{1}{r_{12}}\psi_t^*(r_2)\psi_u(r_2)dr_1dr_2 \\ &= \int \rho_{rs}(r_1)\frac{1}{r_{12}}\rho_{tu}(r_2)dr_1dr_2 \end{aligned} \tag{2.62}$$

The central idea of DF is to approximate the one electron densities $\rho_{rs}(r_1)$ and $\rho_{tu}(r_2)$. Approximated densities $\tilde{\rho}_{rs}(r)$ may be constructed using atom-centred Gaussian type orbitals (GTO's) χ_P as

$$\tilde{\rho}_{rs}(r) = \sum_P c_{rs}^P \chi_P(r) \ , \tag{2.63}$$

where c_{rs}^P represent the fitting coefficients which might be determined by minimizing the functional

$$\begin{aligned}\Delta_{rs} &= \int \left[\rho_{rs}(r_1)r_{12}^{-1}\rho_{rs}(r_2) - 2\rho_{rs}(r_1)r_{12}^{-1}\tilde{\rho}_{rs}(r_2) + \tilde{\rho}_{rs}(r_1)r_{12}^{-1}\tilde{\rho}_{rs}(r_2)\right]dr_1dr_2 \\ &= (rs|rs) - 2\sum_P (rs|P)c_{rs}^P + \sum_{PQ} c_{rs}^P \underbrace{(P|Q)}_{=J_{PQ}} c_{rs}^Q \ . \end{aligned} \tag{2.64}$$

This leads to the following linear equations for the fitting coefficients c_{rs}^P.

$$\sum_Q J_{PQ}c_{rs}^Q = (P|rs) \tag{2.65}$$

The 3-index integrals $(P|rs)$ are used to approximate the 4-index integrals for example as

$$(rs|tu) \approx \sum_{PQ} (rs|P) J^{-1}_{PQ} (Q|tu) \ . \tag{2.66}$$

This leads to computational savings but it has to be mentioned that despite the use of DF in canonical MP2 or CC2 the overall scaling of these methods remains $\mathcal{N}^5$ with $\mathcal{N}$ as the number of orbitals. With further decomposition of the two-electron repulsion integrals as products of two-index quantities, as done bei Hohenstein et al. using the so-called tensor hypercontraction [29, 30], a scaling behaviour of $\mathcal{N}^4$ can be achieved for CC2.
But for further reduction of the computational costs local approximations are applied as described in sections 4.2 and 5.2.

2.6. Laplace transformation

In Coupled Cluster as well as in Møller-Plesset perturbation theory an energy denominator occurs in different expressions. For example the MP2 second order correction to the energy can be written in canonical basis as

$$E^{(2)} = -\frac{1}{4} \sum_{IJAB} \frac{\langle AB \parallel IJ \rangle^2}{\epsilon_A + \epsilon_B - \epsilon_I - \epsilon_J} \ . \tag{2.67}$$

The expression $\langle AB \parallel IJ \rangle$ represents the antisymmetrized two electron integrals and ϵ_X is the orbital energy of the spin orbital ψ_X. In a basis where the occupied-occupied and the virtual-virtual blocks of the Fock matrix are not diagonal, the doubles amplitudes can not be simply expressed as integrals divided by a sum of orbital energies. Hence the residuals equations have to be solved iteratively.
Almlöf and Häser proposed to eliminate the energy denominator using the Laplace

identity [31, 32]

$$\frac{1}{x} = \int_0^\infty \exp\left(-xt\right)dt \ . \tag{2.68}$$

Using quadrature points t_q and corresponding weights w_q to approximate the integral from the Laplace identity, equation (2.67) can be written as

$$E^{(2)} \approx -\frac{1}{4} \sum_{IJAB} \sum_{q=1}^{n_q} \mathrm{w}_q \left\langle A(t_q)B(t_q) \parallel I(t_q)J(t_q) \right\rangle^2 \ . \tag{2.69}$$

The spin orbitals $\psi_A(t_q)$ and $\psi_I(t_q)$, for example, are defined as

$$\begin{aligned} \psi_A(t_q) &= \psi_A \exp\left(-\epsilon_A t_q\right) \\ \psi_I(t_q) &= \psi_I \exp\left(\epsilon_I t_q\right) \ . \end{aligned} \tag{2.70}$$

The form of equation (2.69) allows to express the doubles amplitudes in a general basis, e.g. local basis, as follows. The integrals entering the doubles amplitudes are constructed for example in local basis, transformed to canonical basis, multiplied with the exponential factors in canonical basis and transformed back to local basis as one transformation.

In case of unrestricted CC2 one uses Laplace transformation for the energy denominator which occurs in the expression of the doubles vector in semi-canonical basis (see equation (5.5)).

3. Reference wave function and localized spin orbitals

The starting point is, as already mentioned, a (|ROHF⟩) determinant as it is an eigenfunction of the spin-squared S^2 operator for the high-spin open-shell case. It is well known that due to the restriction of α and β spin orbitals to the same spatial part, the spin orbitals entering |ROHF⟩ are not eigenfunctions of F^α and F^β, the alpha and beta Fock operator, and Brillouin's condition is not fulfilled any more.
In order to get a matrix representation of the Fock operators in which the occupied-occupied and virtual-virtual block is diagonal, the procedure described by Peter J. Knowles et al. [15] is used. There the different occupied-virtual parts of F^α and F^β are set to zero and the rest is diagonalized. Note that by doing this no spin contamination is introduced, because the occupied and virtual space is not mixed and the diagonalization within the α or β occupied space is simply a linear combination of the corresponding MO coefficients. As a result one gets n_α and n_β occuppied and $M - n_\alpha$ and $M - n_\beta$ virtual spin orbitals for a system with n_α plus n_β electrons. M is the total number of the molecular orbitals. By construction these semi-canonical spin orbitals are eigenfunctions of the correspondingly modified Fock matrices.

In semi-canonical basis the Fock operators F^{α} and F^{β} can be defined as

$$F^{\sigma} = \sum_{\bar{i}_{\sigma}} f_{\bar{i}_{\sigma}\bar{i}_{\sigma}} a^{\dagger}_{\bar{i}_{\sigma}} a_{\bar{i}_{\sigma}} + \sum_{\bar{a}_{\sigma}} f_{\bar{a}_{\sigma}\bar{a}_{\sigma}} a^{\dagger}_{\bar{a}_{\sigma}} a_{\bar{a}_{\sigma}} + \sum_{\bar{i}_{\sigma}\bar{a}_{\sigma}} f_{\bar{i}_{\sigma}\bar{a}_{\sigma}} a^{\dagger}_{\bar{i}_{\sigma}} a_{\bar{a}_{\sigma}} \ . \tag{3.1}$$

Having diagonal occupied-occupied and virtual-virtual blocks of the correspondig Fock-matrices is essential for building the effective singles eigenvalue problem for the calculation of excitation energies. In equation (3.1) σ can be only α or β. The sums run over the set of the alpha or beta occupied $\bar{i}_{\sigma}, \bar{j}_{\sigma}, ...$ and virtual semi-canonical spin orbitals $\bar{a}_{\sigma}, \bar{b}_{\sigma}, ...$. The creation and annihilation operators from second quantization formalism are denoted as $a^{\dagger}_{\bar{p}_{\sigma}}$ and $a_{\bar{q}_{\sigma}}$, respectively. The indices $\bar{p}_{\sigma}, \bar{q}_{\sigma}, \bar{r}_{\sigma}...$ denote general semi-canonical orbitals with σ-spin. The orbital indices without a bar correspond to localized spin orbitals. The zeroth order Hamiltonian in semi-canonical basis can be defined as

$$H^{(0)}_{\sigma} = \sum_{\bar{i}_{\sigma}} f_{\bar{i}_{\sigma}\bar{i}_{\sigma}} a^{\dagger}_{\bar{i}_{\sigma}} a_{\bar{i}_{\sigma}} + \sum_{\bar{a}_{\sigma}} f_{\bar{a}_{\sigma}\bar{a}_{\sigma}} a^{\dagger}_{\bar{a}_{\sigma}} a_{\bar{a}_{\sigma}} \ . \tag{3.2}$$

There is no need to go to semi-canonical basis if one starts with the unrestricted Hartree-Fock determinant ($|\text{UHF}\rangle$) because the resulting α and β molecular spin orbitals are already eigenfunctions of F^{α} and F^{β} and Brillouin's condition is fulfilled. The α and β occupied localized spin orbitals are obtained using for example a Pipek-Mezey [33] or Boys [34] localization procedure. Results in this thesis are based on localization procedure according to Pipek-Mezey. The α and β occupied semi-canonical orbitals are localized separately. The occupied semi-canonical spin orbitals are transformed to localized spin orbitals as shown in the following equation.

$$|i_{\sigma}\rangle = \sum_{\bar{i}_{\sigma}} |\bar{i}_{\sigma}\rangle \, W_{\bar{i}_{\sigma} i_{\sigma}} = \sum_{\bar{i}_{\sigma}} |\bar{i}_{\sigma}\rangle \sum_{\mu\nu} (C^{occ}_{\mu\bar{i}_{\sigma}})^{\dagger} S^{AO}_{\mu\nu} L_{\nu i_{\sigma}} \tag{3.3}$$

In equation (3.3) the matrix $\mathbf{L}_{(\sigma)}$ transforms atomic orbitals (AOs) to localized occupied spin orbitals and $\mathbf{C}^{occ}_{(\sigma)}$ transforms AOs to occupied semi-canonical spin orbitals.

There are two sets of $\mathbf{L}_{(\sigma)}$, $\mathbf{C}^{occ}_{(\sigma)}$ and $\mathbf{W}_{(\sigma)}$ matrices, one for $\sigma = \alpha$ and one for $\sigma = \beta$ spin. For the alpha and beta virtual space projected atomic orbitals (PAOs) as introduced by Saebø and Pulay [16] are used. The matrix which transforms semi-canonical virtuals to PAOs is defined as

$$\mathbf{Q}_{(\sigma)} = \mathbf{C}^{vir\dagger}_{(\sigma)}\mathbf{S}^{AO} \ . \tag{3.4}$$

$\mathbf{S}^{AO}$ represents the overlap matrix in AO basis and $\mathbf{C}^{vir}_{(\sigma)}$ transforms AOs to virtual semi-canonical orbitals. Again one has two $\mathbf{Q}_{(\sigma)}$ and $\mathbf{C}^{vir}_{(\sigma)}$ matrices ($\sigma = \alpha, \beta$). Hence there are also two PAO overlap matrices

$$\mathbf{S}^{PAO}_{(\sigma)} = \mathbf{Q}^{\dagger}_{(\sigma)}\mathbf{Q}_{(\sigma)} \tag{3.5}$$

with σ equal α or β. The superscripts AO and PAO over the overlap matrices are not written explicitly when certain elements of these matrices enter any of the following equations, because corresponding greek and latin letters in the subscripts indicate AO and PAO elements, respectively.

4. Local unrestricted CC2 ground state

This chapter contains the derivation of programmable working equations for the spin unrestricted open-shell ground state method. Further the corresponding local approximations for the ground state and there effect on excitation energies will be discussed.

4.1. Diagrams and working equations

The CC2 singles equation (2.10) can be reformulated using the T1-dressed normal-ordered Hamiltonian (2.39) as

$$\begin{aligned}\Omega_{\mu_1} =& \langle \mu_1 | (\hat{\mathbf{H}}_\mathrm{N} + \langle \Phi_0 | \hat{\mathbf{H}} | \Phi_0 \rangle) + [(\hat{\mathbf{H}}_\mathrm{N} + \langle \Phi_0 | \hat{\mathbf{H}} | \Phi_0 \rangle), \mathrm{T}_2] | 0 \rangle \\ =& \langle \mu_1 | \hat{\mathbf{H}}_\mathrm{N} + [\hat{\mathbf{H}}_\mathrm{N}, \mathrm{T}_2] | \Phi_0 \rangle + \langle \Phi_0 | \hat{\mathbf{H}} | \Phi_0 \rangle \underbrace{\langle \mu_1 | \Phi_0 \rangle}_{=0} \\ &+ \langle \mu_1 | \underbrace{[\langle \Phi_0 | \hat{\mathbf{H}} | \Phi_0 \rangle, \mathrm{T}_2]}_{=0} | \Phi_0 \rangle = \langle \mu_1 | \hat{\mathbf{H}}_\mathrm{N} + [\hat{\mathbf{H}}_\mathrm{N}, \mathrm{T}_2] | \Phi_0 \rangle \ . \end{aligned} \tag{4.1}$$

Thus it is obvious that solving the singles equation with $\hat{\mathbf{H}}_\mathrm{N}$ or $\hat{\mathbf{H}}$ makes no difference. But as already mentioned, the use of $\hat{\mathbf{H}}_\mathrm{N}$ simplifies the derivation of working equations via Wicks theorem or diagrammatic techniques as introduced in section

2.3. Writing each part of $\hat{\mathbf{H}}_{\mathrm{N}}$ and T_2 explicitly yields

$$\begin{aligned}\Omega_{\mu_1} = \langle \mu_1 | \hat{\mathrm{F}}_{\mathrm{N}}^{\alpha} + \hat{\mathrm{F}}_{\mathrm{N}}^{\beta} + ((\hat{\mathrm{F}}_{\mathrm{N}}^{\alpha} + \hat{\mathrm{F}}_{\mathrm{N}}^{\beta})(\mathrm{T}_2^{\alpha\alpha} + \mathrm{T}_2^{\beta\beta} + \mathrm{T}_2^{\beta\alpha}))_{\mathrm{c}} \\ + ((\hat{\mathrm{V}}_{\mathrm{N}}^{\alpha\alpha} + \hat{\mathrm{V}}_{\mathrm{N}}^{\beta\beta} + \hat{\mathrm{V}}_{\mathrm{N}}^{\alpha\beta})(\mathrm{T}_2^{\alpha\alpha} + \mathrm{T}_2^{\beta\beta} + \mathrm{T}_2^{\beta\alpha}))_{\mathrm{c}} \, |\Phi_0\rangle \,, \end{aligned} \tag{4.2}$$

where the two electron operators of $\hat{\mathbf{H}}_{\mathrm{N}}$, which would not be connected to any amplitude, are omitted in equation (4.2). The reason is that no diagrams with an excitation level of +1 can be generated where at the same time no external lines go under the operator interaction line. The subscript c indicating connected terms has already been introduced in section 2.3. Matrix elements, corresponding diagrams and algebraic expressions for the σ part ($\sigma = \alpha$ or β) of the singles residuum will be presented in the following.

Before giving all contributions to an element $v_{i_\sigma}^{a_\sigma}$ of the residuum in local basis, where i_σ belongs to localized occupied spin orbitals and a_σ is a projected atomic spin orbital, the fragments of the T1-dressed normal-ordered Hamiltonian are defined in chemist notation as

$$\begin{aligned}\hat{\mathrm{F}}_{\mathrm{N}}^{\sigma} =& \sum_{p_\sigma q_\sigma} \big[\hat{h}_{p_\sigma q_\sigma} + \sum_{i_\sigma} (i_\sigma i_\sigma \hat{|} p_\sigma q_\sigma) - (i_\sigma q_\sigma \hat{|} p_\sigma i_\sigma) + \sum_{i_\tau} (i_\tau i_\tau \hat{|} p_\sigma q_\sigma)\big] \big\{ a_{p_\sigma}^{\dagger} a_{q_\sigma} \big\} \\ \hat{\mathrm{V}}_{\mathrm{N}}^{\sigma\sigma} =& \frac{1}{4} \sum_{p_\sigma q_\sigma r_\sigma s_\sigma} \big[(p_\sigma r_\sigma \hat{|} q_\sigma s_\sigma) - (p_\sigma s_\sigma \hat{|} q_\sigma r_\sigma)\big] \big\{ a_{p_\sigma}^{\dagger} a_{q_\sigma}^{\dagger} a_{s_\sigma} a_{r_\sigma} \big\} \\ \hat{\mathrm{V}}_{\mathrm{N}}^{\sigma\tau} =& \sum_{p_\sigma q_\tau r_\sigma s_\tau} (p_\sigma r_\sigma \hat{|} q_\tau s_\tau) \big\{ a_{p_\sigma}^{\dagger} a_{q_\tau}^{\dagger} a_{s_\tau} a_{r_\sigma} \big\}. \end{aligned} \tag{4.3}$$

For equation (4.3) and all the following equations, it holds that if σ equals α, then τ equals β or vice versa. The dressed one and two electron integrals are written in chemist notation as

$$\hat{h}_{p_\sigma q_\sigma} = \sum_{\mu\nu} h_{\mu\nu} \Lambda_{\mu p_\sigma}^{p} \Lambda_{\nu q_\sigma}^{h} \tag{4.4}$$

$$(p_\sigma q_\sigma \hat{|} r_\tau s_\tau) = \sum_{\kappa\lambda\mu\nu} (\kappa\lambda|\mu\nu) \Lambda_{\kappa p_\sigma}^{p} \Lambda_{\lambda q_\sigma}^{h} \Lambda_{\mu r_\tau}^{p} \Lambda_{\nu s_\tau}^{h}. \tag{4.5}$$

The Lambda matrices transform from AO basis to local spin orbital basis and are defined exactly as given in references [35, 36], except their dependence on spin.

$$\begin{aligned}\Lambda^{p}_{\mu a_\sigma} =& P_{\mu a_\sigma} - L_{\mu i_\sigma} t^{a'_\sigma}_{i_\sigma} S_{a'_\sigma a_\sigma},\ \Lambda^{p}_{\mu i_\sigma} = L_{\mu i_\sigma},\\ \Lambda^{h}_{\mu a_\sigma} =& P_{\mu a_\sigma},\ \Lambda^{h}_{\mu i_\sigma} = L_{\mu i_\sigma} + P_{\mu a_\sigma} t^{a_\sigma}_{i_\sigma}\end{aligned} \tag{4.6}$$

The matrix **P** transforms from AO to PAO basis and **S** represents the PAO overlap matrix. There are in total eight Lambda matrices, four for α and four for β spin. In equation (4.6) summation over repeated indexes is assumed.

In figure 4.1 the matrix elements and the corresponding diagrams of the singles residuum are given. The indexes of the external particle lines emerging from an amplitude bear a prime to indicate that they have to be multiplied by elements of the PAO overlap matrix. After the evaluation of the CC diagrams according to the rules introduced in section 2.3, writing the two electron integrals in chemist notation and simplifying the expressions one arrives at the following equation.

$$\begin{aligned}v^{a_\sigma}_{i_\sigma} =& \hat{f}_{a_\sigma i_\sigma} + \sum_{a'_\sigma} S_{a_\sigma a'_\sigma} \Big[\sum_{j_\sigma} \sum_{b_\sigma \in [i_\sigma j_\sigma]} t^{i_\sigma j_\sigma}_{a'_\sigma b_\sigma} \hat{f}_{j_\sigma b_\sigma} + \sum_{j_\tau} \sum_{b_\tau \in [i_\sigma j_\tau]} t^{i_\sigma j_\tau}_{a'_\sigma b_\tau} \hat{f}_{j_\tau b_\tau} \Big] \\ & - \sum_{a'_\sigma} S_{a_\sigma a'_\sigma} \sum_{k_\sigma P} A^{P}_{k_\sigma a'_\sigma} (P\hat{|}k_\sigma i_\sigma) + \sum_{P} \sum_{c_\sigma \in [i_\sigma]_U} A^{P}_{i_\sigma c_\sigma} (P\hat{|}a_\sigma c_\sigma)\end{aligned} \tag{4.7}$$

The index b_σ lives in the pair domain $[i_\sigma j_\sigma]$. Whereas b_τ belongs to the orbital domain of j_τ which is extended to the length of the pair domain of i_σ & j_τ. And $c_\sigma \in [i_\sigma]_U$ indicates that c_σ lives in the union of all pair domains of localized spin orbitals (LSOs) which build a pair with the fixed LSO i_σ. The dressed Fock elements are defined implicitly in equation (4.3). The quantity $A^{P}_{i_\sigma a_\sigma}$ is constructed using

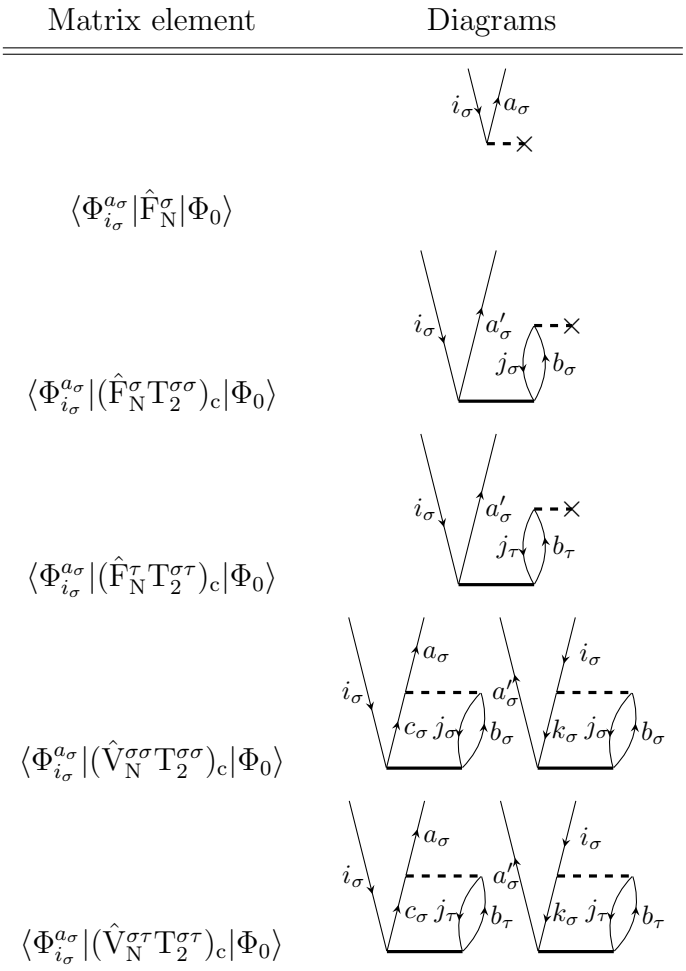

Figure 4.1.: Matrix elements and CC diagrams for $v_{i_\sigma}^{a_\sigma}$

fitting coefficients as

$$\begin{aligned} A_{i_\sigma a_\sigma}^{P} =& \sum_{j_\sigma} \sum_{b_\sigma \in [i_\sigma j_\sigma]} t_{a_\sigma b_\sigma}^{i_\sigma j_\sigma} C_{j_\sigma b_\sigma}^{P} + \sum_{j_\tau} \sum_{b_\tau \in [i_\sigma j_\tau]} t_{a_\sigma b_\tau}^{i_\sigma j_\tau} C_{j_\tau b_\tau}^{P} \\ =& \sum_{j_\sigma} \sum_{b_\sigma \in [i_\sigma j_\sigma]} t_{a_\sigma b_\sigma}^{i_\sigma j_\sigma} \sum_{Q} J_{PQ}^{-1}(Q|j_\sigma b_\sigma) \\ &+ \sum_{j_\tau} \sum_{b_\tau \in [i_\sigma j_\tau]} t_{a_\sigma b_\tau}^{i_\sigma j_\tau} \sum_{Q} J_{PQ}^{-1}(Q|j_\tau b_\tau) \ . \end{aligned} \tag{4.8}$$

Analogously to the singles amplitudes equation, the doubles equation (2.13) can be reformulated using $\hat{\mathbf{H}}_\mathrm{N}$ as

$$\begin{aligned}\Omega_{\mu_2} &= \langle\mu_2|\hat{\mathbf{H}}_\mathrm{N} + (\mathbf{F}_\mathrm{N}\mathrm{T}_2)_\mathrm{c}|\Phi_0\rangle \\ &= \langle\mu_2|(\hat{\mathrm{V}}_\mathrm{N}^{\alpha\alpha} + \hat{\mathrm{V}}_\mathrm{N}^{\beta\beta} + \hat{V}_N^{\alpha\beta}) + ((\mathrm{F}_\mathrm{N}^{\alpha} + \mathrm{F}_\mathrm{N}^{\beta})(\mathrm{T}_2^{\alpha\alpha} + \mathrm{T}_2^{\beta\beta} + \mathrm{T}_2^{\beta\alpha}))_\mathrm{c}|\Phi_0\rangle \ . \end{aligned} \tag{4.9}$$

In the second line of equation (4.9) the one electron parts of $\hat{\mathbf{H}}_\mathrm{N}$ are omitted, because it is not possible to create a doubly excited wave function on the bra side by them alone. The matrix elements and corresponding diagrams which contribute to an element of the $\sigma\sigma$ and $\sigma\tau$ doubles residuum, are shown in figure 4.2. Evaluation of

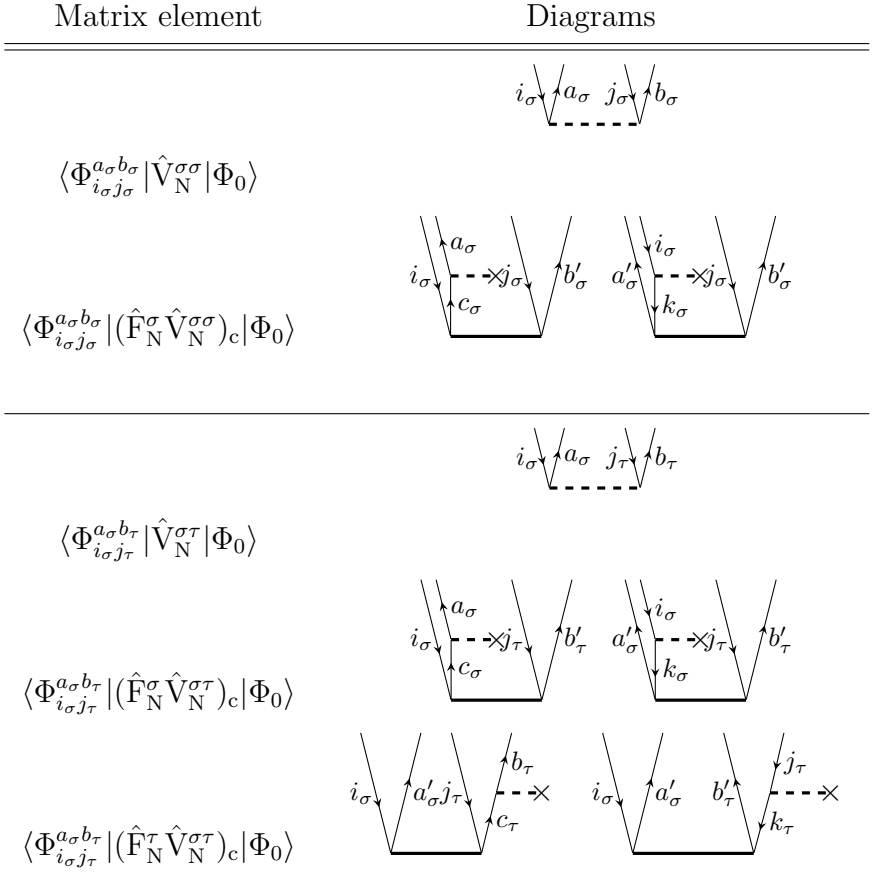

Figure 4.2.: Matrix elements and CC diagrams for $v^{a_\sigma b_\sigma}_{i_\sigma j_\sigma}$ and $v^{a_\sigma b_\tau}_{i_\sigma j_\tau}$

these diagrams leads to the following equations.

$$v_{i_\sigma j_\sigma}^{a_\sigma b_\sigma} = (a_\sigma i_\sigma \hat{|} b_\sigma j_\sigma) - (b_\sigma i_\sigma \hat{|} a_\sigma j_\sigma) + \sum_{c_\sigma} \sum_{b'_\sigma} f_{a_\sigma c_\sigma} t_{c_\sigma b'_\sigma}^{i_\sigma j_\sigma} S_{b'_\sigma b_\sigma} + \sum_{c_\sigma} \sum_{a'_\sigma} S_{a_\sigma a'_\sigma} t_{a'_\sigma c_\sigma}^{i_\sigma j_\sigma} f_{b_\sigma c_\sigma}$$
$$- \sum_{a'_\sigma b'_\sigma} \sum_{k_\sigma} S_{a_\sigma a'_\sigma} \Big(t_{a'_\sigma b'_\sigma}^{k_\sigma j_\sigma} f_{k_\sigma i_\sigma} + t_{a'_\sigma b'_\sigma}^{i_\sigma k_\sigma} f_{k_\sigma j_\sigma} \Big) S_{b'_\sigma b_\sigma} \quad ; \; a_\sigma, b_\sigma \in [i_\sigma j_\sigma]. \tag{4.10}$$

$$v_{i_\sigma j_\tau}^{a_\sigma b_\tau} = (a_\sigma i_\sigma \hat{|} b_\tau j_\tau) + \sum_{c_\sigma} \sum_{b'_\tau} f_{a_\sigma c_\sigma} t_{c_\sigma b'_\tau}^{i_\sigma j_\tau} S_{b'_\tau b_\tau} + \sum_{c_\tau} \sum_{a'_\sigma} S_{a_\sigma a'_\sigma} t_{a'_\sigma c_\tau}^{i_\sigma j_\tau} f_{b_\tau c_\tau}$$
$$- \sum_{a'_\sigma b'_\tau} S_{a_\sigma a'_\sigma} \Big(\sum_{k_\sigma} t_{a'_\sigma b'_\tau}^{k_\sigma j_\tau} f_{k_\sigma i_\sigma} + \sum_{k_\tau} t_{a'_\sigma b'_\tau}^{i_\sigma k_\tau} f_{k_\tau j_\tau} \Big) S_{b'_\tau b_\tau} \quad , \; a_\sigma, b_\tau \in [i_\sigma j_\tau]. \tag{4.11}$$

DF approximation is also applied for the two electron integrals in equations (4.10) and (4.11).

The update of the singles and doubles residuals for the open-shell system is performed according to first order perturbation theory as described in detail by Liu Yu [37]. The central idea is to transform the residuals to a pseudo canonical basis and perform the update in that basis and transform the result back to the local basis. To achieve this, e.g. for the doubles residuum, a pair domain specific virtual Fock matrix is transformed to an orthogonal basis and diagonalized. The product of the transformation matrix which transforms to an orthogonal basis and the unitary transformation matrix, which diagonalizes the corresponding Fock matrix, is used to transform the virtual index of the residuum to the pseudo semi-canonical basis.

4.2. Local approximations for the ground state

The virtual space, as already mentioned, is spanned by PAOs. The excitation domain, orbital domain, for localized occupied spin orbitals (LSOs) is restricted as follows. For each LSO $|i_\sigma\rangle$ (3.3) the formal charge contribution to a certain atom is

calculated according to a Mulliken or Löwdin analysis. Then the atoms are sorted according to decreasing charge and only those are considered to be part of the domain which contribute significantly to the charge. For this thesis all charges are summed up until the difference between this sum and charge one is less than 1.0E−08. Afterwards further atoms are added to the domain of a LSO according to Boughton-Pulay procedure [38] with a threshold of 0.98. This is in complete analogy to what is described for closed-shell systems in reference [39]. These orbital domains are extended by including the next connected neighbours, iext=1, of the already included atoms. Pair domains are constructed by unifying the orbital domains of two LSOs.

For local CC2 ground state calculations, in case of closed-shell systems, usually a distance criterion is used to restrict the pair list. If two occupied orbitals are spatially separated by more then $R_0 = 10$ bohr, they are considered to be very distant pairs and are neglected [21, 35]. All other pairs are taken into account. Applying this distance criterion to doublet alkane radicals can produce, especially for extended chains, large deviations from the canonical excitation energies.
Restriction of the pair list according to an energy criterion has been described by Saebø and Pulay [16]. It turns out to be of great improvement to the excitation energies of alkane radicals, if those pairs are included in the correlation treatment which contribute to the MP2 correlation energy with more than 3 μH. And improved results can be obtained by using a threshold of 1 μH. But as the alkane chains get more extended (e.g. Pentadecane$^+$), the threshold of 1 μH is not enough to always find the lowest excited state. In order to manage finding the lowest lying states and getting a deviation of less than 0.05 eV from the canonical results for each state, a threshold of 0.1 μH is applied.
This behaviour is due to the bad localization of the β-semicanonical orbitals by

which the hole (missing electron) is described. In case of Pentadecane$^+$ 20% of the β-valence orbitals were delocalized on three and four atoms. Also the character of the excitations influences the deviation from the canonical results as will be explained in section 6.1.
In order to be sure that the deviations from canonical excitation energies are due to the ground state pair list, additional calculations have been performed where the excited states pair lists included all pairs and the results remained nearly the same as with restricted excited states pair lists. And in the case where all ground state pairs have been included and ground state orbital domains restricted as described, it was possible to get deviations less than 0.05 eV from canonical excitation energies. So it is concluded that restricting the orbital domains in the ground state has no harmful effect on the excitation energies. One can also exclude the possibility that full orbital domains for the excited state could lead to less deviations of the excitation energies from the canonical results, because corresponding calculations show that the deviations still remain as large as before.

In figure 4.3 one can see the mean absolute error (MAE) in eV for the first three excited states of the alkane radical chains depending on restriction of the ground state pair list according to a distance criterion and different pair energy thresholds. Also the case where all ground state pairs are taken into account is included. The MAE values are based on the results presented in the supplementary in table C.1. Additionally the ratio n_loc/n_can is plotted for the different restrictions of the ground state pair list. (n_loc is the number of pairs included in the local calculation and n_can represents the number of all pairs which would be included in a canonical calculation). It is obvious from figure 4.3 that one does not get closer to the canonical results because of simply including more pairs. Actually one obtains already better results with less ground state pairs using a threshold of 3 μH.

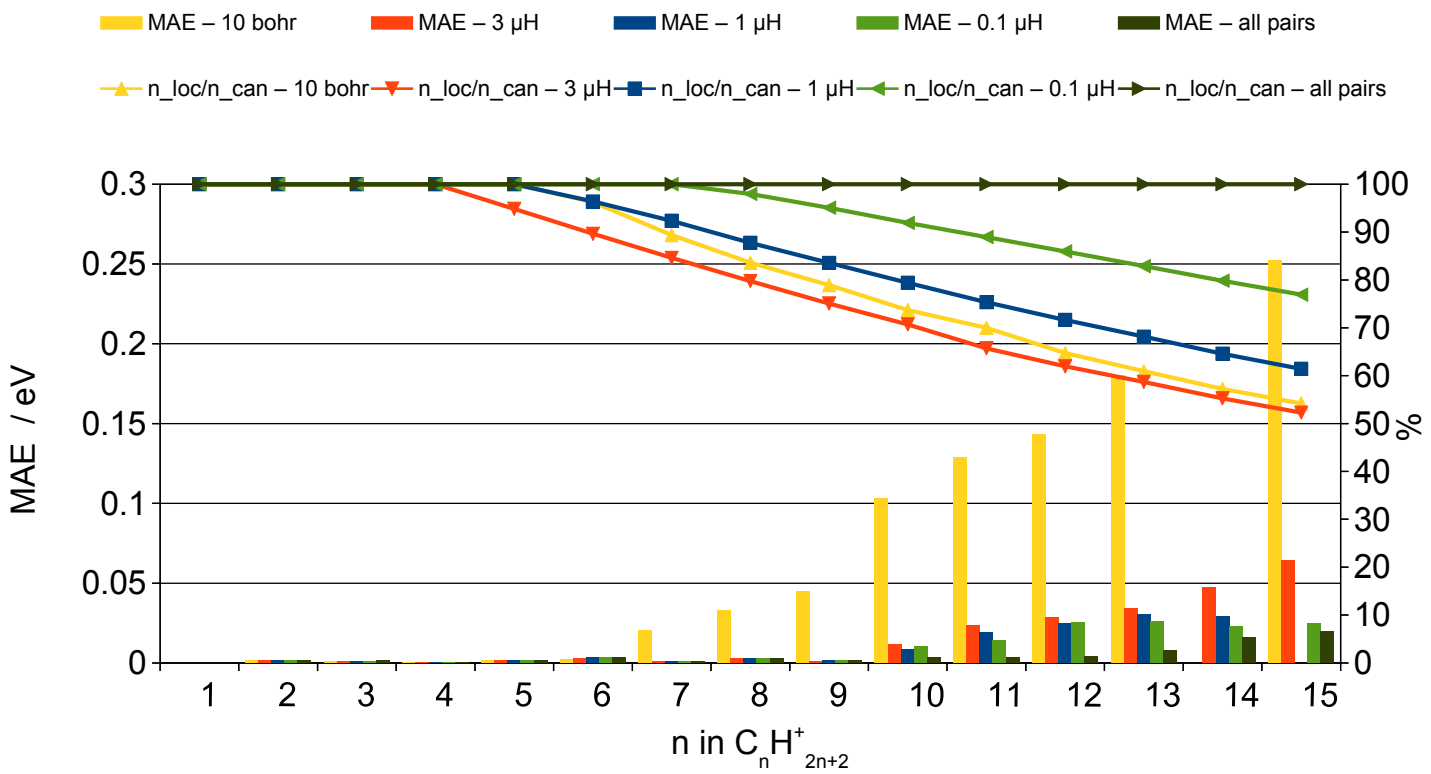

Figure 4.3.: Mean absolute error (MAE) in eV compared to canonical excitation energies for the first three excited states of alkane radicals. n_loc/n_can represents the ratio between the number of pairs included in the local calculation and all possible pairs (canonical). Results due to the restriction of the ground state pair list according to a distance criterion (10 bohr) and different pair energy thresholds as well as not restricting it are shown.

5. Local unrestricted CC2 excited states

5.1. Diagrams and working equations

As shown in section 2.4, excitation energies are obtained as the eigenvalues of the nonsymmetric Jacobian $\mathbf{A}$ which emerges from the second derivative of the time averaged second order Lagrangian $\{^{2n+1}L^{(2)}_{UCC2}\}_T$ (A.4) with respect to the first order multipliers and amplitudes (see eq. (2.60)). The corresponding right eigenvalue problem of the Jacobian can be written as

$$\mathbf{AU} = \begin{array}{c} \\ \mu_1^\alpha \\ \mu_1^\beta \\ \mu_2^{\alpha\alpha} \\ \mu_2^{\beta\beta} \\ \mu_2^{\beta\alpha} \end{array} \begin{array}{c} \begin{array}{ccccc} \nu_1^\alpha & \nu_1^\beta & \nu_2^{\alpha\alpha} & \nu_2^{\beta\beta} & \nu_2^{\beta\alpha} \end{array} \\ \begin{pmatrix} A_{\mu_1^\alpha \nu_1^\alpha} & A_{\mu_1^\alpha \nu_1^\beta} & A_{\mu_1^\alpha \nu_2^{\alpha\alpha}} & 0 & A_{\mu_1^\alpha \nu_2^{\beta\alpha}} \\ A_{\mu_1^\beta \nu_1^\alpha} & A_{\mu_1^\beta \nu_1^\beta} & 0 & A_{\mu_1^\beta \nu_2^{\beta\beta}} & A_{\mu_1^\beta \nu_2^{\beta\alpha}} \\ A_{\mu_2^{\alpha\alpha} \nu_1^\alpha} & 0 & A_{\mu_2^{\alpha\alpha} \nu_2^{\alpha\alpha}} & 0 & 0 \\ 0 & A_{\mu_2^{\beta\beta} \nu_1^\beta} & 0 & A_{\mu_2^{\beta\beta} \nu_2^{\beta\beta}} & 0 \\ A_{\mu_2^{\beta\alpha} \nu_1^\alpha} & A_{\mu_2^{\beta\alpha} \nu_1^\beta} & 0 & 0 & A_{\mu_2^{\beta\alpha} \nu_2^{\beta\alpha}} \end{pmatrix} \end{array} \begin{pmatrix} U_{\nu_1^\alpha} \\ U_{\nu_1^\beta} \\ U_{\nu_2^{\alpha\alpha}} \\ U_{\nu_2^{\beta\beta}} \\ U_{\nu_2^{\beta\alpha}} \end{pmatrix} = \omega \begin{pmatrix} U_{\nu_1^\alpha} \\ U_{\nu_1^\beta} \\ U_{\nu_2^{\alpha\alpha}} \\ U_{\nu_2^{\beta\beta}} \\ U_{\nu_2^{\beta\alpha}} \end{pmatrix}. \tag{5.1}$$

The singles singles, singles doubles, doubles singles and doubles doubles block ele-

ments of **A** are defined as

$$
\begin{aligned}
A_{\mu_1^\rho \nu_1^\sigma} =& \frac{\partial^2 \{^{2n+1} L^{(2)}_{UCC2}\}_T}{\partial \lambda^{(1)}_{\mu_1^\rho} \partial t^{(1)}_{\nu_1^\sigma}} + \omega_k \delta_{\mu_1^\rho \nu_1^\sigma} = \langle \mu_1^\rho | [\hat{H}_N, \tau_{\nu_1^\sigma}] + [[\hat{H}_N, \tau_{\nu_1^\sigma}], T_2^{(0)}] | \Phi_0 \rangle \\
A_{\mu_1^\rho \nu_2^{\sigma\upsilon}} =& \frac{\partial^2 \{^{2n+1} L^{(2)}_{UCC2}\}_T}{\partial \lambda^{(1)}_{\mu_1^\rho} \partial t^{(1)}_{\nu_2^{\sigma\upsilon}}} = \langle \mu_1^\rho | [\hat{H}_N, \tau_{\nu_2^{\sigma\upsilon}}] | \Phi_0 \rangle \\
A_{\mu_2^{\rho\sigma} \nu_1^\upsilon} =& \frac{\partial^2 \{^{2n+1} L^{(2)}_{UCC2}\}_T}{\partial \lambda^{(1)}_{\mu_2^{\rho\sigma}} \partial t^{(1)}_{\nu_1^\upsilon}} = \langle \mu_2^{\rho\sigma} | [\hat{H}_N, \tau_{\nu_1^\upsilon}] | \Phi_0 \rangle \\
A_{\mu_2^{\rho\sigma} \nu_2^{\upsilon\chi}} =& \frac{\partial^2 \{^{2n+1} L^{(2)}_{UCC2}\}_T}{\partial \lambda^{(1)}_{\mu_2^{\rho\sigma}} \partial t^{(1)}_{\nu_2^{\upsilon\chi}}} + \omega_k \delta_{\mu_2^{\rho\sigma} \nu_2^{\upsilon\chi}} = \langle \mu_2^{\rho\sigma} | [F_N, \tau_{\nu_2^{\upsilon\chi}}] | \Phi_0 \rangle \ . \qquad (5.2)
\end{aligned}
$$

$\hat{H}_N$ is the $T_1^{(0)}$-dressed normal-ordered zeroth order Hamiltonian. It is used in order to derive working equations in a more elegant way using the diagrammatic technique presented in section 2.3. The spin combinations for the non vanishing terms of the Jacobian can be seen from equation (5.1). When doing multistate calculations it is essential to build the effective singles eigenvalue problem, $A^{eff}_{\mu_1 \nu_1} U_{\nu_1}$, in order to avoid firstly keeping the doubles vector for several states in memory and secondly to updating them. This is only possible if the doubles doubles blocks of **A** are diagonal and their inversion does not produce further computational costs. Which is the case if one chooses the semi-canonical basis as described above.

$$
\begin{aligned}
A^{eff}_{\mu_1 \nu_1} U_{\nu_1} =& A_{\mu_1^\alpha \nu_1^\alpha} U_{\nu_1^\alpha} + A_{\mu_1^\alpha \nu_1^\beta} U_{\nu_1^\beta} + A_{\mu_1^\alpha \nu_2^{\alpha\alpha}} \frac{A_{\mu_2^{\alpha\alpha} \nu_1^\alpha} U_{\nu_1^\alpha}}{\omega - A_{\mu_2^{\alpha\alpha} \nu_2^{\alpha\alpha}}} \\
&+ A_{\mu_1^\alpha \nu_2^{\beta\alpha}} \frac{A_{\mu_2^{\beta\alpha} \nu_1^\alpha} U_{\nu_1^\alpha} + A_{\mu_2^{\beta\alpha} \nu_1^\beta} U_{\nu_1^\beta}}{\omega - A_{\mu_2^{\beta\alpha} \nu_2^{\beta\alpha}}} \\
&+ A_{\mu_1^\beta \nu_1^\beta} U_{\nu_1^\beta} + A_{\mu_1^\beta \nu_1^\alpha} U_{\nu_1^\alpha} + A_{\mu_1^\beta \nu_2^{\beta\beta}} \frac{A_{\mu_2^{\beta\beta} \nu_1^\beta} U_{\nu_1^\beta}}{\omega - A_{\mu_2^{\beta\beta} \nu_2^{\beta\beta}}} \\
&+ A_{\mu_1^\beta \nu_2^{\beta\alpha}} \frac{A_{\mu_2^{\beta\alpha} \nu_1^\alpha} U_{\nu_1^\alpha} + A_{\mu_2^{\beta\alpha} \nu_1^\beta} U_{\nu_1^\beta}}{\omega - A_{\mu_2^{\beta\alpha} \nu_2^{\beta\alpha}}} = \omega U_{\nu_1} \ . \qquad (5.3)
\end{aligned}
$$

The doubles vector for the $\alpha\alpha$ or $\beta\beta$ spin combination is expressed as

$$
U_{\nu_2^{\sigma\sigma}} = \frac{A_{\mu_2^{\sigma\sigma} \nu_1^\sigma} U_{\nu_1^\sigma}}{\omega - A_{\mu_2^{\sigma\sigma} \nu_2^{\sigma\sigma}}} \ . \qquad (5.4)
$$

A single element of the only contributing term from the expression $A_{\mu_2^\sigma \nu_1^\sigma} U_{\nu_1^\sigma}$ is $\langle \Phi^{a_\sigma b_\sigma}_{i_\sigma j_\sigma} | (\hat{V}_N^{\sigma\sigma} \tau_{\nu_1^\sigma})_c | \Phi_0 \rangle \, U_{\nu_1^\sigma}$. The corresponding diagrams are shown in figure 5.1. One

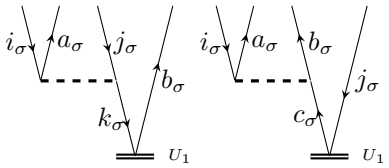

Figure 5.1.: Diagrams for $\langle \Phi^{a_\sigma b_\sigma}_{i_\sigma j_\sigma} | (\hat{V}_N^{\sigma\sigma} \tau_{\nu_1^\sigma})_c | \Phi_0 \rangle \, U_{\nu_1^\sigma}$

element of $U_{\nu_2^{\sigma\sigma}}$ can be written in semi-canonical basis in physicist notation as

$$U^{\bar{i}_\sigma \bar{j}_\sigma}_{\bar{a}_\sigma \bar{b}_\sigma} = \frac{\mathcal{P}(\bar{i}_\sigma, \bar{j}_\sigma) \sum_{\bar{c}_\sigma} \langle \bar{a}_\sigma \bar{b}_\sigma | \hat{|} \bar{c}_\sigma \bar{j}_\sigma \rangle \, u^{\bar{i}_\sigma}_{\bar{c}_\sigma} - \mathcal{P}(\bar{a}_\sigma, \bar{b}_\sigma) \sum_{\bar{k}_\sigma} \langle \bar{k}_\sigma \bar{b}_\sigma | \hat{|} \bar{i}_\sigma \bar{j}_\sigma \rangle \, u^{\bar{k}_\sigma}_{\bar{a}_\sigma}}{\omega - \underbrace{(f_{\bar{a}_\sigma \bar{a}_\sigma} + f_{\bar{b}_\sigma \bar{b}_\sigma} - f_{\bar{i}_\sigma \bar{i}_\sigma} - f_{\bar{j}_\sigma \bar{j}_\sigma})}_{\Delta^{\bar{i}_\sigma \bar{j}_\sigma}_{\bar{a}_\sigma \bar{b}_\sigma}}} \, . \tag{5.5}$$

The permutation operator $\mathcal{P}(x, y)$ acting on a function $f(x, y)$ gives

$$\mathcal{P}(x, y) f(x, y) = f(x, y) - f(y, x) \, . \tag{5.6}$$

It is obvious from the two equations above that elements of the doubles vector $(U^{\bar{a}_\sigma \bar{b}_\sigma}_{\bar{i}_\sigma \bar{i}_\sigma})$ belonging to a diagonal pair vanish. In the local basis, the inversion of the doubles doubles block is not possible as the Fock matrix is not diagonal. Direct transformation of the involved quantities to the semi-canonical basis that would allow the use of expression (5.5) is expensive and would lead to the loss of the savings due to local schemes. The Laplace transform ansatz proposed by Almlöf and Häser [31, 32] (see section 2.6) allows to circumvent the inversion of the Fock matrix in local basis while still remaining in the local framework, thus retaining the efficiency of local approximations.

$$\begin{aligned} U^{\bar{i}_\sigma \bar{j}_\sigma}_{\bar{a}_\sigma \bar{b}^\sigma} \approx - \sum_{q=1}^{n_q} \mathrm{w}_q e^{-(\Delta^{\bar{i}_\sigma \bar{j}_\sigma}_{\bar{a}_\sigma \bar{b}_\sigma} - \omega) t_q} \Big(& \mathcal{P}(\bar{i}_\sigma, \bar{j}_\sigma) \sum_{\bar{c}_\sigma} \langle \bar{a}_\sigma \bar{b}_\sigma | \hat{|} \bar{c}_\sigma \bar{j}_\sigma \rangle \, u^{\bar{i}_\sigma}_{\bar{c}_\sigma} \\ & - \mathcal{P}(\bar{a}_\sigma, \bar{b}_\sigma) \sum_{\bar{k}_\sigma} \langle \bar{k}_\sigma \bar{b}_\sigma | \hat{|} \bar{i}_\sigma \bar{j}_\sigma \rangle \, u^{\bar{k}_\sigma}_{\bar{a}_\sigma} \Big) \end{aligned} \tag{5.7}$$

In equation (5.7) t_q and w_q represent the quadrature points and corresponding weights, respectively. The use of the Laplace transform in context of local correlation methods based on a priori restricted pair lists and excitation domains has been shown in detail in the group of M. Schütz for DF-LMP2 [40]. It is straight forward to adopt the formalism for a high-spin open-shell case.

The integrals entering equation (5.7) are calculated in local and transformed to semi-canonical basis. After multiplying with the exponential factors, the doubles vector is transformed from semi-canonical to local basis following equation (14) of reference [40]. This yields the following expression for the $\alpha\alpha$ or $\beta\beta$ doubles vector in local basis.

$$\begin{aligned} U^{i_\sigma j_\sigma}_{a_\sigma b_\sigma} &= \sum_{a'_\sigma \bar{a}_\sigma \bar{i}_\sigma} \sum_{b'_\sigma \bar{b}_\sigma \bar{j}_\sigma} V^{\dagger(i_\sigma j_\sigma)}_{a_\sigma a'_\sigma} Q^{\dagger}_{a'_\sigma \bar{a}_\sigma} W^{\dagger}_{i_\sigma \bar{i}_\sigma} U^{\bar{i}_\sigma \bar{j}_\sigma}_{\bar{a}_\sigma \bar{b}_\sigma} W_{\bar{j}_\sigma j_\sigma} Q_{\bar{b}_\sigma b'_\sigma} V^{(i_\sigma j_\sigma)}_{b'_\sigma b_\sigma} \\ &= - V^{\dagger(i_\sigma j_\sigma)}_{a_\sigma a'_\sigma} V^{(i_\sigma j_\sigma)}_{b'_\sigma b_\sigma} \Big(\mathcal{P}(i_\sigma, j_\sigma) \mathcal{P}(a'_\sigma, b'_\sigma) \Big) \\ &\quad \times \sum_{q}^{n_q} \mathrm{sgn}(\mathrm{w}_q) e^{\omega t_q} X^{o}_{i_\sigma k_\sigma} X^{v}_{a'_\sigma c'_\sigma} V_{c'_\sigma c_\sigma} \Big(\hat{B}^{P}_{c_\sigma k_\sigma} \hat{C}^{P}_{d_\sigma l_\sigma} \Big) X^{o}_{l_\sigma j_\sigma} V^{\dagger}_{d_\sigma d'_\sigma} X^{v}_{d'_\sigma b'_\sigma} \end{aligned} \tag{5.8}$$

Here

$$\hat{B}^{P}_{a_\sigma i_\sigma} = u^{i_\sigma}_{c_\sigma}(a_\sigma c_\sigma \hat{|} P) - S_{a_\sigma a'_\sigma} u^{k_\sigma}_{a'_\sigma}(k_\sigma i_\sigma \hat{|} P) \text{ and } \hat{C}^{P}_{a_\sigma i_\sigma} = (J^{-1})_{PQ}(Q \hat{|} a_\sigma i_\sigma) \ . \tag{5.9}$$

From the second equality in equation (5.8) it is assumed according to the Einstein convention that summation is carried out over repeated indices, except the localized occupied spin orbital (LSO) indices i_σ and j_σ. Elements of the quadrature point dependent transformation matrices

$$\begin{aligned} X^{o}_{i_\sigma j_\sigma} &= \sum_{\bar{k}_\sigma} W^{\dagger}_{i_\sigma \bar{k}_\sigma} e^{(f_{\bar{k}_\sigma \bar{k}_\sigma} - \epsilon_{F_\sigma}) t_q + \frac{1}{4} ln(\mathrm{w}_q)} W_{\bar{k}_\sigma j_\sigma} \\ X^{v}_{a_\sigma b_\sigma} &= \sum_{\bar{c}_\sigma} Q^{\dagger}_{a_\sigma \bar{c}_\sigma} e^{(-f_{\bar{c}_\sigma \bar{c}_\sigma} + \epsilon_{F_\sigma}) t_q + \frac{1}{4} ln(\mathrm{w}_q)} Q_{\bar{c}_\sigma b_\sigma} \end{aligned} \tag{5.10}$$

are defined in complete analogy to equation (5) of reference [21]. One can clearly see from equation (5.10) that the quadrature point dependent transformation matrices

accomplish in one step the transformation from local to semi-canonical basis and the back transformation to the local basis. The orbital indices decorated with a bar indicate the semi-canonical ones and those without a bar refer to local orbitals. The spin dependent transformation matrices $\mathbf{W}_{(\sigma)}$, $\mathbf{Q}_{(\sigma)}$ and the PAO overlap matrix are given in equations (3.3), (3.4) and (3.5). The diagonal elements $f_{\bar{p}_\sigma \bar{p}_\sigma}$ of F^σ (3.1) in semi-canonical basis are the eigenvalues of $H_\sigma^{(0)}$ (3.2) and ϵ_{F_σ} is the corresponding (HOMO+LUMO)/2. The matrix $\mathbf{V}_{(\sigma)}$, introduced in equations (10) and (11) of reference [40], is the pseudoinverse of the PAO overlap matrix obeying the equation

$$\mathbf{S}_{(\sigma)}^{PAO}\mathbf{V}_{(\sigma)}\mathbf{S}_{(\sigma)}^{PAO} = \mathbf{S}_{(\sigma)}^{PAO} \ . \tag{5.11}$$

The same holds also for the pair specific pseudoinverse $\mathbf{V}^{i_\sigma j_\sigma}$ which lives in the pair domain of the LSOs i_σ and j_σ, given that $\mathbf{S}_{(\sigma)}^{PAO}$ is restricted to the same domain. Diagrams corresponding to terms entering the $\beta\alpha$ part of the doubles vector

$$U_{\nu_2^{\sigma\tau}} = \frac{A_{\mu_2^{\sigma\tau}\nu_1^\tau}U_{\nu_1^\tau} + A_{\mu_2^{\sigma\tau}\nu_1^\sigma}U_{\nu_1^\sigma}}{\omega - A_{\mu_2^{\sigma\tau}\nu_2^{\sigma\tau}}} \tag{5.12}$$

are shown in figure 5.2 (if σ equals α, then τ equals β or vice versa). Note that these do not contain any unique external lines (see section 2.3).

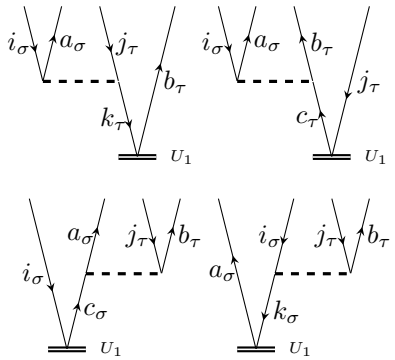

Figure 5.2.: Diagrams for $\langle \Phi_{i_\sigma j_\tau}^{a_\sigma b_\tau} | (\hat{V}_N^{\sigma\tau}\tau_{\nu_1^\tau})_c | \Phi_0 \rangle \, U_{\nu_1^\tau}$ and $\langle \Phi_{i_\sigma j_\tau}^{a_\sigma b_\tau} | (\hat{V}_N^{\sigma\tau}\tau_{\nu_1^\sigma})_c | \Phi_0 \rangle \, U_{\nu_1^\sigma}$
(If σ equals α then τ equals β and vice versa.)

One gets the following expression for a single element of the $\beta\alpha$ doubles vector in local basis.

$$U^{i_\sigma j_\tau}_{a_\sigma b_\tau} = -V^{\dagger(i_\sigma j_\tau)}_{a_\sigma a'_\sigma}\Big\{\sum_{q=1}^{n_q}\mathrm{sgn}(\mathrm{w}_q)e^{\omega t_q}X^v_{a'_\sigma c_\sigma}V_{c_\sigma d_\sigma}X^o_{i_\sigma k_\sigma}\Big(\hat{B}^P_{d_\sigma k_\sigma}\hat{C}^P_{e_\tau l_\tau}+\hat{C}^P_{d_\sigma k_\sigma}\hat{B}^P_{e_\tau l_\tau}\Big) \times X^o_{l_\tau j_\tau}V^\dagger_{e_\tau c_\tau}X^v_{c_\tau b'_\tau}\Big\}V^{(i_\sigma j_\tau)}_{b'_\tau b_\tau}\ . \tag{5.13}$$

The this way constructed doubles vector can be used immediately in the effective singles eigenvalue problem of equation (5.3). The diagrams for the remaining parts of equation (5.3) are given in the supplementary in section B. Using the rules presented in section 2.3, it is possible to write the right matrix vector product $(A^{eff}_{\mu_1\nu_1}U_{\nu_1})$ working equation for a certain state for α or β spin as

$$\begin{aligned}\mathfrak{v}^{i_\sigma}_{a_\sigma} =& \sum_{c_\sigma}\hat{f}_{a_\sigma c_\sigma}u^{i_\sigma}_{c_\sigma}+\sum_{a'_\sigma}S_{a_\sigma a'_\sigma}\Big[\sum_{j_\sigma b_\sigma}U^{i_\sigma j_\sigma}_{a'_\sigma b_\sigma}\hat{f}_{j_\sigma b_\sigma}+\sum_{j_\tau b_\tau}U^{i_\sigma j_\tau}_{a'_\sigma b_\tau}\hat{f}_{j_\tau b_\tau}-\sum_{j_\sigma}u^{j_\sigma}_{a'_\sigma}\hat{f}_{j_\sigma i_\sigma}\Big]\\ &+\sum_{PQ}(a_\sigma i_\sigma\hat{|}Q)J^{-1}_{QP}(C^P_{(\sigma)}+C^P_{(\tau)})-\sum_{j_\sigma b_\sigma}\sum_{PQ}(a_\sigma b_\sigma\hat{|}Q)J^{-1}_{QP}(P\hat{|}j_\sigma i_\sigma)u^{j_\sigma}_{b_\sigma}\\ &-\sum_{a'_\sigma}S_{a_\sigma a'_\sigma}\Big[\sum_{k_\sigma}Z_{i_\sigma k_\sigma}u^{k_\sigma}_{a'_\sigma}+\sum_{Pk_\sigma}A^P_{k_\sigma a'_\sigma}Y^P_{k_\sigma i_\sigma}-\sum_P A^P_{i_\sigma a'_\sigma}C^P_{(\sigma)}+\sum_{j_\sigma b_\sigma}t^{i_\sigma j_\sigma}_{a'_\sigma b_\sigma}X_{j_\sigma b_\sigma}\Big]\\ &+\sum_{a'_\sigma}S_{a_\sigma a'_\sigma}\Big[\sum_P A^P_{i_\sigma a'_\sigma}C^P_{(\tau)}-\sum_{j_\tau b_\tau}t^{i_\sigma j_\tau}_{a'_\sigma b_\tau}X_{j_\tau b_\tau}\Big]\\ &+\sum_{Pc_\sigma}V^P_{i_\sigma c_\sigma}(P\hat{|}a_\sigma c_\sigma)-\sum_{a'_\sigma}S_{a_\sigma a'_\sigma}\sum_{Pk_\sigma}V^P_{k_\sigma a'_\sigma}(P\hat{|}k_\sigma i_\sigma)\end{aligned} \tag{5.14}$$

with the following definitions of the used quantities.

$$C^P_{(\sigma)} = \sum_{k_\sigma c_\sigma} (P|k_\sigma c_\sigma) u^{c_\sigma}_{k_\sigma}$$

$$A^P_{i_\sigma a_\sigma} = \sum_{j_\sigma b_\sigma} t^{i_\sigma j_\sigma}_{a_\sigma b_\sigma} c^P_{j_\sigma b_\sigma} + \sum_{j_\tau b_\tau} t^{i_\sigma j_\tau}_{a_\sigma b_\tau} c^P_{j_\tau b_\tau}$$

$$c^P_{j_\sigma b_\sigma} = \sum_Q (j_\sigma b_\sigma|Q) J^{-1}_{QP} \ , \ Z_{i_\sigma k_\sigma} = \sum_{P c_\sigma} A^P_{i_\sigma c_\sigma} (P|k_\sigma c_\sigma)$$

$$Y^P_{k_\sigma i_\sigma} = \sum_{c_\sigma} (P|k_\sigma c_\sigma) u^{c_\sigma}_{i_\sigma} \ , \ X_{j_\sigma b_\sigma} = \sum_{P k_\sigma} c^P_{k_\sigma b_\sigma} Y^P_{j_\sigma k_\sigma}$$

$$V^P_{i_\sigma a_\sigma} = \sum_{j_\sigma b_\sigma} U^{i_\sigma j_\sigma}_{a_\sigma b_\sigma} c^P_{j_\sigma b_\sigma} + \sum_{j_\tau b_\tau} U^{i_\sigma j_\tau}_{a_\sigma b_\tau} c^P_{j_\tau b_\tau}$$

Again if in the equations above σ equals α then τ equals β or vice versa. Equation (19) of reference [21] is actually the closed-shell formulation of equation (5.14) using contravariant configuration state functions. To solve the effective singles eigenvalue problem and get the corresponding excitation energies, an iterative Davidson method [41] generalised to nonsymmetric matrices [42] as explicitly shown in reference [21] is used. It has to be mentioned that the Davidson subspace in the first iteration is spanned by N (states) basis vectors which are obtained from unrestricted configuration interaction singles (UCIS) calculation instead of unrestricted coupled cluster singles (UCCS). For closed-shell systems CIS is equivalent to CCS but not for open-shell systems, because occupied-virtual Fock elements do not vanish for the latter.

5.2. Local approximations for the excited state

Pair lists and orbital domains for the excited states are restricted following the procedure outlined in reference [21]. There a list of state specific important orbitals is determined after analysing the diagonal pair part of the doubles vector according to a Löwdin alike analysis. This list is extended by including all ground state pairs

and all pairs with a distance of less or equal 5 bohr between the corresponding occupied orbitals. Of course, in case where the ground state pair list is restricted according to the distance criterion of 10 bohr, the extension of the excited state pair list means just that beside important orbital pairs all ground state pairs are included.

In case of spin orbitals a doubles vector with elements $U^{i_\sigma i_\sigma}_{a_\sigma b_\sigma}$ is not available as it vanishes according to equation (5.5). Instead the object

$$\begin{aligned}\tilde{U}^{i_\sigma i_\sigma}_{a_\sigma b_\sigma} = &-V^{\dagger}_{a_\sigma a'_\sigma} V_{b'_\sigma b_\sigma} \Big(1 + \mathcal{P}(a'_\sigma b'_\sigma)\Big) \\ &\times \sum_{q}^{n_q} \mathrm{sgn}(\mathrm{w}_q) e^{\omega t_q} X^{o}_{i_\sigma k_\sigma} X^{v}_{a'_\sigma c'_\sigma} V_{c'_\sigma c_\sigma} \Big(\hat{B}^{P}_{c_\sigma k_\sigma} \hat{C}^{P}_{d_\sigma l_\sigma}\Big) X^{o}_{l_\sigma i_\sigma} V^{\dagger}_{d_\sigma d'_\sigma} X^{v}_{d'_\sigma b'_\sigma} \end{aligned} \quad (5.15)$$

is used and calculated in full PAO basis. The permutation operator $\mathcal{P}(p_\sigma q_\sigma)$ simply permutes the two orbital indices. The other quantities used in equation (5.15) have already been introduced above.

After establishing the list of important orbitals, the state specific truncation of the PAO range for the doubles vector follows the description in reference [21]. The sole difference is that here spin dependent matrices are used.

6. Test calculations

In the following it will be demonstrated that the developed local method is also useful, from a computational point of view, in cases where a good localization of the of the occupied spin orbitals is not possible and yields accurate results compared to the corresponding canonical calculations.

6.1. Computational behaviour and excitaion energies

As already mentioned above, a time factor which is not higher than 3 is expected when the time needed to perform the open-shell (os) calculation in comparison to the corresponding closed-shell (cs) one is considered. This is fulfilled even if one takes all possible ground state pairs, and hence all excited state pairs, for an os calculation into account and let the local cs calculation be performed as usual with a restriction of the ground and excited states pair lists. It can be seen from figure 6.1 that the sum of the averaged elapsed times for an iteration of the os ground and excited state calculation is only around an averaged factor of 2 (2.03 exactly) larger than the corresponding average elapsed times for the local cs calculation. Note that the averaged elapsed time per iteration for the ground state calculation does not include the time for the update, because for os and cs the contribution of the singles to the correlation energy has been computed differently. For os the undressed pre constructed coulomb and exchange (4-index) integrals restricted to pair domains are

multiplied with the corresponding parts of the singles amplitudes. As in case of cs the singles contribution to the correlation energy is calculated using the full singles amplitudes, an explicit construction of the 4-index integrals is avoided using density fitting. But in both cases the elapsed time needed for the update represents nearly the same fraction of the total averaged time per iteration, 32 % for cs and 33 % for os.

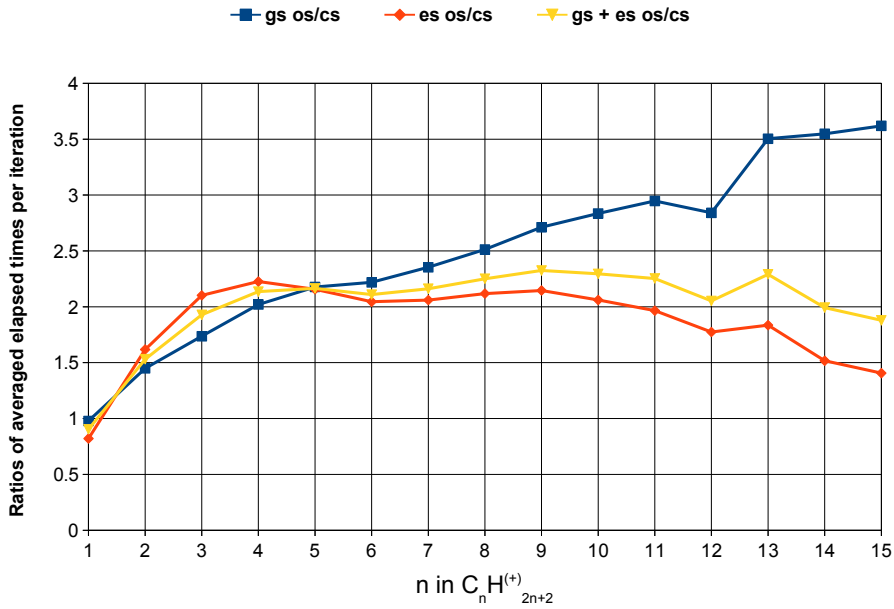

Figure 6.1.: The abbreviation gs os/cs indicates the ratio of averaged elapsed times of the local ground state (gs) of the open-shell (os) and closed-shell (cs) molecule. And es represents the local excited state method. Also the ratio of the sum of the averaged elapsed times of both gs and es for cs and os is shown. All the corresponding calculations are performed on 7 CPUs, AMD Opteron(tm) Processor 6180 SE at 800 MHz. Putting the plus sign into a bracket indicates that one has data from the neutral cs and positively charged os molecule at the corresponding points.

For the comparison of the computational behaviour of the local methods for the

ground and excited state, it is essential to consider also the corresponding averaged pair domain sizes (PDS) and the number of orbital pairs.
If one would use exactly the same criterion to restrict the ground state pair list for os and cs molecules, one would get at maximum 4 times more orbital pairs in os case compared to the cs case. The results for the local os calculations presented in figure 6.1 are based on taking all pairs into account. For cs systems a distance criterion of $R_0 = 10$ bohr is used to truncate the list of pairs treated on CC2 level. The difference in the way of restriction is kept, because firstly for cs molecules this restriction is usually sufficient and secondly for os systems as extended radical alkane chains, a distance criterion fails to produce reasonable results as shown in figure 4.3.

The orbital domains are extended by including the PAOs of the next connected neighbours, i.e. iext=1, for os and cs molecules. For the local ground state methods the average PDS is in average 9 % higher for the os systems in comparison to the cs ones. And as the ratio of the ground state pairs increases with the length of the alkane chain, as can be seen from figure 6.2, also the corresponding time factor is increasing (figure 6.1).
However, one observes for the local excited state method an average PDS which is for os systems in average around 21 % less than for cs molecules. Further, it can be recognized that the number of orbital pairs for the os case compared to the cs one is reaching a factor of 4.0 asymptotically. The reason for this is that for os molecules one always has all pairs and for cs molecules the corresponding number is increasing. In case of having in both cases all pairs, the expected factor of four would be observed. The reduced average PDS for os molecules compared to the cs ones leads to computational saving for the excited state and finally to the overall time factor of 2.

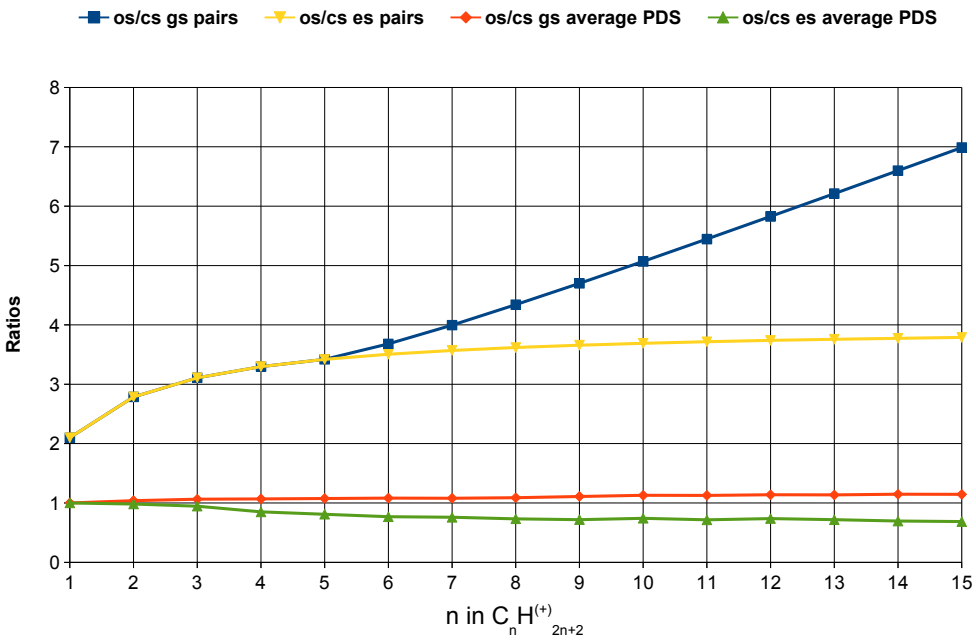

Figure 6.2.: Ratios of the number of pairs and of the averaged pair domain sizes (PDS) are plotted for local ground state (gs) and excited state (es) methods of open-shell (os) alkane radicals and closed-shell (cs) alkanes. For os molecules all pairs are included, whereas for the gs pair list restriction of cs molecules a distance criterion of $R_0 = 10$ bohr has been applied. The state specific es pair list is restricted as described in section 5.2.

In figure 6.3 absolute deviations of the excitation energies from canonical results, obtained with TURBOMOLE [20], are plotted for the first three excited states of the singly positively charged alkane radicals. As one can see, the largest deviation from the canonical result is only about 0.030 eV. This can be regarded as acceptable within an accuracy of 0.3 eV for the canonical CC2 response method for closed-shell molecules (see Tables IV and V of reference [43]). It can be clearly seen that the deviations from the canonical excitation energies are increasing with the chain length. For the first excited state this is more obvious but it is also true for the

second and third one. One has to keep in mind that the effective singles eigenvalue problem is solved, where the doubles vector (U_2) of the Jacobian is calculated in local basis with restricted pair domains. This approximation of the doubles vector can lead to increasing deviations from the canonical results in cases where the type of the excitation is of an increased double replacement character. In figure 6.4 one can see that the doubles character of the excitations of the first three excited states is increasing with chain length.

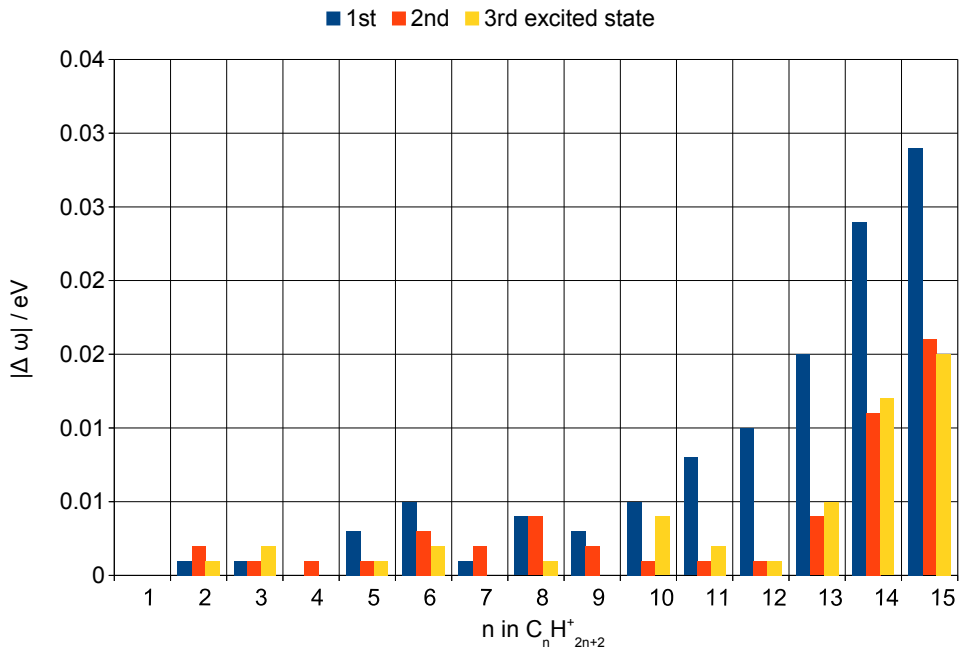

Figure 6.3.: Absolute deviations of the excitation energies of the first three excited states from canonical results. The orbital domains are restricted using the Boughton-Pulay procedure and are extended by the next connected neighbours with iext=1. The excited state orbital domains are restricted as described in section 5.2. The ground and excited state pair lists contain all pairs. A cc-pVDZ orbital basis is chosen for all molecules.

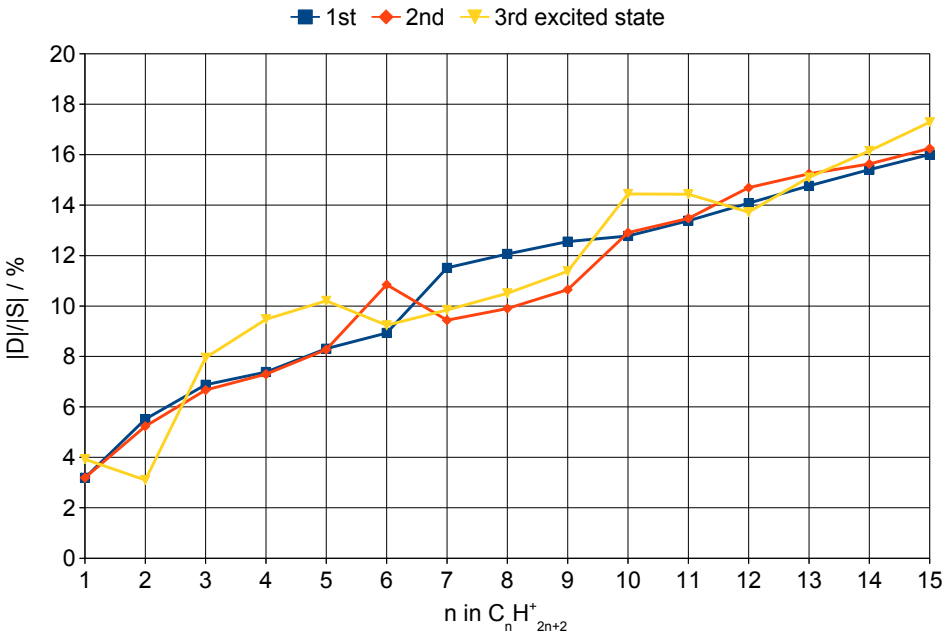

Figure 6.4.: Ratio of the norms of the doubles |D| and singles |S| eigenvector of the UCC2 Jacobian for the first three excited states of singly positively charged alkane radicals.

Besides, examining the singles eigenvector of the Jacobian for the first excited state in semi-canonical basis for Dodecane$^+$, it turns out that the largest contribution ($\approx$ 98 %) to it arises from the excitation from the highest β occupied to the first β virtual orbital. However in local basis, there is not a certain very large contribution but several ones around 30 % and from occupied spin orbitals which are not well localized, i.e. delocalized over three or four atoms. This might be the reason for the larger deviation from canonical results for the first excited state, because the other states correspond in most cases to excitations from bettter localized spin orbitals (distributed over 2 atoms) into the first unoccupied β orbital.

Table 6.1 shows for a set of doublet radicals the first three excitation energies calculated using a threshold of 1.0 μH to restrict the ground state pair list. Two cases are presented. First, the ground state orbital domains obtained with Boughton-Pulay (BP=0.98) are kept unchanged, i.e. iext=0. Second, the domains are extended by including the next connected neighbours, i.e. iext=1. Results based on ROHF and UHF determinants are shown. For these small molecules the energy threshold of 1.0 μH leads to inclusion of nearly all pairs, except for DMABN$^+$ where at most around 9% of the ground state pairs are not included.

For the case of iext=0 the average local errors are 0.044 eV and 0.038 eV for results based on ROHF and UHF, respectively. In case of iext=1 the average deviations are 0.008 eV and 0.004 eV (ROHF and UHF), respectively. As the average values show, similar deviations for ROHF and UHF based calculations from the corresponding canonical values are observed. An exception is seen for Thymine$^+$ where for the calculation based on UHF the lowest lying excited state is not found and the third excited state did not converge when using iext=0. The largest deviations of the excitation energies from the canonical results are found for Adenine$^+$. In case of iext=0 the deviation is 0.175 eV. Whereas in the case of iext=1, the largest deviation is 0.021 eV.

From these results it can be concluded that for the calculation of the excitation energies of high-spin open-shell radicals, the ground state orbital domains obtained from the BP-Procedure have to be extended using iext=1, in order to get acceptable deviations (< 0.05 eV) from the canonical results.

Table 6.1.: Vertical excitation energies for the first three excited states of doublet radicals calculated with the presented local method. The numbers in brackets indicate the local error in eV compared to the canonical results. Results based on a restricted open-shell Hartree-Fock (ROHF) and unrestricted Hartree-Fock (UHF) determinant are presented. The orbital domains are restricted using the Boughton-Pulay (BP=0.98) procedure. For the case iext=0 they are not changed and for iext=1 they are extended by the next connected neighbours. A threshold of 1.0 μH to restrict the ground state pair list is applied. The calculations are performed using a cc-pVDZ orbital basis set. A represents $\frac{n_{loc}}{n_{can}}$, i.e. the ratio between the local and canonical number of ground state pairs. B symbolizes the ratio between the local and canonical ground state average pair domain sizes.

		iext=0		ω/eV			iext=1		ω/eV		
Molecule	Reference	A / %	B / %	1st	2nd	3rd	A/ %	B/ %	1st	2nd	3rd
Water$^+$	|ROHF⟩	100.0	79.2	2.038 (0.002)	6.870 (0.002)	13.394(0.004)	100.0	100.0	2.040 (0.000)	6.868 (0.000)	13.398 (0.000)
	|UHF⟩	100.0	79.2	2.074 (0.002)	6.927 (0.002)	13.385 (0.004)	100.0	100.0	2.076 (0.000)	6.925 (0.000)	13.389 (0.000)
Furan$^+$	|ROHF⟩	100.0	53.3	1.394 (0.017)	3.906 (0.026)	4.88 (0.021)	100.0	88.9	1.407 (0.004)	3.925 (0.007)	4.905 (0.004)
	|UHF⟩	100.0	53.3	1.528 (0.015)	3.983 (0.026)	5.012 (0.020)	100.0	88.9	1.539 (0.004)	4.003 (0.006)	5.028 (0.004)
Thymine$^+$	|ROHF⟩	98.1	32.1	0.509 (0.032)	1.247 (0.043)	1.497 (0.025)	98.9	63.5	0.558 (0.017)	1.291 (0.001)	1.533 (0.011)
	|UHF⟩	98.1	32.1	[a]	1.232 (0.041)	[b]	98.7	62.2	0.764 (0.007)	1.270 (0.003)	1.685 (0.000)
Adenine$^+$	|ROHF⟩	100.0	33.3	0.610 (0.095)	1.087 (0.175)	1.708 (0.087)	100.0	66.1	0.694 (0.011)	1.241 (0.021)	1.795 (0.000)
	|UHF⟩	100.0	32.7	0.694 (0.093)	1.123 (0.146)	1.835 (0.068)	100.0	65.5	0.783 (0.004)	1.259 (0.010)	1.901 (0.002)
DMABN$^+$	|ROHF⟩	92.5	25.5	1.893 (0.048)	2.590 (0.064)	3.955 (0.022)	93.3	52.0	1.948 (0.007)	2.657 (0.003)	4.008 (0.031)
	|UHF⟩	91.2	25.0	2.204 (0.034)	2.880 (0.044)	4.169 (0.002)	92.1	51.0	2.247 (0.009)	2.928 (0.004)	4.182 (0.011)

[a] This state is not found.

[b] This state does not converge during 50 iterations of the Davidson procedure.

For a calculation on a bigger molecule (98 atoms) the singly positively charged 3-(5-(5-(4-(bis(4-(hexyloxy)phenyl)amino)phenyl)thiophene-2-yl)thiophene-2-yl)-2-cyanoacrylic acid (D21L6$^+$) is chosen. The corresponding closed-shell molecule (see figure 6.5) functions as an organic sensitizer in dye-sensitized solar cells [44].

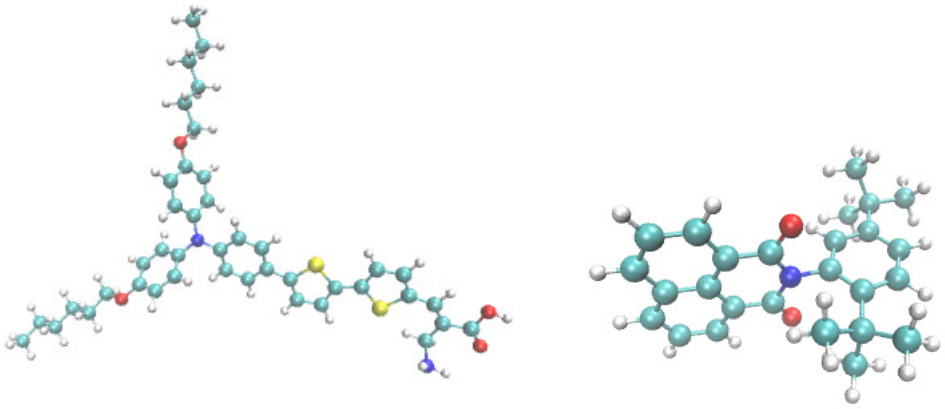

Figure 6.5.: D21L6 (left) and N-(2,5-di-tert-butylphenyl)-1,8-naphthalimide (right)

Table 6.2 shows the DF-LUCC2 ground state (gs) energy as well as the first five excited state (es) energies for D21L6$^+$. Also the total time needed to perform the gs calculation and the averaged total time to compute one es is given. Further is shown the fraction between the gs pairs included in the local calculation (n_loc) and all possible pairs (n_can) and the averaged gs pair domain size (PDS). By restricting the ground state orbital domains (see section 4.2), the number of elements belonging to the doubles amplitude of one pair reduces in average from 898704 to 17956. Using the pair energy threshold of 0.1 μH to restrict the gs pair list, reduces the number of the pairs from 33930 to 15195. In total the size of the gs doubles amplitudes is reduced from 227.2 GB to 2.03 GB. One can see that this restriction of the gs pair list is hardly changing the obtained excitation energies, i.e. the largest deviation from the results with full pair list is around 0.014 eV. The time needed to perform the gs calculation is reduced by a factor of 4.4 compared to the calculation with full pair list. The factor by which the averaged time needed to calculate one excited

state is reduced, is only about 1.27. This is due to the fact that the es PDS is in both cases nearly the same (228) and the averaged number of the es pairs is 20566 which is about 61 % of all pairs.

	A	**B**
E_{UCC2}/H	-2828.77731	-2828.77683
gs $\frac{\text{n\_loc}}{\text{n\_can}}$	1.00	0.45
gs PDS	134	134
time for DF-LUCC2 gs [h]	8.02	1.81
1st ω/eV	0.881	0.880
2nd ω/eV	1.876	1.890
3rd ω/eV	1.967	1.979
4th ω/eV	2.300	2.300
5th ω/eV	2.485	2.484
time for LT-DF-LUCC2 es per state [h]	5.04	3.96

Table 6.2.: Results for D21L6$^+$. **A** and **B** symbolize taking all ground state (gs) pairs into account and restricting the gs pair list using a threshold of 0.1 μH, respectively. The gs orbital domains are restricted using the Boughton-Pulay procedure and are extended by the next connected neighbours with iext=1. n_loc/n_can represents the ratio between the number of gs pairs included in the local calculation and all possible pairs (canonical). $\overline{\text{PDS}}$ is the average gs pair domain size. Local approximations for the excited state are applied as described in section 5.2. A cc-pVDZ orbital basis set is used. Both calculations are performed in parallel mode on 11 CPUs, Intel(R) Xeon(R) Gold 6128 at 3.40 GHz.

Excitation energies for the radical anion N-(2,5-di-tert-butylphenyl)-1,8-naphthalimide$^-$, shown in figure 6.5, are calculated. Results based on calculations with cc-pVDZ and aug-cc-pVDZ basis as well as experimentally determined excitation energies are shown in table 6.3. This molecule and other imides and diimides radical anions have been examined because of their potential to be used as electron donors in photo induced electron transfer reactions [45].

The ground state structure of the anion is optimized with the restricted open-shell Kohn-Sham program using B3LYP implemented in MOLPRO [22]. The lowest lying excited state obtained with cc-pVDZ basis deviates about 0.323 eV from the value of the lowest excited state determined experimentally. And the second lowest excited state from the calculation with cc-pVDZ basis set deviates from the corresponding experimental value about 0.178 eV. But the two lowest lying states calculated using aug-cc-pVDZ basis differ only about 0.02 eV from the corresponding experimental values. It is observed that the virtual states to which the excitation is performed are different for both basis sets.

The excitation energies starting from the third excited state obtained with aug-cc-pVDZ basis might probably correspond to Rydberg states which are not seen in the experiment. But as at the present level of the developed method no oscillator strengths are available, an unambiguous assignment of the calculated excitation energies to the experimental values is not possible.

LT-DF-LUCC2 / DF-ROHF				Experiment[a]	
cc-pVDZ		aug-cc-pVDZ			
ω/eV	λ/ nm	ω/eV	λ/ nm	ω/eV	λ/ nm
1.813	684	1.468	845	1.490	832
1.840	674	1.644	754	1.662	746
2.679	463	1.751	708	2.525	491
2.758	450	1.772	700	2.952	420
2.830	438	1.848	671	4.558	272
3.378	367	2.017	615		
3.982	311	2.056	603		

Table 6.3.: Vertical excitation energies in eV and corresponding wave lengths in nm for N-(2,5-di-tert-butylphenyl)-1,8-naphthalimide$^-$, obtained with the presented local response methode (LT-DF-LUCC2) based on DF-ROHF. For the calculation with cc-pVDZ and aug-cc-pVDZ all ground and excited state pairs are included. The ground state orbital domains for the local calculations are constructed according to the Boughton-Pulay procedure with a criterion of BP=0.98 and extended with inclusion of the next connected neighbours (iext=1). Excited state orbital domains and pair lists are restricted as described in section 5.2.

[a] Experimental values are taken from **TABLE 2** of reference [45].

6.2. Ionisation potentials

It is possible to calculate vertical ionisation potentials (IP) in addition to excitation energies. It is already possible to get the first IP using the presented ground state method for an open-shell system. One needs solely to perform the corresponding ground state closed-shell calculation in addition. The first IP is calculated according to

$$\mathrm{IP}_0 = \mathrm{E}^{\mathrm{N-1}}_{\mathrm{UCC2}} - \mathrm{E}^{\mathrm{N}}_{\mathrm{CC2}}, \tag{6.1}$$

where $\mathrm{E}^{\mathrm{N}}_{\mathrm{CC2}}$ and $\mathrm{E}^{\mathrm{N-1}}_{\mathrm{UCC2}}$ represent the closed-shell and open-shell ground state CC2 energies, respectively. Thus IP_0 corresponds to the ΔCC2 method which includes orbital relaxation by construction.
Higher IPs are available using

$$\mathrm{IP}_{\mathrm{n}} = \mathrm{IP}_0 + \omega_{\mathrm{n}} \ , \ \mathrm{n} = 1, 2, \ldots \ . \tag{6.2}$$

IP_{n} refers to the higher vertical ionisation potential of the closed-shell molecule and ω_{n} represents the corresponding excitation energy of the open-shell system. From equation (6.2) it is obvious that excitation energies of open-shell systems can be also obtained if the IPs of the corresponding closed-shell molecule are available. This has been demonstrated in context of local CC methods for vertical ionisation potentials [36]. Table 6.4 shows for some of the test molecules used in Ref. [36] the first three IPs calculated with different methods and the one presented here.
For this set of molecules an average deviation of 0.13 eV from the ΔCCSD(T) method is observed, if one considers the calculation of the IPs based on a ROHF determinant with the application of local approximations as given in table 6.4. This is a strong improvement compared to bare CC2 IPs (IP_CCSD[0]_CC2) which in average deviate about 0.7 eV from the ΔCCSD(T) results as shown in [36]. The reason is that in the here presented method additional to dynamic electron correlation also full orbital

relaxation is included. The IP_CCSD[f]_CC2 method, for which the Jacobi matrix contains all the CCSD diagrams, gives for this set an average deviation of 0.11 eV which is approximately the same as for ΔCC2(-LR)/ROHF.

Due to the spin contamination in the ground state, my results based on a UHF determinant deviate in average about 0.27 eV from the ΔCCSD(T) method for this set of molecules. The ΔHF method itself shows in average a deviation, like IP_CCSD[0]_CC2, of 0.7 eV from the ΔCCSD(T) results.

Table 6.4.: The first three vertical IPs in eV for a set of five molecules. The abbreviation ΔCC2(-LR) represents the local response method presented here. Results based on a ROHF and a UHF determinant are given. These results can be compared to IPs calculated with the methods ΔHF, IP_CCSD[0]_CC2, IP_CCSD[f]_CC2 [36] and ΔCCSD(T). Deviations from ΔCCSD(T) results are given in round brackets. The canonical values (no local approximations) in the last three columns have been taken from reference [46]. All calculations have been performed with a cc-pVDZ orbital basis set. Local approximations have been applied as described in figure 6.3 except the usage of an energy threshold of 1.0 μH to restrict the ground state pair list.

Molecule		ΔHF	ΔCC2(-LR)/UHF	ΔCC2(-LR)/ROHF	A	B	ΔCCSD(T)
Water	IP_0	10.736 (1.094)	12.000 (-0.170)	11.997 (-0.167)	10.847 (0.983)	11.651 (0.179)	11.830
	IP_1	12.696 (1.146)	14.076 (-0.234)	14.037 (-0.195)	12.947 (0.895)	13.652 (0.190)	13.842
	IP_2	17.505 (1.097)	18.925 (-0.323)	18.865 (-0.263)	17.966 (0.636)	18.460 (0.142)	18.602
Furan	IP_0	7.717 (0.986)	8.812 (-0.109)	8.772 (-0.069)	8.390 (0.313)	8.730 (-0.027)	8.703
	IP_1	9.752 (0.375)	10.351 (-0.224)	10.179 (-0.052)	9.549 (0.578)	10.174 (-0.047)	10.127
	IP_2	12.311 (0.717)	12.817 (0.211)	12.697 (0.331)	11.715 (1.313)	12.991 (0.037)	13.028
Thymine	IP_0	8.360 (0.357)	8.905 (-0.188)	8.677 (0.040)	8.271 (0.446)	8.854 (-0.137)	8.717
	IP_1		9.669	9.235	8.449	9.849	
	IP_2		10.175	9.968	9.408	10.206	
Adenine	IP_0	7.443 (0.603)	8.155 (-0.109)	8.041 (0.005)	7.555 (0.491)	8.170 (-0.124)	8.046
	IP_1		8.938	8.732	7.898	9.130	
	IP_2		9.414	9.279	8.780	9.440	
DMABN	IP_0	7.062 (0.352)	8.026 (-0.612)	7.444 (-0.030)	6.793 (0.621)	7.533 (-0.119)	7.414
	IP_1		10.273	9.392	8.951	9.494	
	IP_2		10.954	10.101	9.494	10.244	

A=IP_CCSD[0]_CC2 and B= IP_CCSD[f]_CC2.

The IPs for the closed-shell molecule D21L6 (see figure 6.5), are given in table 6.5 for the method presented here and IP_CCSD[f]_CC2 [36]. In case of ΔCC2(-LR)/ROHF all the higher IPs are based on IP_0 as is apparent from equation (6.2). As there is a difference of around 0.6 eV for IP_0 between the both methods, also the higher IPs show in average this deviation. The value of IP_0 calculated according to equation (6.1) is expected to be more accurate as it corresponds to a pure ΔCC2 method. On the other hand, the excitation energies obtained from both methods are virtually the same (average deviation ≈ 0.03 eV).

Table 6.5.: Vertical ionization potentials in eV for D21L6. Results obtained with the presented local method are based on excitation energies given in round brackets. The values in round brackets for the method IP_CCSD[f]_CC2 are calculated as IP_n-IP_0, taken from reference [36].

	IP_CCSD[f]_CC2	ΔCC2(-LR)/ROHF	
		A	**B**
IP_0	6.258	5.662	5.672
IP_1	7.188 (0.930)	6.543 (0.881)	6.552 (0.880)
IP_2	8.145 (1.887)	7.538(1.876)	7.562 (1.890)
IP_3	8.241 (1.983)	7.629 (1.967)	7.651 (1.979)
IP_4	8.701 (2.443)	7.962 (2.300)	7.972 (2.300)
IP_5	8.794 (2.536)	8.147 (2.485)	8.156 (2.484)

A Results correspond to inclusion of all ground and excited state pairs.

B Results correspond to thr_pair_en=0.1 μH for the restriction of the ground state pair list.

6.3. Electron affinities

Electron affinities (EAs) of a neutral closed-shell molecule can be calculated as shown in the following two equations.

$$\mathrm{EA}_0 = \mathrm{E}^{\mathrm{N}}_{\mathrm{CC2}} - \mathrm{E}^{\mathrm{N+1}}_{\mathrm{UCC2}} \tag{6.3}$$

$$\mathrm{EA}_\mathrm{n} = \mathrm{EA}_0 - \omega_\mathrm{n} \ , \ \mathrm{n} = 1, 2, \ldots \tag{6.4}$$

Where EA_0 represents the difference between the CC2 ground state energies of the closed-shell ($\mathrm{E}^{\mathrm{N}}_{\mathrm{CC2}}$) and the ($\mathrm{E}^{\mathrm{N+1}}_{\mathrm{UCC2}}$) open-shell molecule, respectively. Thus EA_0 corresponds to the ΔCC2 method. Higher electron affinities are obtained by subtracting the corresponding excitation energies (ω_n) of the open-shell system from EA_0.

EAs are calculated for Water, Furan, the DNA bases Adenine, Guanine and Thymine and for N-(2,5-di-tert-butylphenyl)-1,8-naphthalimide.

In table 6.6 one can see that the higher EAs of Furan are not given. The reason is that the higher EAs obtained from ΔCCSD(T) for certain symmetry states are energetically so high that, even after the calculation of 14 excited states of the Furan anion, they can not be reached.

It is observed that the highest deviation of the calculated EAs from the results obtained by ΔCCSD(T) is still less than 0.1 eV. The ΔHF method gives results which in average deviate around 0.25 eV from the ΔCCSD(T) results.

N-(2,5-di-tert-butylphenyl)-1,8-naphthalimide (**A** in table 6.6) shows already at the HF level a positive value of 0.443 eV for EA_0. The ΔCC2(-LR)/ROHF method gives a value of 1.424 eV. In other words, both methods indicate that the ground state energy of the closed-shell molecule **A** is lowered when an additional electron is attached to it. Calculated excitation energies of $\mathbf{A}^-$ are compared to experimental values in section 6.1. To the best of my knowledge, no experimental EAs are available for **A**.

Molecule		ΔHF	ΔCC2(-LR)/ROHF	ΔCCSD(T)
Water	EA_0	-0.954(-0.209)	-0.745 (0.000)	-0.745
	EA_1		-1.534	
	EA_2		-4.423	
	$EA_{(6)}$	-6.605 (0.270)	-6.912 (-0.037)	-6.875
	$EA_{(12)}$	-10.301 (-0.458)	-9.938 (-0.095)	-9.843
Furan	EA_0	-0.961 (-0.215)	-0.727 (0.019)	-0.746
Adenine	EA_0	-0.614 (-0.206)	-0.339 (0.069)	-0.408
	EA_1		-0.707	
	EA_2		-0.839	
Guanine	EA_0	-0.442(-0.241)	-0.165(0.036)	-0.201
	EA_1		-0.479	
	EA_2		-0.921	
Thymine	EA_0	-0.455 (-0.174)	-0.242 (0.039)	-0.281
	EA_1		-0.392	
	EA_2		-0.772	
A	EA_0	0.443	1.424	
	EA_1		-0.044	
	EA_3		-0.220	

Table 6.6.: Vertical electron affinities in eV for a set of six molecules. The orbital basis set aug-cc-pVDZ is used. Local approximations for ΔCC2(-LR)/ROHF are applied as described in sections 4.2 and 5.2 with an energy threshold of 1.0 μH to restrict the ground state pair list. For **A**=N-(2,5-di-tert-butylphenyl)-1,8-naphthalimide all pairs are included. The numbers in round brackets are calculated as EA's of the different methods minus the ΔCCSD(T) results.

6.4. T1-diagnostics

A very important point is the ability to judge in which cases the developed method can be used and in which it may fail to produce reasonable results. In general, one has to be careful not to treat a clear multi-reference case with a single reference method. Thus it is very helpful to get a corresponding signal from the single reference method itself when the examined system might be a multi-reference case and has probably energetically degenerate or quasi-degenerate states. This is especially helpful for large systems for which corresponding CASSCF and CASPT2 calculations with a reasonable active space are very time consuming.

As the singles Coupled Cluster operator $\mathbf{T}_1$ is used to describe the single replacements of occupied orbitals by virtuals, the values of the corresponding amplitudes will be a hint towards the significance of such replacements for the description of the ground state. Thus the larger the values of the singles amplitudes, the more important will be the inclusion of more than a single determinant to appropriately describe the ground state.

For closed-shell systems T. J. Lee et al. proposed to take the Euclidian norm of the ground state singles amplitudes ($\mathbf{t}_1$) [47] and to divide it by the square root of the number of the correlated electrons (n_{elec}) [48] as

$$\mathcal{T}_1 = \sqrt{\frac{\mathbf{t}_1\mathbf{t}_1}{n_{elec}}}. \tag{6.5}$$

This is the so-called T1-diagnostics. Others proposed to take the 2-norm of the $\mathbf{T}$ matrix [49], which contains n_{occ} rows and n_{vir} columns, i.e. in each row one has all n_{vir} elements of $\mathbf{t}_1$ for the corresponding occupied orbital. The 2-norm of $\mathbf{T}$ is based on the square root of the largest eigenvalue of the matrix ($\mathbf{T}^{\mathrm{T}}\mathbf{T}$). This is referred to as the D1-diagnositcs.

Also for open-shell systems T1- and D1-diagnostics have been described [50–52]. It has been shown that both diagnostics are highly correlated [52]. In both diagnostics

reference to singly and doubly occupied orbitals is present. As for the local method presented here, after going to the semi-canonical basis (see chapter 3), only a clear reference to α and β spin orbitals is available, the following T1-diagnostics definition is chosen.

$$\mathcal{T}_1 = \sqrt{\frac{\mathbf{t}_1^\alpha \mathbf{t}_1^\alpha + \mathbf{t}_1^\beta \mathbf{t}_1^\beta}{n_{elec}^\alpha + n_{elec}^\beta}} \tag{6.6}$$

The core electrons are not included in n_{elec}^α and n_{elec}^β. It has been reported for closed-shell molecules that $\mathcal{T}_1$ values, based on a CCSD calculation, which are larger than 0.02 indicate the importance of static correlation [48].

Table 6.7 shows the T1-diagnostics values for the open-shell molecules treated in this thesis. All the examined doublet radicals show $\mathcal{T}_1$ values which are larger than 0.02 except H_2O^+. For the alkane radicals one can see that in general the T1-diagnostics values increase with the chain length. The exceptions are Ethane$^+$, Propane$^+$ and Butane$^+$. Ethane$^+$ has the largest $\mathcal{T}_1$ value (0.084) of all alkane radicals examined here. The largest T1-diagnostics value of 0.165 is observed for the dipeptide Glycylglycine$^+$.

Molecule	$\mathcal{T}_1$	Molecule	$\mathcal{T}_1$	Molecule	$\mathcal{T}_1$	Molecule	$\mathcal{T}_1$
Methane$^+$	0.026	Nonane$^+$	0.034	H_2O^+	0.018	H_2O^-	0.027
Ethane$^+$	0.084	Decane$^+$	0.035	Furan$^+$	0.030	Furan$^-$	0.055
Propane$^+$	0.046	Undecane$^+$	0.037	Thymine$^+$	0.046	Thymine$^-$	0.038
Butane$^+$	0.052	Dodecane$^+$	0.039	Adenine$^+$	0.069	Adenine$^-$	0.039
Pentane$^+$	0.032	Tridecane$^+$	0.041	DMABN$^+$	0.036	Guanine$^-$	0.041
Hexane$^+$	0.033	Tetradecane$^+$	0.042	Glycylglycine$^+$	0.165	**A**$^-$	0.025
Heptane$^+$	0.032	Pentadecane$^+$	0.044	D21L6$^+$	0.027		
Octane $^+$	0.033						

Table 6.7.: $\mathcal{T}_1$ values for doublet radicals. **A**=N-(2,5-di-tert-butylphenyl)-1,8-naphthalimide

In order to judge if the calculated $\mathcal{T}_1$ values larger than 0.02 indeed indicate a multi-reference case and a degenerate ground state, some CASSCF and CASPT2 calculations are performed.

For H_2O^+ and H_2O^- a full valence active space is chosen for the CASSCF and CASPT2 calculations. The dominant ground state configuration state function (CSF) for H_2O^+ with the occupation string 222a00 has a weight of 0.99 in CASSCF and CASPT2. For H_2O^- the ground state CSF with the occupation string 2222a0 has a weight of 0.98. The first three excitation energies for these two molecules are shown in table 6.8. For H_2O^+ the first two excitation energies obtained with the developed method are in good agreement with CASPT2 results. For the Water anion, which has a $\mathcal{T}_1$ value of 0.027, the first excitation energy is still in good agreement with the CASPT2 result and no indication of degeneracy in the ground state is found. Also for the Furan cation and anion CASSCF and CASPT2 calcula-

Table 6.8.: The first three excitation energies in eV for H_2O^+ and H_2O^-. For the CASSCF and CASPT2 calculations a full valence active space is chosen. A state averaged calculation over four states is performed. No local approximations are applied for LT-DF-LUCC2. A cc-pVDZ and a aug-cc-pVDZ are chosen for H_2O^+ and H_2O^-, respectively. The occupation string of the dominant configuration state function (CSF) belonging to the corresponding CASPT2 excited state is given. The numbers in round brackets indicate absolute deviation from the CASPT2 excitation energies.

Molecule	Excited state	Dominant CSF	CASSCF	LT-DF-LUCC2	CASPT2
H_2O^+	1^{st}	22a200	2.088 (0.064)	2.040 (0.026)	2.014
	2^{nd}	2a2200	7.234 (0.400)	6.868 (0.034)	6.834
	3^{rd}	2220a0	14.458 (0.047)	14.753 (0.346)	14.407
H_2O^-	1^{st}	22220a	0.502 (0.232)	0.789 (0.055)	0.734
	2^{nd}	222a20	5.127 (0.917)	6.167 (0.123)	6.044
	3^{rd}	222aba	[a]	[a]	6.857

[a] This state is not found.

tions are done and the results are shown in table 6.9. The dominant ground state CSFs for the cation and the anion with the occupation string 222a000000 (7,10) have the weights 0.96 and 0.89, respectively. For the cation especially the first and third excitation energies of the local method are in very good agreement with the CASPT2 results (absolute deviation < 0.05 eV). But the corresponding CASSCF results deviate in average about 0.70 eV from the CASPT2 excitation energies. However for the anion CASSCF is in very good agreement (MAE = 0.057 eV) with CASPT2. This can be interpreted as an increasing importance of static correlation for Furan$^-$. Also the local method gives quite acceptable results (MAE = 0.07 eV) compared to CASPT2.

Table 6.9.: The first three excitation energies in eV for Furan$^+$ and Furan$^-$. For the CASSCF and CASPT2 calculations a (7,10) active space is chosen. A state averaged calculation over four states is performed. The local method is carried out with restriction of the ground state domains with a Boughton-Pulay criterion of 0.98 and inclusion of the next connected neighbours (iext=1). Pair lists are not restricted. A cc-pVDZ and a aug-cc-pVDZ are chosen for the cation and the anion, respectively. The occupation string of the dominant configuration state function (CSF) belonging to the corresponding CASPT2 excited state is given. The numbers in brackets indicate absolute deviation from the CASPT2 excitation energies.

Molecule	Excited state	Dominant CSF	CASSCF	LT-DF-LUCC2	CASPT2
Furan$^+$	1st	22a2000000	1.846 (0.402)	1.407 (0.037)	1.444
	2nd	2a22000000	4.936 (0.838)	3.925 (0.173)	4.098
	3rd	a222000000	5.719 (0.840)	4.905 (0.026)	4.879
Furan$^-$	1st	2220a00000	0.200 (0.045)	0.304 (0.059)	0.245
	2nd	22200a0000	0.296 (0.044)	0.391 (0.051)	0.340
	3rd	222000a000	0.631 (0.082)	0.803 (0.090)	0.713

The local method for the calculation of IPs presented in [36,46] starts from a closed-shell ground state. By comparison of IP_0 and IP_1 of that method, table A.1 in [46],

for the non-alkane ions given in table 6.7, no degenerate ground state of the corresponding open-shell molecule can be found.

One of the exceptions in table A.1 in [46] represents N-acetylglycine which differs only by an amine group from Glycylglycine. The difference between IP_0 and IP_1 for N-acetylglycine is 0.064 eV. This shows that the ground state of the corresponding cation is energetically quasi degenerate.

Glycylglycine$^+$ has indeed the largest $\mathcal{T}_1$ value (0.165) of all the radicals presented in table 6.7. A CASSCF calculation with a (11,11) CAS, using a cc-pVDZ basis set, reveals a doubly near degenerate ground state for this cation. The dominant CSFs with the occupation strings 2222a200000 and 22222a00000 correspond to states with the energies -489.46405042 H and -489.46152732 H, respectively. The energy difference between both is 0.069 eV. Thus also CASSCF shows a near degenerate ground state. Neither the local method presented here nor the canonical unrestricted CC2 of TURBOMOLE [20] finds both quasi degenerate states. The UCC2 ground state energy found by the local method is -490.79455668 H and the canonical value is -490.79752302 H. The energy difference between both is 0.081 eV, which is very close to the CASSCF result. Hence the local method finds one of the degenerate states and the canonical method the other. And the difference between the corresponding first excitation energies, which are 0.462 eV and 0.538 eV, is 0.076 eV, i.e. approximately the same as the difference between the corresponding ground state energies. As for the local and canonical method the first excitation energy corresponds to an excited state with the occupation string 2222a200000, one would expect a value around 0.07 eV.

For Methane$^+$ (T_d) and Ethane$^+$ (D_{3d}) an energetically degenerate ground state is expected due to molecular symmetry. For Methane$^+$ a CASPT2 calculation with a (7,10) CAS averaged over four states using a cc-pVDZ basis set yields for the three states with the dominant occupation strings 222a000000, 22a2000000 and

2a22000000 the energies -39.85447039 H, -39.85386619 H and -39.85384712 H, respectively. For each of these CSFs the weight factor is 0.97. The energy difference between the first and the second and between the first and the third state is 0.016 eV and 0.017 eV, respectively. The corresponding CASSCF calculation yields the excitation energy of 0.023 eV for the second and third states, i. e. the three degenerate states are found. The developed method and the canonical UCC2 find both an excitation energy of 0.221 eV and 0.222 eV, see table C.1, for the second and third excited state, respectively. Thus the second and third state are identified as energetically equal but around 0.2 eV larger than the ground state.

For Ethane$^+$, which has the largest $\mathcal{T}_1$ value of the alkane radicals, a CASPT2 calculation with a (13,13) CAS averaged over four states, using a cc-pVDZ basis set, yields an excitation energy of 0.038 eV for the first excited state. Thus the ground state is energetically doubly degenerate. The dominant CSFs have a weight factor above 0.94 for all four states. The corresponding CASSCF calculation and the UCC2 methods, local and canonical, give an excitation energy of 0.120 eV and 0.115 eV for the first excited state, respectively. In this case CASSCF and UCC2 indicate approximately a degenerate ground state. The second excited state found by UCC2 corresponds to the third excited state of CASSCF and CASPT2, with respect to single excitations, but with an energy value corresponding to the second excited state of CASSCF and CASPT2. The same problem occurs for the third excited state found by UCC2, i.e. this state corresponds schematically to the second state of CASSCF and CASPT2, but energetically it has the value of the third excited state.

For Propane$^+$ one finds a degenerate ground state with the UCC2 method. This can be seen from the excitation energy of 0.002 eV for the first excited state (see table C.1). Corresponding CASSCF and CASPT2 calculations with a (11,11) CAS, averaged over four states, yield for the first excited state the excitation energies of

0.189 eV and 0.127 eV , respectively. Using a (15,15) CAS in a CASSCF calculation yields an excitation energy of 0.079 eV. For both active spaces the dominant ground state CSF has a weight factor larger than 0.92. However the occupation string describing the first excited state is different in all three calculations, but it can be described with a single excitation from the ground state. A calculation with a larger active space would be needed to decide if the first excited state described by the UCC2 method is the correct one. The UCC2 excitation energy hints at least at a degenerate ground state in agreement with the CASSCF calculation for which a (15,15) CAS is used.

Butane$^+$, which has the second largest $\mathcal{T}_1$ value of the alkane radicals, seems to be a rather complicated case. A CASSCF calculation with a (9,9) CAS yields an excitation energy of 0.182 eV for the first excited state. For the same state the corresponding CASPT2 calculation yields a negative excitation energy of -0.051 eV. In both calculations the ground state CSF with the occupation string 2222a0000 has a weight factor of 0.95. The first excited state has, in both calculations, the two dominant occupation strings 2a2220000 and 222a20000 with weight factors 0.72 and 0.67, respectively. A CASSCF calculation with a (11,11) CAS yields an excitation energy of 0.238 eV for the first excited state. With an active space of (13,13) the first excitation energy obtained via CASSCF is 0.292 eV. With the UCC2 method one finds a first excitation energy of 0.410 eV belonging to an excited state which can be described by the occupation string 222a20000. Also in this case CASSCF and CASPT2 calculations with larger active space are needed to decide how reasonable the UCC2 results are.

One can conclude for the developed method that $\mathcal{T}_1$ values larger than 0.02, especially for the alkane radicals, may indeed indicate a degenerate ground state. And it can happen that the method fails to find the degenerate states as is the case for $Methane^+$ and $Ethane^+$. However, for the other molecules shown in table 6.7 the developed method may produce reasonable results for the first excited state even up to $\mathcal{T}_1$ values around 0.05. But it may fail for a value larger than 0.1.

7. Summary

A local multistate response method for the description of high-spin open-shell molecules is presented. Going from a ROHF-MO basis to semi-canonical basis, enables the building of the effective singles eigenvalue problem. Further the Laplace-transform trick allows for an efficient way to calculate the doubles vector of the Jacobian in local basis.

An energy based criterion to restrict the ground state pair list, instead of a distance criterion, turns out to be the better choice, especially in case of the extended alkane doublet radicals. And is in general recommended in cases where strong localization of the occupied spin orbitals is not possible due to the nature of the molecule. To get acceptable deviations (< 0.05 eV) from canonical excitation energies, it is necessary to extend the Boughton-Pulay domains by inclusion of the next connected neighbours with iext=1. The presented results for excitation energies, ionisation potentials and electron affinities do in average not exceed an error of 0.13 eV compared to the ΔCCSD(T) method. The lowest two excitation energies calculated for N-(2,5-di-tert-butylphenyl)-1,8-naphthalimide anion are in very good agreement with the experimental values (deviation < 0.025 eV).

The so-called T_1-diagnostics for the developed method is defined. For alkane radicals, already values slightly larger than 0.02 may indicate a clear multi-reference

case and thus methods describing static correlation have to be applied. For other radicals tested in this thesis, the developed method produces reasonable results up to $\mathcal{T}_1$ values of 0.05. When going to larger values, it is always recommended to check if static correlation has to be taken into account.

From the computational point of view one needs only around twice more time than a corresponding local closed-shell calculation. Due to the local scheme, this method shows a lower scaling behaviour with system size than a corresponding canonical one. This makes the method applicable to extended molecular systems. In this work the method is successfully tested on systems containing up to 98 atoms.

A. The second order UCC2 Lagrangian and its time average

$$
\begin{aligned}
{}^{2n+1}L^{(2)}_{UCC2}(t) = \langle\Phi_0|\,[V(t), T_1^{(1)} + T_2^{(1)}] \\
&+ \frac{1}{2}\big([[H_0, T_1^{(1)}], T_1^{(1)} + T_2^{(1)}] + [[H_0, T_2^{(1)}], T_1^{(1)} + T_2^{(1)}]\big)\exp(T_1^{(0)} + T_2^{(0)})\,|\Phi_0\rangle \\
&+ \sum_{\zeta=\alpha,\beta}\sum_{\mu_1^\zeta}\lambda^{(0)}_{\mu_1^\zeta}\Big(\Big\langle\mu_1^\zeta\Big|\,[\hat{V}(t), T_1^{(1)} + T_2^{(1)}] + [[\hat{H}_0, T_1^{(1)}], T_2^{(1)}] + [[\hat{V}_{(t)}, T_1^{(1)}], T_2^{(0)}] \\
&\qquad + \frac{1}{2}\big([[\hat{H}_0, T_1^{(1)}], T_1^{(1)}] + [[[\hat{H}_0, T_1^{(1)}], T_1^{(1)}], T_2^{(0)}]\big)\,|\Phi_0\rangle\Big) \\
&+ \sum_{\zeta=\alpha,\beta}\sum_{\mu_1^\zeta}\lambda^{(1)}_{\mu_1^\zeta}\Big\langle\mu_1^\zeta\Big|\,\hat{V}(t) + [\hat{H}_0, T_1^{(1)} + T_2^{(1)}] + [\hat{V}(t), T_2^{(0)}] + [[\hat{H}_0, T_1^{(1)}], T_2^{(0)}]\,|\Phi_0\rangle \\
&+ \sum_{\zeta,\sigma}\sum_{\mu_2^{\zeta\sigma}}\lambda^{(0)}_{\mu_2^{\zeta\sigma}}\Big(\Big\langle\mu_2^{\zeta\sigma}\Big|\,[\hat{V}(t), T_1^{(1)} + T_2^{(1)}] + [[\hat{V}(t), T_1^{(1)}], T_2^{(0)}] \\
&\qquad + \frac{1}{2}[[\hat{H}_0, T_1^{(1)}], T_1^{(1)}]\,|\Phi_0\rangle\Big)(\delta_{\zeta\alpha}\delta_{\zeta\sigma} + \delta_{\zeta\beta}\delta_{\zeta\sigma} + \delta_{\zeta\alpha}\delta_{\sigma\beta}) \\
&+ \sum_{\zeta,\sigma}\sum_{\mu_2^{\zeta\sigma}}\lambda^{(1)}_{\mu_2^{\zeta\sigma}}\Big(\Big\langle\mu_2^{\zeta\sigma}\Big|\,\hat{V}(t) + [\hat{H}_0, T_1^{(1)}] + [F, T_2^{(1)}] \\
&\qquad + [\hat{V}(t), T_2^{(0)}]\,|\Phi_0\rangle\Big)(\delta_{\zeta\alpha}\delta_{\zeta\sigma} + \delta_{\zeta\beta}\delta_{\zeta\sigma} + \delta_{\zeta\alpha}\delta_{\sigma\beta}) \\
&- i\sum_{\zeta=\alpha,\beta}\sum_{\mu_1^\zeta}\lambda^{(1)}_{\mu_1^\zeta}\frac{\partial t^{(1)}_{\mu_1^\zeta}}{\partial t} - i\sum_{\zeta,\sigma}\sum_{\mu_2^{\zeta\sigma}}\lambda^{(1)}_{\mu_2^{\zeta\sigma}}\frac{\partial t^{(1)}_{\mu_2^{\zeta\sigma}}}{\partial t}(\delta_{\zeta\alpha}\delta_{\zeta\sigma} + \delta_{\zeta\beta}\delta_{\zeta\sigma} + \delta_{\zeta\alpha}\delta_{\sigma\beta})
\end{aligned}
\tag{A.1}
$$

The dressed quantities are similarity transformed with the zeroth order singles Cluster operator $T_1^{(0)}$ and the explicit time dependence of the first order amplitudes and multipliers is omitted. V_0 is part of the zeroth order Hamiltonian H_0. The given orders are with respect to time. The following definitions are assumed:

$$T_1^{(1)} = \sum_{\zeta=\alpha,\beta} \sum_{\mu_1^\zeta} t_{\mu_1^\zeta}^{(1)} \tau_{\mu_1^\zeta};\ t_{\mu_1^\zeta}^{(1)} = \sum_{k=-N}^{N} \exp\left(-i\omega_k t\right) \sum_X \epsilon_X(\omega_k) t_{\mu_1^\zeta}^X(\omega_k)$$

$$T_2^{(1)} = \sum_{\zeta,\sigma} \sum_{\mu_2^{\zeta\sigma}} t_{\mu_2^{\zeta\sigma}}^{(1)} \tau_{\mu_2^{\zeta\sigma}} (\delta_{\zeta\alpha}\delta_{\zeta\sigma} + \delta_{\zeta\beta}\delta_{\zeta\sigma} + \delta_{\zeta\alpha}\delta_{\sigma\beta});\ t_{\mu_2^{\zeta\sigma}}^{(1)} = \sum_{k=-N}^{N} \exp\left(-i\omega_k t\right) \sum_X \epsilon_X(\omega_k) t_{\mu_2^{\zeta\sigma}}^X(\omega_k)$$

$$V(t) = \sum_{k_1=-N}^{N} \exp\left(-i\omega_k t\right) \sum_X \epsilon_X(\omega_k) X \tag{A.2}$$

$\lambda_{\mu_1^\zeta}^{(1)}$ and $\lambda_{\mu_2^{\zeta\sigma}}^{(1)}$ are defined in analogy to $t_{\mu_1^\zeta}^{(1)}$ and $t_{\mu_2^{\zeta\sigma}}^{(1)}$.

With $V(\omega_k) = \sum_X \epsilon_X(\omega_k) X$,

$$T_1^{(1)}(\omega_k) = \sum_{\zeta=\alpha,\beta} \sum_{\mu_1^\zeta} t_{\mu_1^\zeta}^{(1)}(\omega_k) \tau_{\mu_1^\zeta};\ t_{\mu_1^\zeta}^{(1)}(\omega_k) = \sum_X \epsilon_X(\omega_k) t_{\mu_1^\zeta}^X(\omega_k)\ . \tag{A.3}$$

and analogous definition of $T_2^{(1)}(\omega_k)$, $\lambda_{\mu_1^\zeta}^{(1)}(\omega_k)$ and $\lambda_{\mu_2^{\zeta\sigma}}^{(1)}(\omega_k)$, taking the time average of equation (A.1) leads to equation (A.4).

$$\{{}^{2n+1}L^{(2)}_{UCC2}\}_T =$$

$$\sum_{k=-N}^{N} \Big\{ \langle\Phi_0| \, [V(-\omega_k), T_1^{(1)}(\omega_k) + T_2^{(1)}(\omega_k)]$$

$$+ \frac{1}{2}[[H_0, T_1^{(1)}(-\omega_k) + T_2^{(1)}(-\omega_k)], T_1^{(1)}(\omega_k) + T_2^{(1)}(\omega_k)] \exp(T_1^{(0)} + T_2^{(0)}) \, |\Phi_0\rangle$$

$$+ \sum_{\zeta=\alpha,\beta} \sum_{\mu_1^\zeta} \lambda^{(0)}_{\mu_1^\zeta} \Big(\Big\langle \mu_1^\zeta \Big| \, [\hat{V}(-\omega_k), T_1^{(1)}(\omega_k) + T_2^{(1)}(\omega_k)] + [[\hat{H}_0, T_1^{(1)}(-\omega_k)], T_2^{(1)}(\omega_k)]$$

$$+ [[\hat{V}(-\omega_k), T_1^{(1)}(\omega_k)], T_2^{(0)}] + \frac{1}{2}[[\hat{H}_0, T_1^{(1)}(-\omega_k)], T_1^{(1)}(\omega_k)]$$

$$+ \frac{1}{2}[[[\hat{H}_0, T_1^{(1)}(-\omega_k)], T_1^{(1)}(\omega_k)], T_2^{(0)}] \, |\Phi_0\rangle \Big)$$

$$+ \sum_{\zeta=\alpha,\beta} \sum_{\mu_1^\zeta} \lambda^{(1)}_{\mu_1^\zeta}(-\omega_k) \Big(\Big\langle \mu_1^\zeta \Big| \, \hat{V}(\omega_k) + [\hat{H}_0, T_1^{(1)}(\omega_k) + T_2^{(1)}(\omega_k)] + [\hat{V}(\omega_k), T_2^{(0)}]$$

$$+ [[\hat{H}_0, T_1^{(1)}(\omega_k)], T_2^{(0)}] \, |\Phi_0\rangle \Big)$$

$$+ \sum_{\zeta,\sigma} \sum_{\mu_2^{\zeta\sigma}} \lambda^{(0)}_{\mu_2^{\zeta\sigma}} \Big(\Big\langle \mu_2^{\zeta\sigma} \Big| \, [\hat{V}(-\omega_k), T_1^{(1)}(\omega_k) + T_2^{(1)}(\omega_k)] + \frac{1}{2}[[\hat{H}_0, T_1^{(1)}(-\omega_k)], T_1^{(1)}(\omega_k)]$$

$$+ [[\hat{V}(-\omega_k), T_1^{(1)}(\omega_k)], T_2^{(0)}] \, |\Phi_0\rangle \Big) (\delta_{\zeta\alpha}\delta_{\zeta\sigma} + \delta_{\zeta\beta}\delta_{\zeta\sigma} + \delta_{\zeta\alpha}\delta_{\sigma\beta})$$

$$+ \sum_{\zeta,\sigma} \sum_{\mu_2^{\zeta\sigma}} \lambda^{(1)}_{\mu_2^{\zeta\sigma}}(-\omega_k) \Big(\Big\langle \mu_2^{\zeta\sigma} \Big| \, \hat{V}(\omega_k) + [\hat{H}_0, T_1^{(1)}(\omega_k)] + [F, T_2^{(1)}(\omega_k)]$$

$$+ [\hat{V}(\omega_k), T_2^{(0)}] \, |\Phi_0\rangle \Big) (\delta_{\zeta\alpha}\delta_{\zeta\sigma} + \delta_{\zeta\beta}\delta_{\zeta\sigma} + \delta_{\zeta\alpha}\delta_{\sigma\beta})$$

$$- \omega_k \sum_{\zeta=\alpha,\beta} \sum_{\mu_1^\zeta} \lambda^{(1)}_{\mu_1^\zeta}(-\omega_k) t^{(1)}_{\mu_1^\zeta}(\omega_k)$$

$$- \omega_k \sum_{\zeta,\sigma} \sum_{\mu_2^{\zeta\sigma}} \lambda^{(1)}_{\mu_2^{\zeta\sigma}}(-\omega_k) t^{(1)}_{\mu_2^{\zeta\sigma}}(\omega_k) (\delta_{\zeta\alpha}\delta_{\zeta\sigma} + \delta_{\zeta\beta}\delta_{\zeta\sigma} + \delta_{\zeta\alpha}\delta_{\sigma\beta}) \Big\} \tag{A.4}$$

B. Diagrams for the effective singles eigenvalue problem $A^{eff}_{\mu_1\nu_1}U_{\nu_1}$

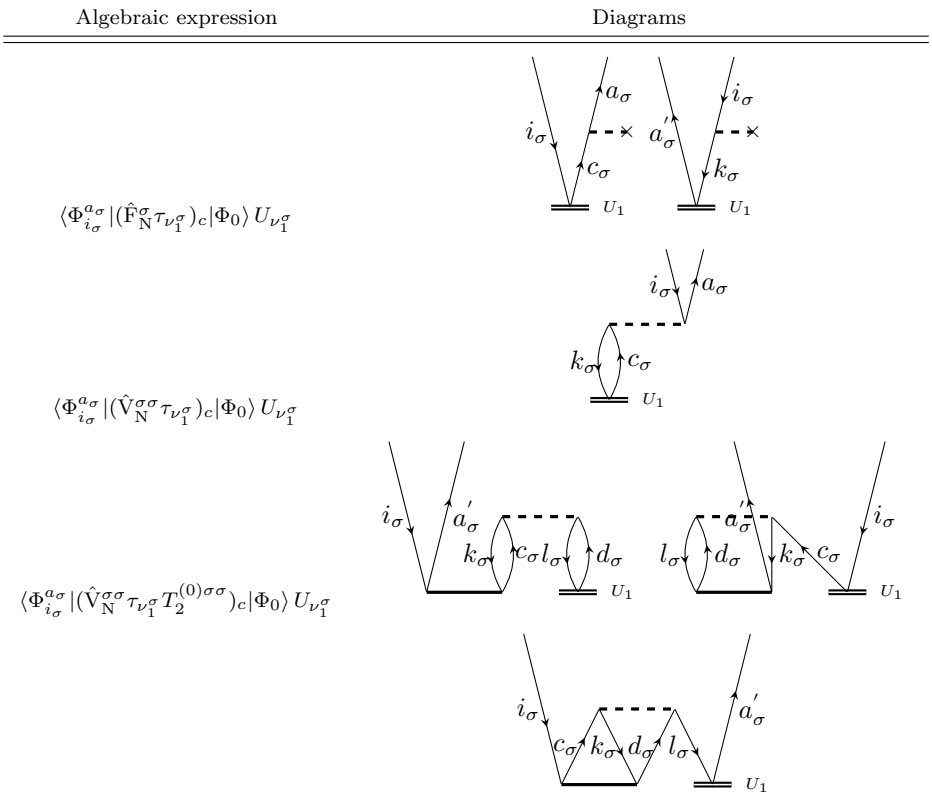

Figure B.1.: Diagrams for $A_{\mu_1^\sigma\nu_1^\sigma}U_{\nu_1^\sigma}$ (σ is α or β).

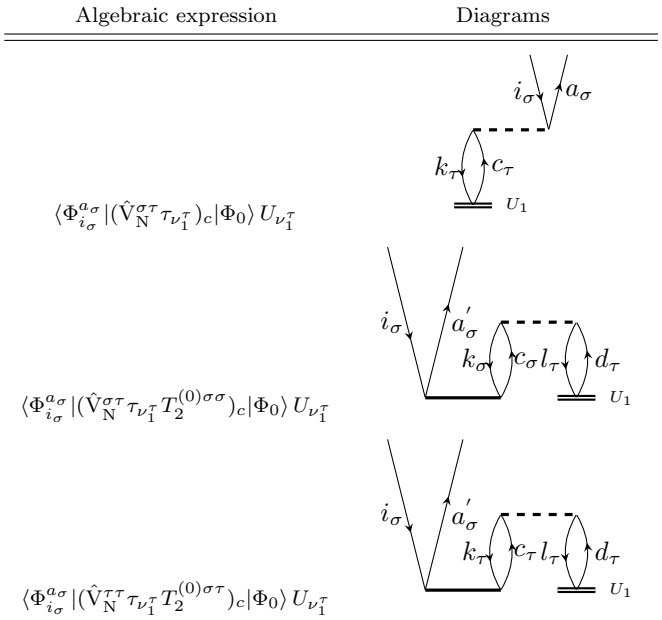

Figure B.2.: Diagrams for $A_{\mu_1^\sigma\nu_1^\tau}U_{\nu_1^\tau}$. If σ equals α then τ equals β and vice versa.

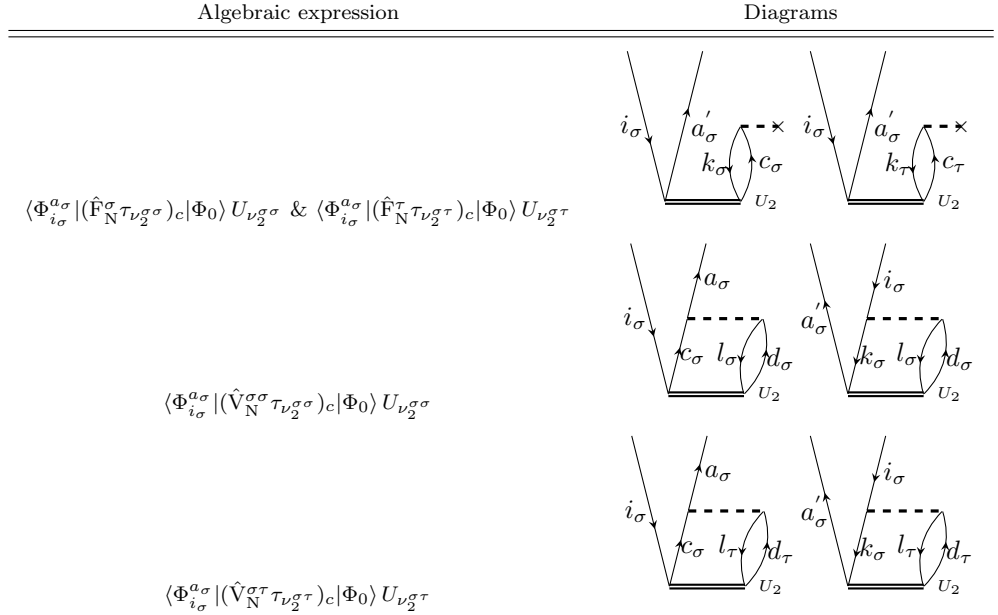

Figure B.3.: Diagrams for $A_{\mu_1^\sigma\nu_2^{\sigma\sigma}}U_{\nu_2^{\sigma\sigma}}$ and $A_{\mu_1^\sigma\nu_2^{\sigma\tau}}U_{\nu_2^{\sigma\tau}}$. If σ equals α then τ equals β and vice versa.

C. Excitation energies of alkane radicals

Table C.1.: Vertical excitation energies for doublet alkane radicals in eV. The ground state orbital domains for the local calculations are constructed according to the Boughton-Pulay procedure with a criterion of BP=0.98 and extended with inclusion of the next connected neighbours (iext=1). The ground state pair list is restricted according to a distance criterion of R_0 =10 bohr and different MP2 pair energy thresholds (thr_pair_en). Excited state orbital domains and pair lists are restricted as described in section 5.2. Also results for local calculations with all pairs and canonical UCC2 excitation energies obtained with TURBOMOLE [20] are presented.

		LT-DF-LUCC2					
			thr_pair_en				
Molecule		R_0=10 bohr	3 μH	1 μH	0.1 μH	all pairs	canonical
Methane$^+$	ω_1	0.221	0.221	0.221	0.221	0.221	0.221
	ω_2	0.222	0.222	0.222	0.222	0.222	0.222
	ω_3	9.557	9.557	9.557	9.557	9.557	9.557
Ethane$^+$	ω_1	0.115	0.114	0.115	0.114	0.115	0.116
	ω_2	0.727	0.727	0.727	0.727	0.727	0.729
	ω_3	2.917	2.917	2.917	2.917	2.917	2.918
Propane$^+$	ω_1	0.002	0.002	0.002	0.002	0.002	0.003
	ω_2	0.233	0.233	0.233	0.233	0.233	0.234
	ω_3	1.655	1.655	1.655	1.655	1.654	1.656
Butane$^+$	ω_1	0.410	0.410	0.410	0.410	0.410	0.410
	ω_2	0.665	0.665	0.665	0.665	0.665	0.666
	ω_3	1.199	1.199	1.199	1.199	1.199	1.199

Table continues on next page

Table C.1.: Continued from previous page

		LT-DF-LUCC2					
			thr_pair_en				
Molecule		R_0=10 bohr	3 μH	1 μH	0.1 μH	all pairs	canonical
Pentane$^+$	ω_1	0.733	0.733	0.733	0.733	0.733	0.730
	ω_2	0.876	0.876	0.876	0.876	0.876	0.875
	ω_3	1.070	1.070	1.070	1.070	1.070	1.069
Hexane$^+$	ω_1	1.009	1.010	1.010	1.010	1.010	1.005
	ω_2	1.116	1.116	1.117	1.117	1.117	1.114
	ω_3	1.118	1.119	1.119	1.119	1.119	1.117
Heptane$^+$	ω_1	1.202	1.222	1.224	1.224	1.224	1.223
	ω_2	1.208	1.229	1.229	1.229	1.229	1.227
	ω_3	1.278	1.299	1.299	1.299	1.299	1.299
Octane$^+$	ω_1	1.311	1.346	1.347	1.347	1.347	1.343
	ω_2	1.373	1.409	1.410	1.410	1.410	1.406
	ω_3	1.425	1.460	1.459	1.459	1.459	1.458
Nonane$^+$	ω_1	1.416	1.458	1.460	1.460	1.461	1.458
	ω_2	1.509	1.551	1.553	1.553	1.553	1.551
	ω_3	1.522	1.570	1.571	1.572	1.572	1.572
Decane$^+$	ω_1	1.376	1.518	1.537	1.542	1.543	1.548
	ω_2	1.496	1.563	1.569	1.570	1.560	1.561
	ω_3	1.560	1.635	1.638	1.648	1.636	1.632
Undecane$^+$	ω_1	1.161	1.334	1.372	1.383	1.383	1.391
	ω_2	1.573	1.657	1.670	1.666	1.651	1.650
	ω_3	1.594	1.681	1.692	1.692	1.676	1.674
Dodecane$^+$	ω_1	0.995	1.174	1.216	1.235	1.236	1.246
	ω_2	1.624	1.720	1.736	1.755	1.720	1.721
	ω_3	1.646	1.740	1.757	1.758	1.728	1.727
Tridecane$^+$	ω_1	0.810	1.026	1.075	1.100	1.101	1.116
	ω_2	1.650	1.774	1.792	1.794	1.763	1.767
	ω_3	1.673	1.797	1.816	1.825	1.786	1.791
Tetradecane$^+$	ω_1	[a]	0.881	0.938	0.976	0.979	1.003
	ω_2	1.649	1.804	1.825	1.832	1.801	1.812
	ω_3	1.674	1.829	1.851	1.863	1.829	1.841
Pentadecane$^+$	ω_1	0.522	0.759	[a]	0.869	0.873	0.902
	ω_2	1.668	1.832	1.862	1.876	1.837	1.853
	ω_3	1.681	1.843	1.873	1.891	1.857	1.872

[a] The corresponding excited state does not converge during 50 iterations.

D. Ionization potentials of alkanes

Table D.1.: Vertical ionization potentials in eV for alkanes. The ground state orbital domains for the local calculations are constructed according to the Boughton-Pulay procedure with a criterion of BP=0.98 and extended with inclusion of the next connected neighbours (iext=1). The ground state pair list is restricted according to a distance criterion of R_0 =10 bohr and a MP2 pair energy thresholds (thr_pair_en) of 0.1 μH. Excited state orbital domains and pair lists are restricted as described in section 5.2. Also ΔHF and canonical UCC2 results obtained with TURBOMOLE [20] are presented. The numbers in brackets represent the absolute deviation from the canonical values.

			ΔCC2(-LR) / ROHF		
Molecule		ΔHF	R_0=10 bohr	0.1 μH	canonical
Methane	IP_0	13.372	14.198 (0.000)	14.198 (0.000)	14.198
	IP_1		14.419 (0.000)	14.419 (0.000)	14.419
	IP_2		14.420 (0.000)	14.420 (0.000)	14.420
Ethane	IP_0	12.285	12.396 (0.000)	12.396 (0.001)	12.396
	IP_1		12.511 (0.001)	12.510 (0.003)	12.512
	IP_2		13.123 (0.002)	13.123 (0.003)	13.125
Propane	IP_0	11.539	11.916 (0.005)	11.916 (0.005)	11.922
	IP_1		11.918 (0.006)	11.918 (0.006)	11.925
	IP_2		12.149 (0.006)	12.149 (0.006)	12.156
Butane	IP_0	10.936	11.261 (0.005)	11.261 (0.005)	11.266
	IP_1		11.671 (0.005)	11.671 (0.005)	11.676
	IP_2		11.926 (0.006)	11.926 (0.006)	11.932
Pentane	IP_0	10.683	10.787 (0.009)	10.787 (0.009)	10.796
	IP_1		11.520 (0.006)	11.520 (0.006)	11.526
	IP_2		11.663 (0.008)	11.663 (0.008)	11.671

Table continues on next page

Table D.1.: Continued from previous page

			ΔCC2(-LR) / ROHF		
Molecule		ΔHF	R_0=10 bohr	0.1 μH	canonical
Hexane	IP_0	10.477	10.421 (0.009)	10.421 (0.009)	10.430
	IP_1		11.430 (0.005)	11.431 (0.004)	11.435
	IP_2		11.537 (0.007)	11.538 (0.006)	11.544
Heptane	IP_0	10.330	10.168 (0.028)	10.138 (0.002)	10.140
	IP_1		11.370 (0.007)	11.362 (0.001)	11.363
	IP_2		11.376 (0.009)	11.367 (0.000)	11.367
Octane	IP_0	10.222	9.956 (0.047)	9.906 (0.004)	9.910
	IP_1		11.267 (0.015)	11.253 (0.000)	11.253
	IP_2		11.329 (0.014)	11.316 (0.000)	11.316
Nonane	IP_0	10.145	9.781 (0.060)	9.718 (0.003)	9.721
	IP_1		11.197 (0.018)	11.178 (0.001)	11.179
	IP_2		11.290 (0.018)	11.271 (0.001)	11.272
Decane	IP_0	10.088	9.671 (0.105)	9.566 (0.000)	9.566
	IP_1		11.047 (0.067)	11.108 (0.006)	11.114
	IP_2		11.167 (0.040)	11.136 (0.009)	11.127
Undecane	IP_0	10.046	9.549 (0.113)	9.439 (0.003)	9.436
	IP_1		10.710 (0.117)	10.822 (0.005)	10.827
	IP_2		11.122 (0.036)	11.105 (0.019)	11.086
Dodecane	IP_0	10.015	9.490 (0.164)	9.331 (0.005)	9.326
	IP_1		10.485 (0.087)	10.566 (0.006)	10.572
	IP_2		11.114 (0.067)	11.086 (0.039)	11.047
Tridecane	IP_0	9.992	9.433 (0.201)	9.244 (0.011)	9.233
	IP_1		10.243 (0.105)	10.344 (0.005)	10.349
	IP_2		11.083 (0.084)	11.038 (0.038)	11.000
Tetradecane	IP_0	9.974	9.412 (0.261)	9.176 (0.024)	9.152
	IP_1		[a]	10.152 (0.003)	10.155
	IP_2		11.061 (0.098)	11.008 (0.044)	10.964
Pentadecane	IP_0	9.961	9.373 (0.291)	9.114 (0.032)	9.082
	IP_1		9.895 (0.089)	9.983 (0.001)	9.984
	IP_2		11.041 (0.106)	10.990 (0.055)	10.935

[a] The corresponding excited state does not converge during 50 iterations.

Bibliography

[1] R. G. Parr and Y. Weitao. *Density-Functional Theory of Atoms and Molecules.* Oxford University Press, (1994).

[2] E. J. Baerends and O. V. Gritsenko. *J. Phys. Chem. A*, **101**:5383, (1997).

[3] A. Dreuw and M. Head-Gordon. *Chem. Rev.*, **105**:4009, (2005).

[4] J. Cizek. *J. Chem. Phys.*, **45**:4256, (1966).

[5] J. Cizek. *Adv. Chem. Phys.*, **14**:35, (1969).

[6] G. D. Purvis and R. J. Bartlett. *J. Chem. Phys.*, **76**:1910, (1982).

[7] G. E. Scuseria and H. F. Schaefer III. *J. Chem. Phys.*, **90**:3700, (1989).

[8] P. J. Knowles, C. Hampel, and Hans-Joachim Werner. *J. Chem. Phys.*, **99**:5219, (1993).

[9] P. Neogrady, M. Urban, and I. Hubac. *J. Chem. Phys.*, **100**:3706, (1994).

[10] X. Li and J. Paldus. *J. Chem. Phys.*, **101**:8812, (1994).

[11] P. G. Szalay and Jürgen Gauss. *J. Chem. Phys.*, **107**:9028, (1997).

[12] P. G. Szalay and Jürgen Gauss. *J. Chem. Phys.*, **112**:4027, (2000).

[13] G. E. Scuseria. *Chem. Phys. Lett.*, **176**:27, (1991).

[14] O. Christiansen, H. Koch, and P. Jørgensen. *Phys. Chem. Lett.*, **243**:409, (1995).

[15] P. J. Knowles, J. S. Andrew, R. D. Amos, and N. C. Handy. *Chem. Phys. Lett.*, **186**:130, (1991).

[16] S. Saebø and P. Pulay. *Annu. Rev. Phys. Chem.*, **44**:213, (1993).

[17] E. J. Baerends, D. E. Ellis, and P. Ros. *Chem. Phys.*, **2**:41, (1973).

[18] J. L. Whitten. *J. Chem. Phys.*, **58**:4496, (1973).

[19] B. I. Dunlap, J. W. D. Connolly, and J. R. Sabin. *J. Chem. Phys.*, **71**:3396, (1979).

[20] TURBOMOLE V6.2 2010, a development of University of Karlsruhe and Forschungszentrum Karlsruhe GmbH, 1989-2007, TURBOMOLE GmbH, since 2007; available from
`http://www.turbomole.com`.

[21] D. Kats and M. Schütz. *J. Chem. Phys.*, **131**:124117, (2009).

[22] H.-J. Werner, P. J. Knowles, G. Knizia, F. R. Manby, M. Schütz, et al. Molpro, version 2015.1, a package of ab initio programs, 2015. see http://www.molpro.net.

[23] A. Szabo and N. S. Ostlund. *Modern Quantum Chemistry: Introduction to advanced electronic structure theory*. Dover publications, (1996).

[24] H. Kock, O. Christiansen, P. Jørgensen, A. M. Sanchez de Merás, and T. Helgaker. *J. Chem. Phys*, **106**:1808, (1995).

[25] T. Helgaker, P. Jørgensen, and J. Olsen. *Molecular Electronic-Structure Theory*. John Wiley & Sons Ltd, (2012).

[26] T. D. Crawford and H. F. Schaefer III. An introduction to coupled cluster theory for computational chemists. In K. B. Lipkowitz and D. B. Boyd, editors, *Reviews in Computational Chemistry*, volume 14, pages 33–124. VCH Publisher, (2000).

[27] O. Christiansen, P. Jørgensen, and C. Hättig. *Int. J. Quantum Chem.*, **68**:1, (1998).

[28] H.-J. Werner, F. R. Manby, and P. J. Knowles. *J. Chem. Phys.*, **118**:8149, (2003).

[29] E. G. Hohenstein, S. I. L. Kokkila, R. M. Parrish, and T. J. Martínez. *J. Chem. Phys.*, **138**:124111, (2013).

[30] E. G. Hohenstein, S. I. L. Kokkila, R. M. Parrish, and T. J. Martínez. *J. Chem. Phys. B*, **117**:12972, (2013).

[31] J. Almlöf. *Chem. Phys. Lett.*, **181**:319, (1991).

[32] M. Häser and J. Almlöf. *J. Chem. Phys.*, **96**:489, (1992).

[33] J. Pipek and P. G. Mezey. *J. Chem. Phys.*, **90**:4916, (1989).

[34] S. F. Boys. *in Quantum Theory of Atoms, Molecules, and the Solid State.* Academic Press, (1996). ed. P. O. Löwdin.

[35] D. Kats, T. Korona, and M. Schütz. *J. Chem. Phys.*, **125**:104106, (2006).

[36] G. Wälz, D. Usvyat, T. Korona, and M. Schütz. *J. Chem. Phys.*, **144**:084117, (2016).

[37] Y. Liu. *Linear scaling high-spin open-shell local correlation methods.* PhD thesis, University Stuttgart, Stuttgart, 2011. http://dx.doi.org/10.18419/opus-1324.

[38] J. W. Boughton and P. Pulay. *J. Comput. Chem.*, **14**:736, (1993).

[39] C. Hampel and Hans-Joachim Werner. *J. Chem. Phys.*, **104**:16, (1996).

[40] D. Kats, D. Usvyat, and M. Schütz. *Phys. Chem. Chem. Phys.*, **10**:3430, (2008).

[41] E. R. Davidson. *J. Comput. Phys.*, **17**:87, (1975).

[42] K. Hirao and H. Nakatsuji. *J. Comput. Phys.*, **45**:246, (1982).

[43] M. Schreiber, M. Silva-Junior, S. Sauer, and W. Thiel. *J. Chem. Phys.*, **128**:134110, (2008).

[44] J.-H. Yum, D. P. Hagberg, S.-J. Moon, K. M. Karlsson, T. Marinado, L. Sun, A. Hagfeldt, M. K. Nazeeruddin, and M. Grätzel. *Angewandte Chemie, International Edition*, **48**:1576, (2009).

[45] D. Gosztola, M. P. Niemczyk, W. Svec, A. S. Lukas, and M. R. Wasielewski. *J. Phys. Chem. A*, **104**:6545, (2000).

[46] G. Wälz. *Development of local coupled cluster response methods for vertical Ionization Potentials*. PhD thesis, University Regensburg, Regensburg, 2017. urn:nbn:de:bvb:355-epub-356062.

[47] T. J. Lee, J. E. Rice, G. E. Scuseria, and H. F. Schaefer III. *Theor. Chim. Acta.*, **75**:81, (1989).

[48] T. J. Lee and P. R. Taylor. *International Journal of Quantum Chemistry: Quantum Chemistry Symposium*, **23**:199, (1989).

[49] C. L. Janssen and I. M. B. Nielsen. *Chem. Phys. Lett.*, **290**:423, (1998).

[50] D. Jayatilaka and T. J. Lee. *J. Chem. Phys.*, **98**:9734, (1993).

[51] M. L. Leininger, I. M. B. Nielsen, T. D. Crawford, and C. L. Janssen. *Chem. Phys. Lett.*, **328**:431, (2000).

[52] T. J. Lee. *Chem. Phys. Lett.*, **372**:362, (2003).